UNIVERSITÁ DEGLI STUDI DI TORINO

Department of Clinical and Biological Sciences

PhD Programme in Experimental Medicine and Therapy

Cycle XXXIV

Effects of metformin on skeletal muscle in an *in vivo* and *in vitro* model

Supervisors
Prof.ssa Silvia Racca
Prof.ssa Fiorella Biasi

Thesis' author
Eleonora Maniscalco

PhD Programme Co-ordinator
Prof. Pasquale Pagliaro

Code of scientific discipline: BIO14

Academic years of enrollment: *2018-2022*

TABLE OF CONTENTS

INTRODUCTION

1.1. Skeletal muscle and satellite cells

Skeletal muscle is one of the most plastic tissues in humans, it can rapidly adapt in response to metabolic changes, and it also has an incredible regenerative capacity. It accounts for the 40% of body weight and it is mainly composed of 75% water, 20% protein and 5% of other compounds such as carbohydrates, fats, inorganic salts, and minerals [1,2].

Skeletal muscle is one of the most metabolically active tissues in human body: it is a reservoir of proteins, as it contains the 50-75% of all body proteins and it also constitutes the 30-50% of whole-body protein turnover. The two most abundant proteins in muscle are actin and myosin, and they approximately account for the 70-80% of the total protein content of each fiber. Muscle mass depends on the equilibrium between protein synthesis and protein degradation [2,3].

Moreover, skeletal muscle is involved in the transduction of the chemical energy in mechanical energy to generate power, it contributes to the basal energy metabolism, thermogenesis, oxygen and energy consumption during physical activity and exercise [2].

Skeletal muscle uses different substrates according to the type, the duration, and the intensity of the physical activity. The main substrates involved are glucose, obtained from the hepatic glycogen demolition and hepatic gluconeogenesis, and fatty acids, that comes from the mobilization of triglycerides of the adipose tissue [4].

As regards its structure, skeletal muscle is made up of muscle fibers and connective tissue. Moreover, each fiber's number and size contribute to determine the size of the muscle (*Figure 1*).

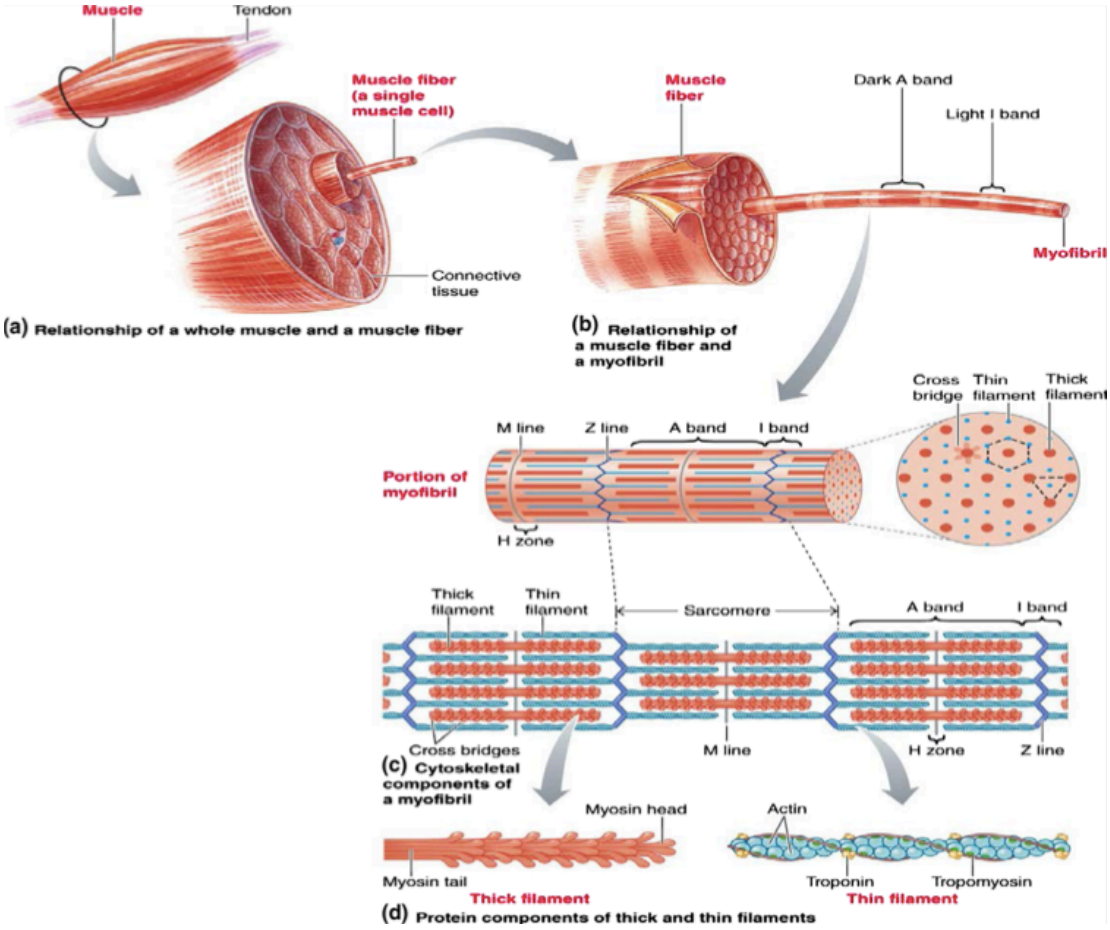

Figure 1. Structure of skeletal muscle (from: Frontera *et al.* 2014 [2])

Muscle fibers are constituted of myofibrils containing actin and myosin filaments, and they are multinucleated. Each myonucleus is post mitotic, therefore no more able to divide, and controls the type of protein synthetized in the specific region of the cell [2].

Muscle fibers are classified in type I, IIa, IIb, IIx, and they differ in the expression of the myosin heavy chain isoform and in the correlate contractile abilities as regards speed and resistance to fatigue. In skeletal muscle the expression of the different fiber types is not always the same, and it can vary during the entire lifespan. Type I fibers are slow, resistant to fatigue, they mainly have an oxidative metabolism and a higher mitochondria content. Type IIa are fast, oxidative, they have intermediate metabolic properties and high levels of glycolytic and oxidative enzymes. Type IIb fibers are mainly glycolytic, fast twitch, and quickly fatigable.

Type IIx have intermediate contractile and metabolic properties between type I and type IIb fibers [3]. Slow fibers are used to maintain the posture, as it is needed a prolonged contractile activity, whereas the fast fibers play a key role when speed and power are needed.

Muscle mass growth or hypertrophy is associated with increased protein accumulation but also with proliferation and fusion of satellite cells (SCs). SCs are tissue resident adult stem cells with a high nucleus-to-cytoplasm *ratio* with few organelles, located in proximity of the muscle fibers underneath the basal lamina (*Figure 2*).

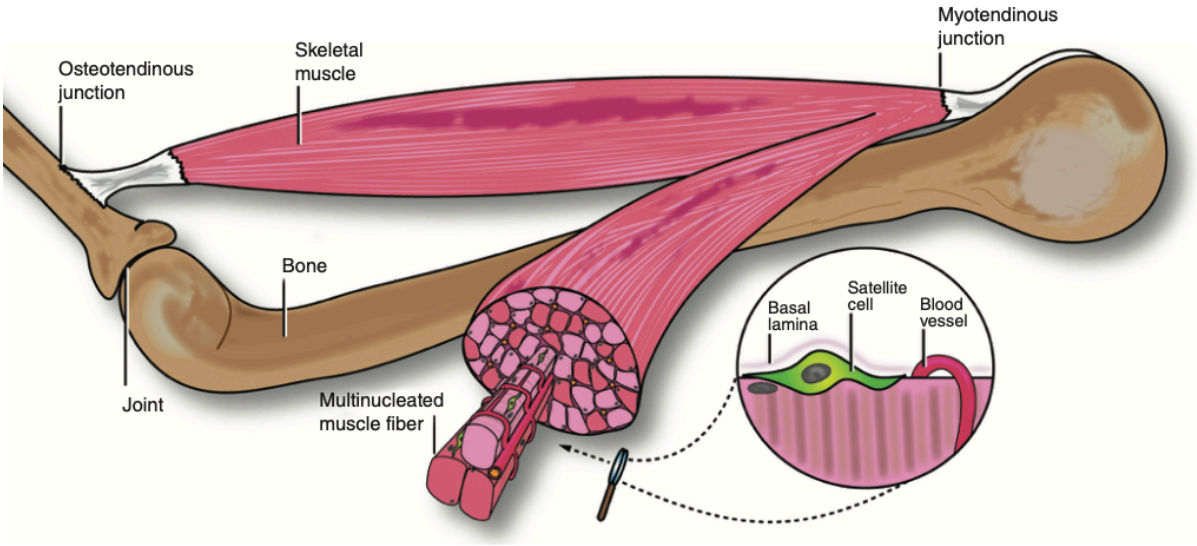

Figure 2. Skeletal muscle anatomy: location of satellite cells (from: Dumont *et al.* 2015 [5])

They are responsible of muscle growth, tissue reparation, regeneration, and homeostasis [2,5–7]. SCs are quiescent mononuclear precursor cells that upon activation proliferate either to become quiescent again or to differentiate and fuse with existing muscle fibers or form new myofibers. Quiescence is a reversible cell cycle arrested state characterized by the absence of cell proliferation but unlike terminally differentiated cells, quiescent cells maintain the ability to enter cell cycle and resume proliferation. To maintain the regenerative capability of muscle tissue it is imperative to keep the homeostasis of SCs and their quiescent status. Age-associated decrease in stem cell function is observed in several stem cell populations,

including SCs, but the exact mechanisms involved in stem cell exhaustion are not known. In muscle, aged SCs fail to maintain quiescence and the capacity to self-renew once activated [4]. There are lots of SCs markers such as paired box 7 (PAX7), myogenic factor 5 (Myf5), and myoblast determination protein 1 (MyoD); during quiescence, they are expressed in an inactive form, even though they are ready to be activated. PAX7 is constantly expressed in SCs, but it is not a specific marker of quiescence. MyoD and Myf5 are called determination factors and they are required to define the myogenic identity (*Figure 3*).

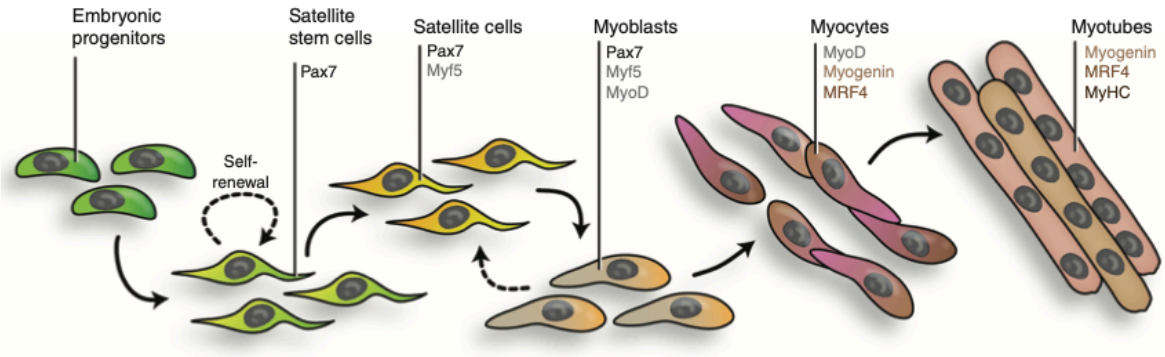

Figure 3. Myogenic lineage progression (from: Dumont *et al.* 2015 [5])

When muscle injury occurs, the damaged environment stimulates the SCs to reach the injured site by releasing cytokines and growth factor. Therefore, SCs re-enter the cell cycle, proliferate and then differentiate to form myocytes that can fuse either to the damaged myofibers or to form new muscle fibers (*Figure 4*). During all these stages there is a different expression of the myogenic markers [2,6].

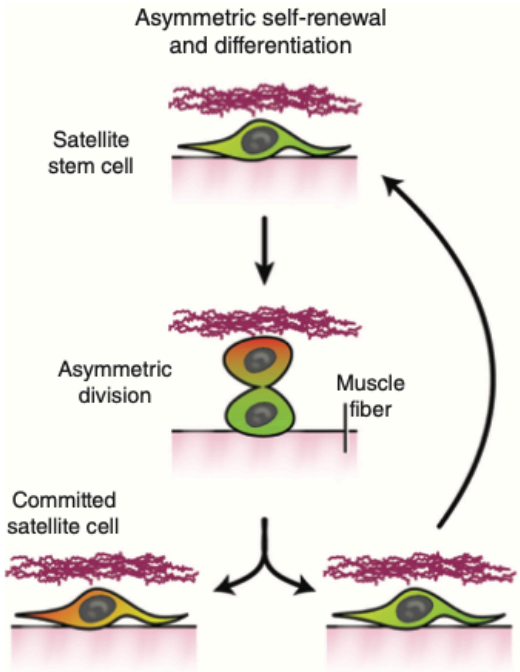

Figure 4. Asymmetric and stochastic self-renewal (modified from: Dumont *et al.* 2015 [5])

1.2. Physical exercise

Physical activity is defined as "any bodily movement produced by skeletal muscles that requires energy expenditure". Instead, physical exercise is "a variety of planned, structured, and repetitive physical activities" which intent is the maintainance and/or progress of the physical fitness. Moreover, exercise exerts beneficial effects on the human body health, and it is very important in the prevention of obesity, but also cardiovascular and metabolic diseases. It is known that exercise improves muscle metabolism, increases muscle protein synthesis and this leads to an increase in muscle weight and size. During physical exercise there is also an increase in mitochondrial biogenesis, and this leads to the synthesis of mitochondrial proteins, together with an enhancement in muscle oxidative capacity and improvement in the extraction and use of blood oxygen. The effects of physical exercise are not only limited to the muscle, as an augmented physical activity enhances insulin sensitivity but also glucose and lipid

metabolism. On the other hand, lack of exercise raises the risk to develop type 2 diabetes and obesity, as well as diseases related to brain function [1,3,8–10].

There are two types of physical exercise: endurance and resistance training.

Endurance training is mainly based on aerobic exercise as the main work is done by the cardiorespiratory system, the loads are low and repeated, high frequency exercises are performed, moreover there is low-power consumption. Endurance exercise activates large muscle groups with a high request of oxygen transport and release, and this causes an increase in capillaries per muscle fiber to facilitate O_2 transport, accompanied by an increase in mitochondria, reinforcement of fat and glycogen. The new capillaries increase the blood flow and provide a bigger surface for the gases exchange during physical exercise. Endurance training also activates the AMPK-MAPK-PGC1α cascades, that result in mitochondrial biogenesis and metabolic adaptations such as angiogenesis and muscle fibers type transition. Furthermore, it also increases the levels of the enzymes of the Krebs cycle, essential for aerobic ATP production [1,3,10].

Indeed, resistance training is more focused on the neuromuscular and the anaerobic system. It is based on the strength exercise, with low frequency, high load, and short duration and it maintains muscle mass protecting from muscle atrophy. Resistance exercise activates the PI3K-AKT-mTOR cascade, leading to a regulation of the protein synthesis/degradation that, together with the activation and fusion of the satellite cells, lead to muscle hypertrophy [1,3,10].

Apart from the effects on skeletal muscle due to the two types of exercise, it has been observed that the combination of endurance and resistance training can augment bone density and insulin sensitivity, helping to prevent from type 2 diabetes [1] (*Figure 5*).

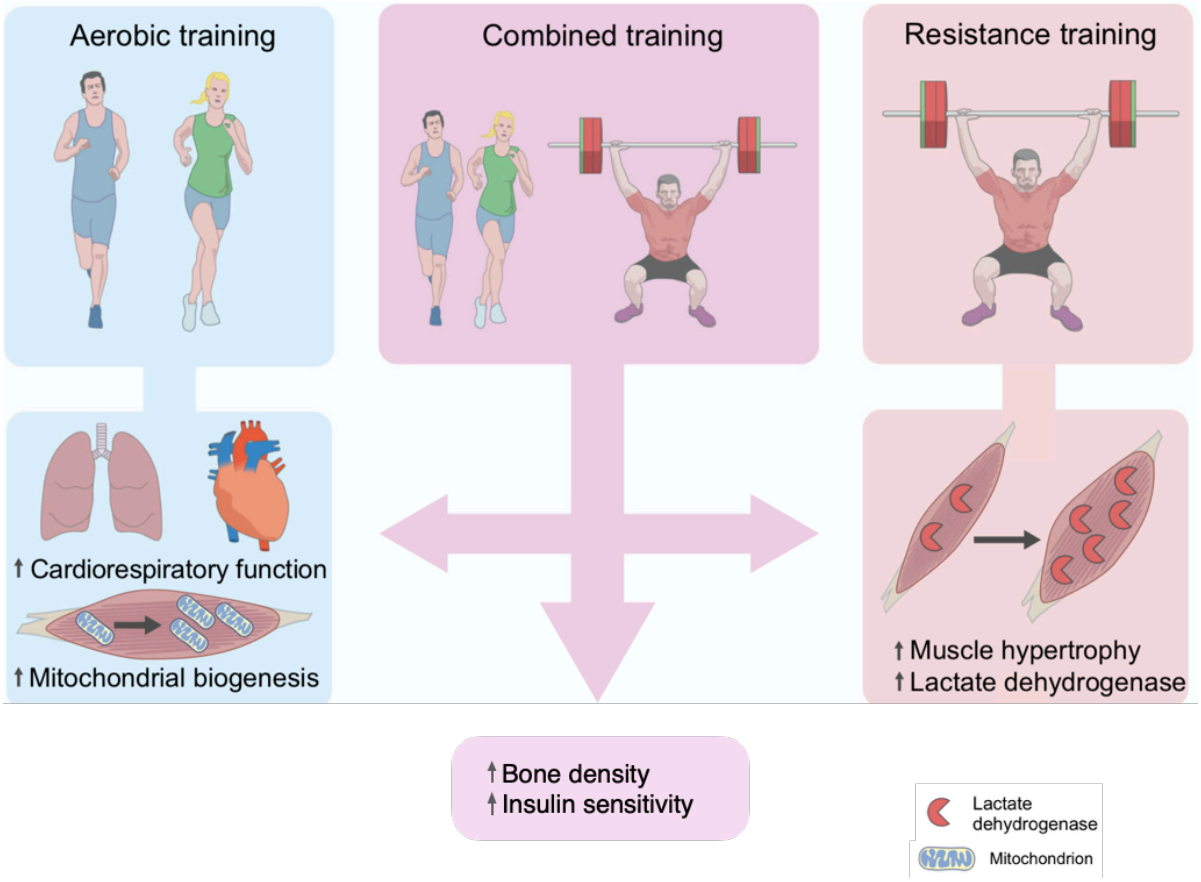

Figure 5. Adaptations to endurance and resistance exercise (modified from: Savikj *et al.* 2020 [11])

1.3. Insulin

Insulin is a hormone secreted by pancreatic ß-cells. It is a peptide made up of two chains, alpha and beta, respectively of 21 and 30 amino acids. The hormone is first secreted as pre-proinsulin, degraded to proinsulin and then, thanks to the action of ß cells peptidases, it becomes active insulin with the release of peptide C, composed by 31 amino acids [12] (*Figure 6*).

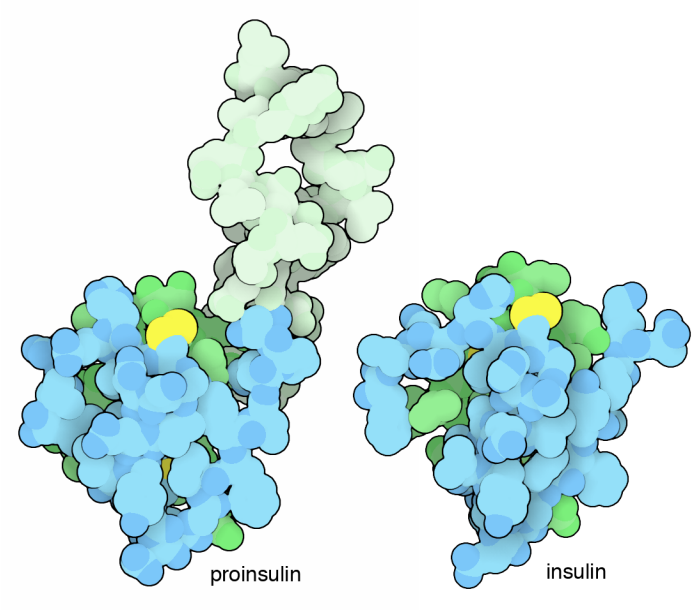

Figure 6. Insulin and proinsulin, with A-chain in green, B-chain in blue and disulfide linkages in yellow [13].

Insulin in responsible of the regulation of glucose uptake, glycogen synthesis, gluconeogenesis, lipid metabolism, and many other activities. It is secreted when glycemia is high, with the aim to restore the homeostasis of the hematic glucose. Insulin action is mediated by its receptors located in the cell membranes of liver, muscle tissue and adipose tissue, whose sensitivity is physiologically regulated by circulating factors. The interaction insulin-receptor activates a tyrosine protein kinase that phosphorylates the receptor and the downstream factors [14].

Insulin increases glycogen production by inducing hepatic, muscle, and adipose cells to internalize the hematic glucose so that it can be then converted in glycogen. This product will then be used by the target cells as an energetic stock. Insulin inhibits lipolysis, stimulates protein synthesis by facilitating the transfer of amino acids from the blood flow to the cells. Moreover, insulin stimulates cell proliferation and the glucose usage for an energetic scope and facilitates the entrance of potassium inside the cells.

In type I diabetes, caused by the absence of insulin production by pancreas, a substitutive therapy with recombinant insulin is done. It is currently employed human insulin produced in bacteria with techniques of recombinant DNA. The various available insulins differ in terms of speed and duration of their action. Indeed, there are preparations with fast and brief action and others with intermediate and prolonged action [12,15].

1.4. Non-insulin antidiabetic drugs

There are a variety of molecules that are used as secretagogues to stimulate insulin release or to increase tissue sensitivity to insulin: these molecules are the antidiabetic drugs used in the therapy of type 2 diabetes. Insulin resistance and abnormal insulin secretion are central to the development of this type of diabetes. Until now, glucose-lowering agents are subdivided into agents that increase insulin secretion (sulfonylureas, glinides, incretins), increase insulin sensitivity (metformin, thiazolidinediones), inhibit intestinal absorption of glucose, such as alpha glycosidase inhibitor, or promote urinary excretion of glucose, inhibiting its reabsorption by the proximal renal tubule [12].

The classification of non-insulin antidiabetic drugs is constantly updated, and the new categorization lists four classes: insulin secretagogues, insulin sensitizers, calorie restrictors, calorie restriction mimetics. Risk of hypoglycemia, weight loss, and reduction of the cardiovascular risk are some of the features considered to list the above-mentioned four categories [16] (*Table 1*).

Insulin Secretagogues	Insulin Sensitizers	Calorie Restriction Mimetics (CRMs)	Calorie Restrictors & CRMs
Direct: • Sulfonylureas	Conventional: • Metformin • Pioglitazone	Acting on Urinary tract: • SGLT2i	Dual Agonists*
Indirect: • DPP4i, GLP1-RAs	Modern: • GLP1-RAs	Acting in the gut: • AGIs, GLP1-RAs	Intermediate & long acting GLP1-RAs

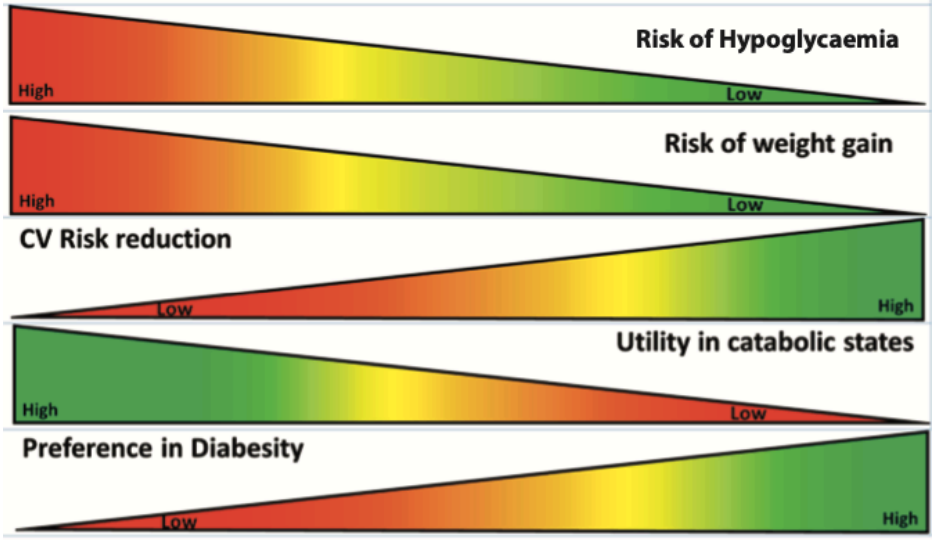

Table 1. Classification of non-insulin antidiabetic drugs (from: Kalra *et al.* 2022 [16])

1.5. Metformin

Metformin (Met) belongs to the biguanides family and is the most prescribed oral antidiabetic drug used for the treatment of type 2 diabetes.

At the beginning of the XX sec it was reported that diguanidines and *Galega officinalis*, a plant rich in guanidine, lowered blood glucose in animals, even though they caused a high toxicity. Met, also named dimethyl biguanide, was synthetized by the fusion of two guanidines to obtain biguanide (*Figure 7*).

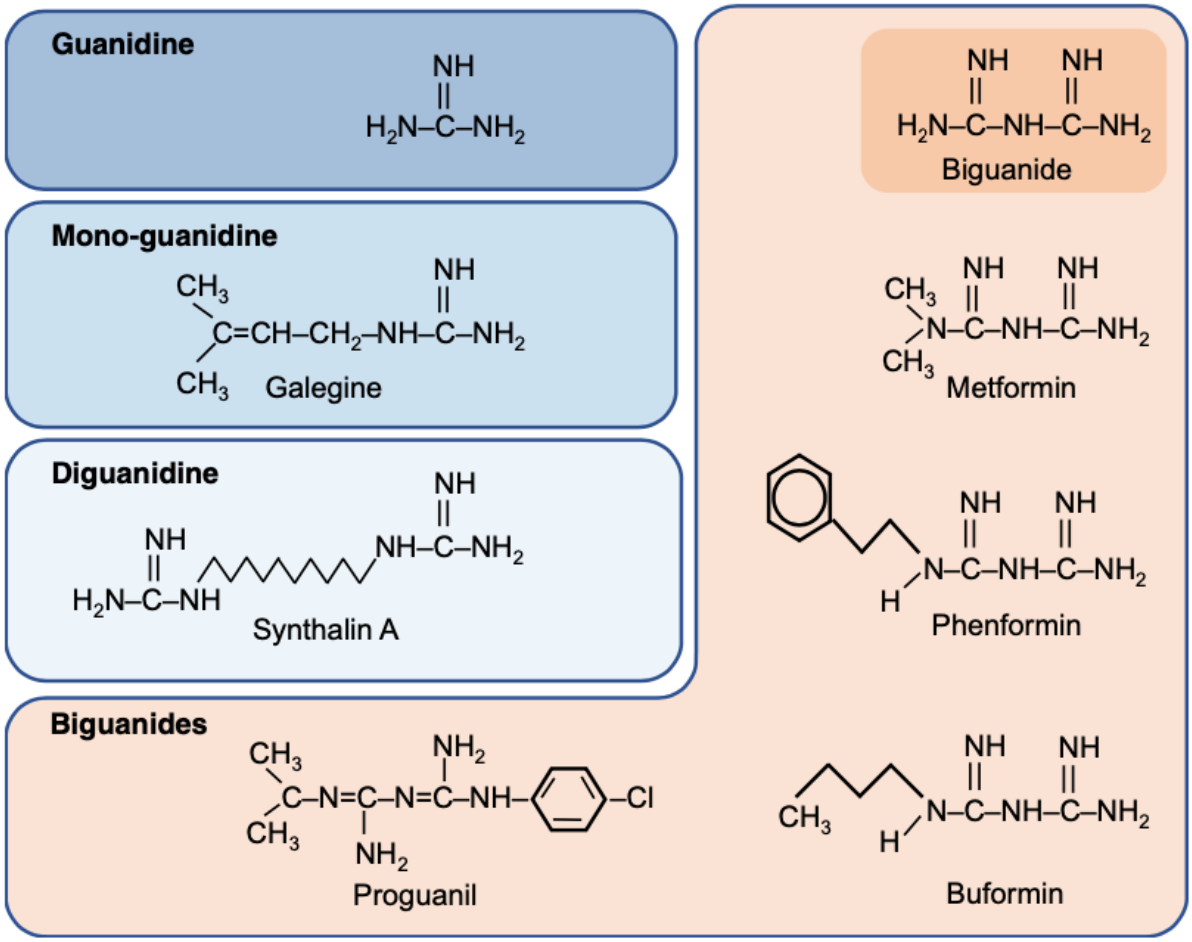

Figure 7. Structure of guanidine and related compounds (from: Bailey *et al.* 2017 [17])

It took many years to understand the utility of Met, only after the 1970s when other biguanides (phenformin and buformin) were withdrawn because of the links to the incidence of lactic acidosis. Only in 1995 Met employment was introduced in the USA, and after many studies on pharmacokinetics and pharmacodynamics, it was discovered that Met had lots of beneficial effects with a low risk ratio, therefore it began to be used as the preferred pharmacological therapy for type 2 diabetes. Indeed, Met has an extraordinary safety profile, as it improves glycemic control in diabetic patients and hardly causes hypoglycemia [17,18].

Met oral bioavailability is around 50% - 60%, the drug is mainly absorbed in the small intestine and accumulates in the liver. It is a stable drug, it does not bind to plasmatic proteins, and is

rapidly excreted unmodified in urines. The biological half-life ($t_{1/2}$) of Met is about three hours, and the maximal recommended dosage is of 2,5 grams per day.

Even though the pharmacologically active dose is high (0,5 to 2g/day), Met is well tolerated and used as antidiabetic drug since the side effects spontaneously resolve [19]. Patients receive doses from 1g/day to 2g/day, and this results in a plasma concentration from 0,1mg/l to 4mg/l. In healthy subjects who received an oral treatment of 1g Met, plasma concentrations reached 25µM within 3 hours. As regards the *in vivo* studies, it has been observed that treated rats with *ad libitum* access to Met dissolved in drinking water had inconsistent plasma concentrations, likely due to differences in drinking and gut absorption [18].

Several studies reported that Met can prevent or reduce the progression from prediabetes to type 2 diabetes, but it can also be used to treat gestational diabetes [17]. Met action on the reduction of hematic glucose levels is associated to potential beneficial effects on hematic lipid profiles and improvements in the macro- and micro-vascular parameters. Indeed, it can exert its beneficial effects in case of dyslipidemia as Met administration can decrease levels of LDL and increase the hematic concentration of HDL. Met can also exert an anti-inflammatory effect with consequent beneficial for what concerns the prevention of - for examples - cardiovascular complications. Moreover, Met does not lead to a weight increase and reduces the hyperglycemia, useful to contrast insulin-resistance and the related clinical implications. Typically, Met reduces basal hyperglycemia from 1 to 3 mmol/l and A_{1c} hemoglobin (HbA_{1c}) from 1 to 2%. It is to note that this drug alone cannot markedly decrease glycemia. It also seems that Met requires insulin to diminish the hematic glucose levels, even though this drug does not stimulate insulin secretion but only reduces insulin-resistance. As before mentioned, the principal glucose lowering effects of Met are attributed to an inhibition of hepatic glucose production and an increase in glucose utilization in skeletal muscle [20–23]. Beyond the type 2 diabetes, Met has also been shown to have beneficial effects on multiple

other disorders such as cancer, anxiety, polycystic ovary syndrome, cardiovascular and Alzheimer diseases [17,24–27]. As regards diseases of the musculoskeletal system, Met treatment has been shown to preserve skeletal muscle from cardiotoxin damage by protecting myotubes from necrosis without influencing muscle regeneration [28]. Furthermore, it has been reported that Met treatment can improve muscle function and diminish neuromuscular deficits in a murine model of Duchenne Muscular Dystrophy and delay SCs activation maintaining a quiescent, low metabolic SCs state. Conversely, it has been demonstrated that metformin treatment impairs muscle function through the regulation of myostatin in skeletal muscle cells via AMPK-FoxO3a-HDAC6 axis [29–31].

2. AIM OF THE STUDY

Since 1999, considering its anabolic effects, insulin has been inserted in the list of the substances and methods banned by the World Anti-Doping Agency (WADA) [32,33]. Therefore, insulin assumption by healthy athletes is not allowed, except for those affected by type 2 diabetes [34]. Even though few data on insulin assumption by healthy athletes are available to date, some evidence suggest that insulin abuse is common among body builders that aim to increase muscle mass and strength.

Particular attention must be paid on molecules such as oral antidiabetic drugs that stimulate, amplify, or modulate insulin secretion or its biological effects, but are not inserted in the prohibited substances list. Therefore, these drugs could represent an alternative to insulin for those athletes who want to take advantage of the hormone action on skeletal muscle to enhance their physical performance.

The use of oral antidiabetics as abuse substances is not only related to the stimulation of insulin secretion, but also to the influence on the number of ß-pancreatic cell, increase in sensibility and activity of insulin on target cells and tissues, greater use of peripheral glucose and activation of the proliferator-activated receptor gamma (PPARγ).

Unfortunately, less is known about the effects of oral antidiabetic drugs on muscle in terms of physical performance. Indeed, all the available information come from studies conducted on patients and in literature there are not enough data that can be used to evaluate the possible effects of oral antidiabetics on healthy skeletal muscle and related physical performances.

Since Met is not inserted in the list of prohibited substances and ameliorates insulin sensibility by increasing glucose uptake and use without causing hypoglycemia neither in diabetic patients nor in healthy subjects, it can be used by non-diabetic athletes to enhance physical performance without falling into risk of positive doping test and side effects.

For this reason, in the first part of the study we aimed to investigate the effects of Met on physical performance *in vivo* on a murine model to clarify if this drug could be considered a doping substance.

Later, to better understand the effects of Met treatment on skeletal muscle observed in the *in vivo* study and to elucidate by which mechanism it acts, we decided to analyze Met effects on C2C12 cells, an *in vitro* model that allowed us to study the outcomes of the drug treatment on proliferating, differentiating myoblast and on myotubes [35].

At the same time, with the *in vitro* experiments we intended to clarify the effects of Met on muscle metabolism, as recent studies reported controversial Met actions on skeletal muscle. Some stated that Met administration could prevent from muscle hypotrophy subsequential to aging or neuromuscular diseases such as Duchenne muscular dystrophy [29], while others reported an impairment of muscle function through the regulation of myostatin in muscle cells [31], secondary to Met treatment.

3. MATERIALS AND METHODS

3.1. *In vivo* experiments

3.1.1. Animals and pharmacological treatment

Twenty-four two-month-old male Wistar rats weighing 250 g (Harlan Laboratories, San Pietro al Natisone, Udine, Italy) were housed in groups of two or three in polycarbonate cages with ad libitum access to food and water and maintained in a controlled environment (12:12 light–dark cycle, room temperature 20-24° C, and humidity 50-60%). They were allowed 1 week of acclimatization before the experiment began. Institutional ethical committee approval was obtained for this study; all experimental procedures were performed in accordance with EC Directive 86/609/EEC and Italian law regulating experiments on animals (*Figure 8*).

Figure 8. Male Wistar rat.

The animal experimentation was conducted in the animal enclosure of the Neuroscience Institute Cavalieri Ottolenghi (NICO), adjacent to the hospital San Luigi Gonzaga in Orbassano.

The following analyses were carried out in the Pharmacology laboratory of the Department of Clinical and Biological Sciences.

Animals were submitted to physical exercise by using a five-lane motorized rodent treadmill (2Biological Instruments) connected to the software SEDACOM, that allowed us to set up the training protocol and analyze the outcomes (*Figure 9a and 9b*). For each animal it was possible to record different parameters such as covered distance, effective time taken, speed, so that the physical performance of every rat could be evaluated as good as possible.

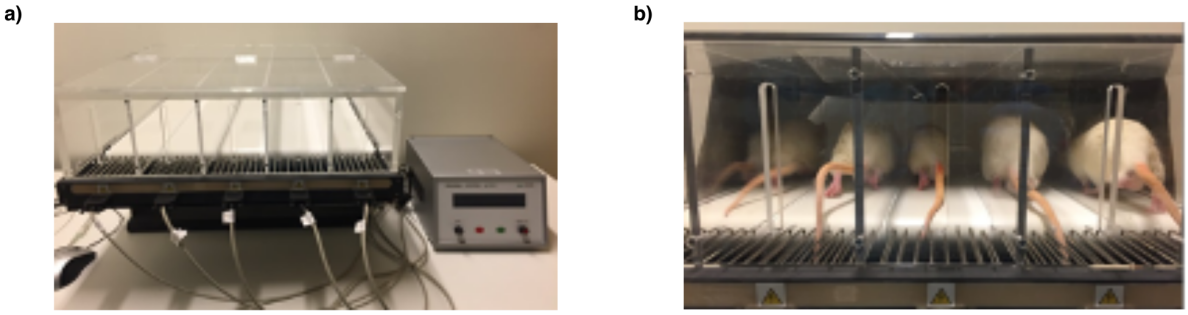

Figure 9. Motorized rodent treadmill (a). Rats during physical exercise (b).

The drug used was Met (metformin hydrochloride, 98% - Bosche Scientific), which the rats received dissolved in the drinking water with a daily dose of 250mg/kg, based upon previous reports [36].

Our pilot study showed that rats consumed *circa* 35ml water per day and Met addition did not influence water consumption. Water and Met were changed daily, and the dose adjusted to weight gain each week. The treatment was maintained until the sacrifice of the animals.

3.1.2. Experimental protocol

3.1.2.1. Preliminary phase

This step was fundamental to divide the twenty-four rats into the five experimental groups. In this adaptive phase, the animals were randomly split into five groups and each of them was exposed to handling and to a treadmill run at a speed of 25cm/sec, 5 minutes a day, for five days (*Figure 10*). This phase allowed us both to identify the animals less willing to run and to let the rats become confident with the type of exercise. The animals with very low propensity to run were inserted in the sedentary group.

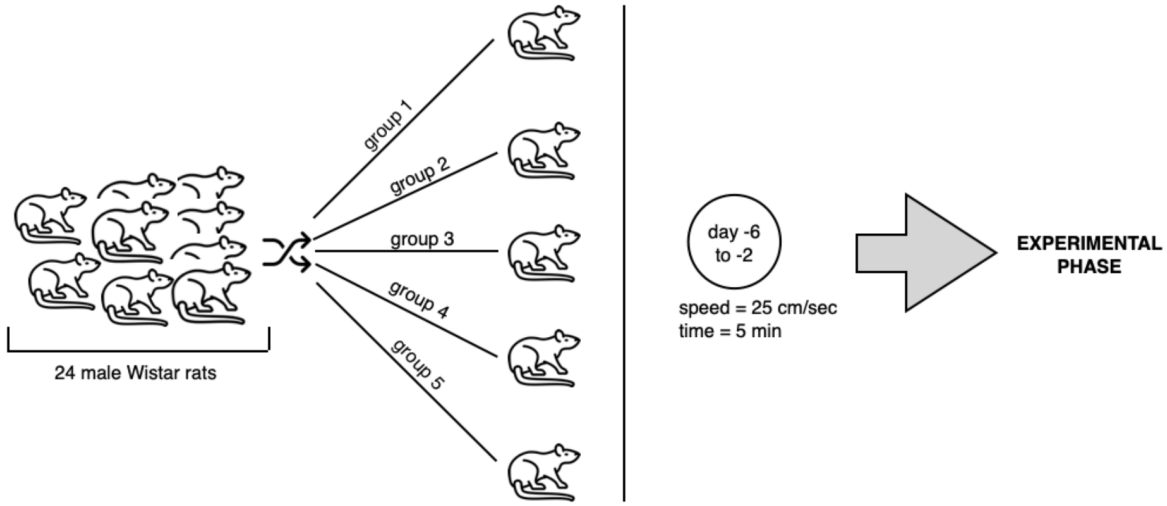

Figure 10. Preliminary phase.

3.1.2.1. Experimental phase

Rats were divided into five groups and treated as follows:

Group I: sedentary control (*SED,* n=4,). Rats were placed on a stationary treadmill daily for 5 min.

Group II and III: control. Untreated rats (*C*-, n=5) and treated rats (*C*+, n=5) that received Met dissolved in their drinking water for the entire experimental period. Both groups were placed on a stationary treadmill daily for 5 min.

Group IV and V: exercise training rats (*EX-, n=5*) and exercise training rats that received Met dissolved in their drinking water for the entire experimental period (*EX+, n=5*). Both groups conducted training on treadmill daily for 8 weeks.

All experimental groups except SED were submitted to graded endurance exercise (GEE) as described below.

Animals were weighted once a week to evaluate the increase in body mass and to determine the correct Met dose to administer. Food intake was evaluated twice a week to evaluate the potential anorexic effect of exercise and Met. We also evaluated daily the water consumption, to observe the possible effects of exercise and Met, but also to determine the appropriate drug dose for each treated group. After 8 weeks, all the animals were sacrificed 24 h after the last training session with an excess of anesthetic, composed of 5% isoflurane associated with a mixture of oxygen and nitrous oxide (*Figure 11*).

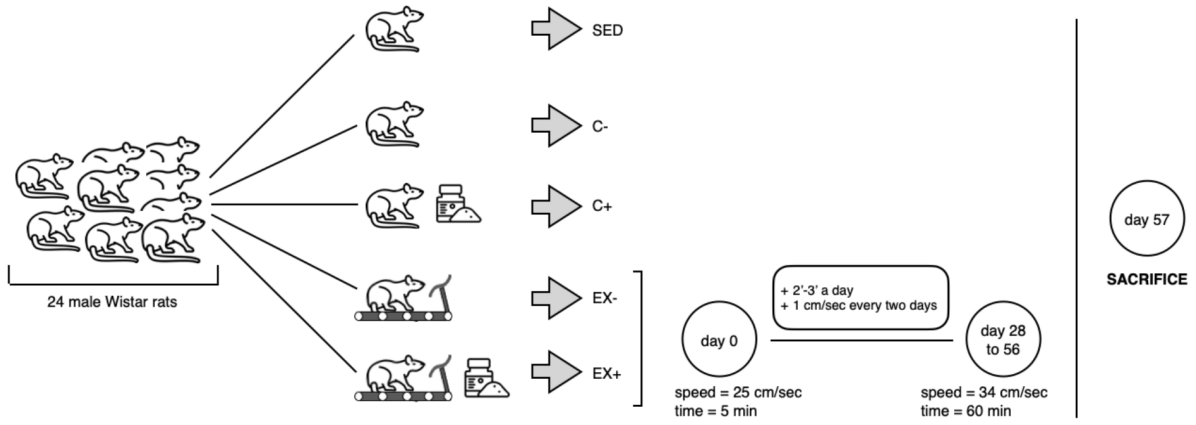

Figure 11. Experimental phase.

3.1.2.3. Training protocol

The training protocol consisted in daily treadmill run sessions, submitting rats to a moderate exercise [37–40]. The training protocol was carried out for all the experimental period, 5 days per week, at the same time each day. Mild electric shocks were used to motivate rats and to ensure a continuous run.

The intensity of exercise was lower in the first week, consisting of a run at a speed of 25 cm/sec for 5 minutes at zero inclination. Thereafter, the duration of the treadmill run increased (2-3 minutes) daily and the speed augmented by about 1cm/sec every two days, until they train for 60 minutes/day at a speed of 34 cm/sec with no inclination. These last parameters were maintained from the fifth week until the end of the experimental period, which globally lasted 8 weeks (*Table 2*).

After every run, the treadmill was cleaned with 70% ethanol solution before the next set of rats was put on the treadmill.

Week	Belt speed (cm/sec)	Inclination (degrees)	Total time (min)
1	25	0	5
2	27	0	15
3	30	0	30
4	32	0	45
5	34	0	60
6	34	0	60
7	34	0	60
8	34	0	60

Table 2. Rats' exercise training protocol on treadmill

3.1.2.4. Graded Endurance Exercise (GEE) test

The GEE test was performed to evaluate the effects of training, Met and their combination on the rats' physical performance. This test consisted in a treadmill run at an initial speed of 8 cm/sec for three minutes with a progressive increase of about 8 cm/sec every three minutes. GEE ended when the animals reached their maximal resistance and cannot run anymore, as judged by the rat spending more than 20 consecutive seconds on the electrical stimulus and resistance to mechanical prodding [41].

All rats were submitted to this test, except for the SED group, three times during the whole experimental period: the day before the beginning of the training protocol (GEE I), the 28th day (GEE II) and the 54th day (GEE III) of the experimental period. The last GEE was performed 48 hours before the sacrifice of the animals (*Figure 12*).

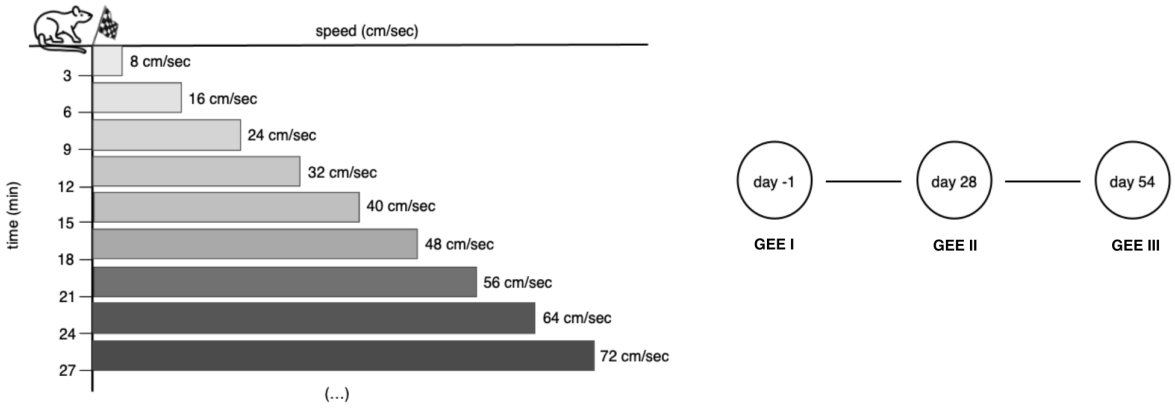

Figure 12. Graded Endurance Exercise (GEE) protocol.

3.1.3. Sample collection

At the end of the experimental period, all rats underwent a surgical intervention to collect gastrocnemius from each back limb. Before their sacrifice, rats were anesthetized, and then an incision was made from the popliteal fossa to the calcaneus to get access to the gastrocnemius (*Figure 13a and 13b*). A longitudinal incision was made to expose the muscle, locate the reference tendinous insertions, and collect gastrocnemius. Every muscle was weighed, split into two parts, immediately frozen in liquid N_2, and stored at -80°C until processing and analysis.

After the rats' sacrifice, blood samples were also collected in an appropriate test tube for serum separation.

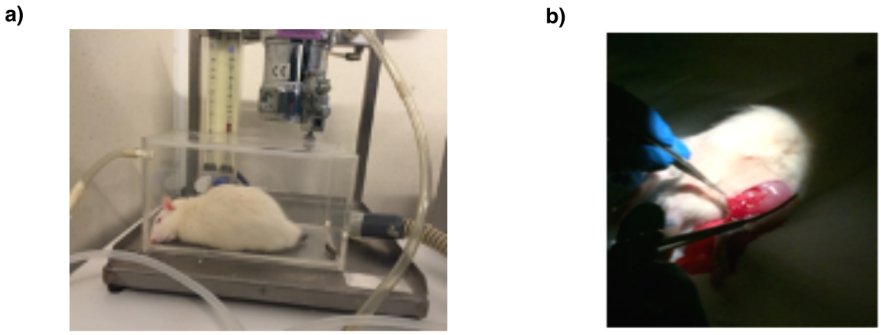

Figure 13. Anesthetic administration (a). Gastrocnemius collection (b).

3.1.4. Analytical methods

3.1.4.1. Serum extraction and blood analysis

Blood samples were centrifuged at 2800 rpm for 10 minutes at 4°C using a Heraeus Megafuge 16R centrifuge (Thermo Scientific) to obtain serum. Samples were then stored at -20°C until their use. Blood analysis was performed at the Laboratorio Analisi of "Centro Antidoping Alessandro Berinara". The following parameters were evaluated:

- ALT (U/L)
- AST (U/L)
- Total cholesterol (mg/dl)
- HDL cholesterol (mg/dl)
- Creatinine (mg/dl)
- Glucose (mg/dl)
- LDH (U/L)
- CK-MB (U/L)
- Myoglobin (ng/dl)
- C-reactive protein (mg/dl)
- Triglycerides (mg/dl)
- Urea (mg/dl)

3.1.4.2. Total muscle lysate and mitochondrial fraction

Muscle samples were homogenized in RIPA lysis buffer (150mM NaCl, 1.0% IGEPAL® CA-630, 0.5% sodium deoxycholate, 0.1% SDS, 50mM Tris, Sigma-Aldrich) supplemented with protease inhibitor cocktail 100X (Cell Signaling), by using a Potter homogenizer and then centrifuged at 16100 xg for 30 min at 4℃. The supernatant was collected and stored at -80℃. Mitochondrial fraction was extracted as described by Penna *et al.* [42], starting from muscle samples.

Protein concentrations of muscle total lysate and mitochondrial extract were determined by Bradford colorimetric assay (Bio-Rad) [43].

3.1.4.3. Myokines assay

For a quantitative evaluation of myokines in plasma and in muscle total lysate, we used the kit Milliplex® Map-Rat Myokine Magnetic Bead Panel (EMD Millipore), based on the Luminex xMAP technology, that allows to screen in the same sample and at the same time a panel of myokines and identify for each of them their involvement in conditions of rest, exercise, and treatment (associated or not with physical activity).

The Luminex® technology, using specific concentrations of two fluorescent pigments can get 100 sets of labeled microspheres, each of them covered by a specific primary antibody capable of binding to a specific analytic contained in the sample. Once the analytic binds to the microsphere, after an antigen-antibody reaction, a biotinylated primary antibody is added to the system and the reaction is completed by adding to the mixture streptavidin conjugated with phycoerythrin (red pigment).

All samples are then read with MAGPIX® (Millipore): the microspheres go rapidly through the first laser that excites the fluorescent pigments, marker of each microspheres' set, while the second laser excites the phycoerythrin conjugated to streptavidin.

Lastly, a processor system identifies the signals emitted and quantifies the analytics concentration based on the number of fluorescent signals (*Figure 14*).

Our kit could identify 12 myokines: brain-derived neurotrophic factor (BDNF), erythropoietin (EPO), interleukin-15 (IL-15), fibroblast growth factor 21 (FGF21), fractalkine (FKN), interleukin-6 (IL-6), follistatin like 1 (FSTL-1), myostatin (MSTN/GDF8), irisin, leukemia inhibitory factor (LIF), osteocrin, secreted protein acid and cysteine rich (SPARC).

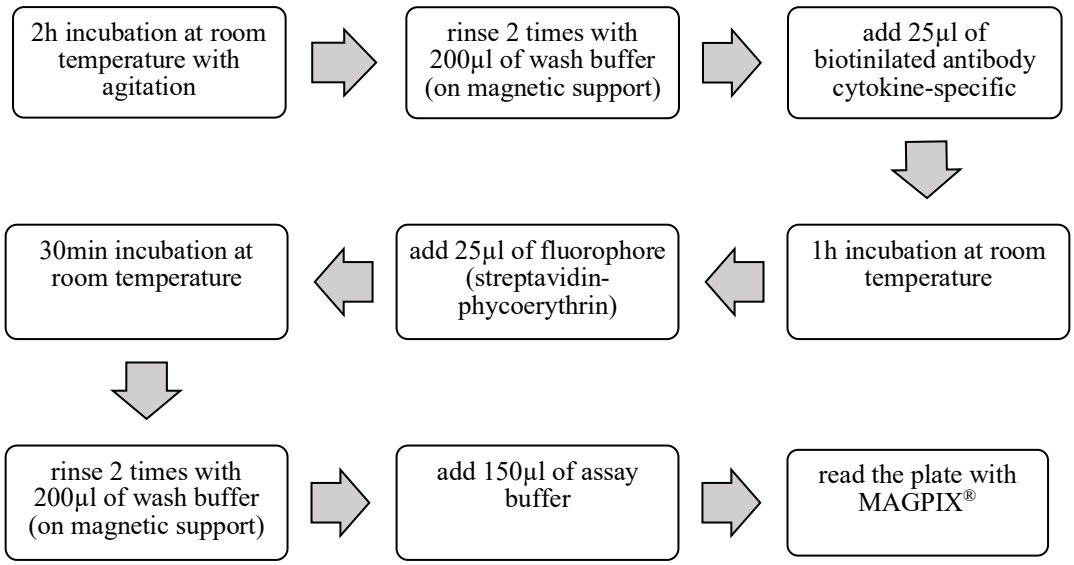

Figure 14. Myokines assay protocol.

3.1.4.4. Western Blot (WB)

Protein extracts from total muscle lysates (40µg) and mitochondrial fraction (2,5 µg) were separated by SDS-PAGE. Gels were transferred to membranes, saturated with blocking solution (5% milk and 0.1% Tween-20 in PBS), and incubated with the suitable primary antibody (*Table 3*) overnight at 4℃. The membranes were then rinsed three times and incubated with the appropriate concentrations of anti-mouse or anti-rabbit secondary antibody conjugated with horseradish peroxidase for 1h at room temperature. Blots were developed with Clarity Western ECL Substrate (Bio-Rad) using ChemiDoc™ Touch Image System (Bio-Rad). Densitometric analysis was performed using ImageLab Software. Non-phosphorylated

proteins were normalized to GAPDH or vinculin. Phosphorylation level is presented as the *ratio* between phosphorylated and total protein.

ACCß	rabbit	1:1000	Cell Signaling	3662
p-ACC (Ser79)	rabbit	1:1000	Cell Signaling	3661
AKT	mouse	1:2000	Cell Signaling	2920
p-AKT (Ser473)	rabbit	1:1000	Cell Signaling	9271
AMPK	rabbit	1:1000	Cell Signaling	2532
p-AMPK (Thr172)	rabbit	1:1000	Cell Signaling	2535
Cytochrome C	mouse	1:1000	Invitrogen	45-6100
GAPDH	mouse	1:25000	Ambion	AM4300
GSK3ß	rabbit	1:1000	Cell Signaling	9315
p- GSK3ß (Ser9)	rabbit	1:1000	Cell Signaling	9323
mTOR	mouse	1:1000	Cell Signaling	4517
p-mTOR (Ser2448)	rabbit	1:1000	Cell Signaling	2971
Myf5	rabbit	1:10000	Abcam	ab125078
MYH1/2	mouse	1:500	Santa Cruz	sc-53088
MyoD	mouse	1:500	BD Pharmingen	554130
PAX7	rabbit	1:1000	Abcam	ab34360
PGC-1α	rabbit	1:1000	Abcam	ab54481
p21	mouse	1:500	Santa Cruz	sc-6246
p70S6K	mouse	1:1000	Santa Cruz	sc-8418
p-p70S6K (Thr389)	mouse	1:1000	Cell Signaling	9206
vinculin	mouse	1:1000	Santa Cruz	sc-25336

Table 3. List of employed primary antibodies for Western Blot analysis.

3.2 *In vitro* experiments

3.2.1 Cell culture and treatments

C2C12 myoblasts (American Type Culture Collection, CRL-1772, kindly gifted by the unit of General Pathology of our Department) were seeded on dishes at 37˚C with 5% CO_2 in growth medium (GM, High Glucose DMEM), supplemented with 10% fetal bovine serum, 1% penicillin-streptomycin, 4mM glutamine and 1mM sodium pyruvate (*Figure 15*).

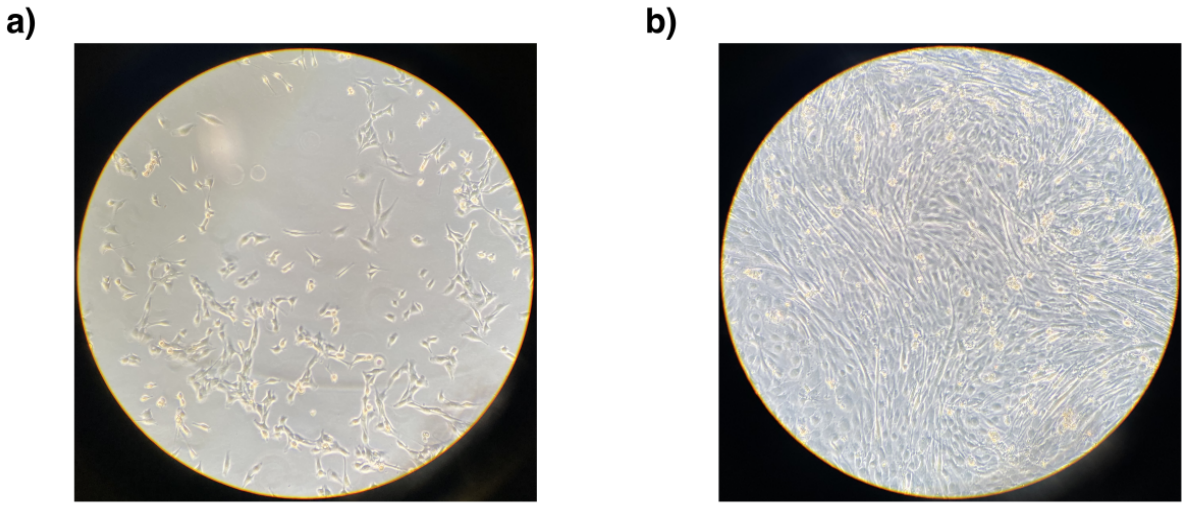

Figure 15. C2C12 cells: undifferentiated (a) and differentiated (b).

For proliferation experiments, C2C12 myoblasts were cultured in GM and treated with or without Met at the final concentrations of 250µM, 1mM and 10mM for 24h, 48h and 72h. Met was added fresh to the medium every 24h.

To evaluate the effects of Met on cell differentiation, GM was replaced by differentiation medium (DM, 2% horse serum in High Glucose DMEM) when cells reached 80% confluence. The following 4 days, cells were treated with or without Met at the final concentration of 10mM. Met was added fresh to the medium every 24h.

For experiments on myotubes, proliferating myoblasts at ~ 80% confluence were induced to differentiate for 5-7 days by incubation in DM. The indicated concentrations of Met,

Compound C (CC) or lithium chloride (LiCl) were added at the end of the differentiation process and again every 24h, when cells were provided with fresh DM. Myotubes from different conditions were harvested at the indicated time points.

3.2.2 Cell proliferation assay

Cell proliferation was evaluated by using MTT colorimetric assay, in which the conversion of 3-(4,5-dimethylthiazol-2-yl)-2,5-diphenyltetrazolium bromide to insoluble tetrazolium by NAD(P)H-dependent cellular oxidoreductase was measured by recording the cell absorbance at 570 nm with a 96-well plate reader [44].

C2C12 myoblasts were seeded at 1000 cells/cm^2 in GM on 96-well plates. After 24h, absorbance of four plates was recorded to define the time point "0h". The remaining plates were treated with or without Met (final concentrations 250µM, 1mM, and 10mM) for 24h, 48h and 72h. Met was added fresh to the medium every 24h. Four replicates were analyzed at each time point, and an average of the values was calculated.

3.2.3 Measurement of cell toxicity

Cell toxicity was assessed by trypan blue (TB) exclusion test and lactate dehydrogenase (LDH) release in C2C12 myoblasts exposed to different concentrations of Met (250µM, 1mM, 10mM) for 24h, 48h and 72h.

The TB exclusion assay is based on the principle that viable cells possess intact cell membranes that exclude certain dyes, such as TB. We used a commercially available TB preparation (TB solution 0.4%, Sigma-Aldrich) to perform the counts. The percentage of cell

toxicity was calculated as the ratio between the number of total dead cells (stained) and total cells (stained and unstained) x100. Cells were counted by using a hemocytometer and a light microscope.

LDH release was determined in culture medium by using a photometric assay based on the conversion of pyruvic acid to lactic acid by this enzyme, in the presence of reduced NADH. Results were expressed as percentages of total LDH released by untreated cells (100%), which were lysed with PBS plus 5% Triton X-100.

3.2.4 Cell cycle FACS analysis

Myoblasts exposed to Met250µM, 1mM and 10mM for 24h, 48h and 72h were trypsinized, washed three times with PBS and fixed in 70% ethanol overnight at -20°C. The cells were further washed two times with PBS and incubated with 200µl staining solution containing 0,1mg/ml RNAse, 25µg/ml propidium iodide, 0,02% Triton X-100 for 40 min at 37°C. DNA content was measured by propidium iodide intensity by using a BD FACSVerse flow cytometer (BD Bioscience). The cell cycle phases were analyzed with 162 FlowJO10.5.3.

3.2.5 Western Blot

C2C12 myoblasts and myotubes were washed in the culture dish with ice-cold PBS and homogenized in RIPA lysis buffer (150mM NaCl, 1.0% IGEPAL® CA-630, 0.5% sodium deoxycholate, 0.1% SDS, 50mM Tris, Sigma-Aldrich) supplemented with protease inhibitor cocktail 100X (Cell Signaling). Samples were incubated in ice for 30 min with the lysis buffer and cell debris were separated by centrifugation at 14,000 rpm for 30 min at 4℃. The

supernatant was collected and stored at -80℃. Protein concentrations were determined by Bradford colorimetric assay (Bio-Rad) [43].

Total protein extracts (30µg) were then separated by SDS-PAGE. The next steps were performed as described for the *in vivo* study (see paragraph 3.1.4.4).

3.3 Statistical analysis

All data are presented as mean values±SD of at least four independent experiments. Statistical analyses were performed with t-test, one-way or two-way ANOVA, followed by Bonferroni or Tukey multiple comparison tests by using GraphPad Prism 8.0 software. The differences were considered significant with *$p < 0.05$, **$p < 0.01$, ***$p < 0.001$ and ****$p < 0.0001$.

4. RESULTS

4.1. *In vivo* study

The SED group was inserted in the experimental protocol to analyse potential effects of the GEE tests, in particular the last one performed 48h before the rats' sacrifice, on the studied parameters. For this reason, we first performed a t-test between SED and C- for each analysed parameter, that reported statistical differences only as regards alanine transferase (ALT), the main myogenic regulatory factors (MRFs) such as Myf5, MyoD, PAX7, and AMPK activation values.

4.1.1. Food consumption and body weight increase

We evaluated food consumption and the percentage of body weight increase to determine potential anorexic effects due to physical exercise or Met administration.

Food consumption was evaluated in each group two times a week, whereas body weight increase was evaluated for each rat once a week. Both the data were collected during the entire experimental period.

From the two-way ANOVA no differences emerged among groups, suggesting that neither physical exercise, Met treatment nor the association of them altered rats' food consumption and body weight (*Figure 16*).

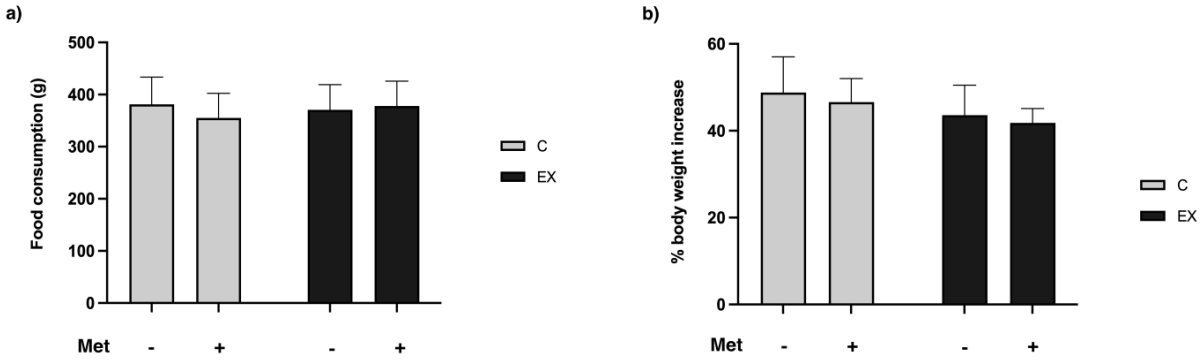

Figure 16. Evaluation of food consumption and body weight increase. No effect of physical training or Met administration on food consumption (a) and body weight increase (b) was reported by two-way ANOVA ($p>0.05$).

4.1.2. Muscle weight/body weight *ratio*

To point out the possible changes in muscle weight due to drug treatment and/or physical exercise, we compared each rat's muscle weight with the last measurement of its body weight. We evaluated for each muscle the muscle weight/body weight *ratio*.

Two-way ANOVA reported that drug administration accounted for the alterations observed in muscle weight (F (1,16) = 11.25, p = .004). Statistical differences emerged in C+ and EX+ groups compared with C- (*Figure 17*).

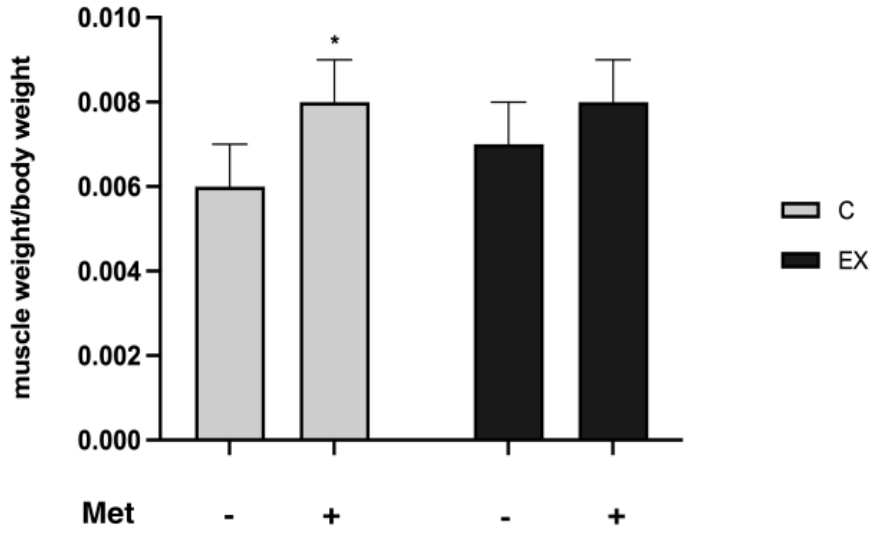

Figure 17. Evaluation of muscle weight/body weight *ratio*. Met administration increases the muscle weight/body weight *ratio*. Statistical analysis was performed using two-way ANOVA followed by Tukey test. * ($p<0.05$) for differences *versus* C-.

4.1.3. Physical performance

Rats were submitted to the GEE test at three different times of the experimental period, to evaluate how they perform an endurance exercise in conditions of drug administration, training, and association of them.

We evaluated the physical performance variations during the period under study by determining the average increase in the distance covered by each group at every subsequent GEE. We compared:

- GEE I and GEE II
- GEE II and GEE III
- GEE I and GEE III

EX and EX+ rats' performance was always significantly higher than C and C+. Two-way ANOVA reported that drug administration (F (1,16) = 10.34, p = .005) and training (F (1,16) = 332.1, p < 0.001) accounted for the improvement in performance observed by comparing GEE I with GEE II. Tukey post hoc test evidenced a significant increase in EX- and EX+ compared with C- and C+ respectively (*Figure 18a*).

As regards the comparison between GEE II and GEE III, two-way ANOVA evidenced an involvement of training (F (1,16) = 55.09, p < 0.001) and interaction (F (1,16) = 15.90, p = .001) in improving rats' physical performance. From multiple comparison emerged that both C+ and EX- increased their covered distance with respect to C- (*Figure 18b*).

From the last comparison (GEE I *versus* GEE III) two-way ANOVA reported that drug administration (F (1,16) = 7.511, p = .014), training (F (1,16) = 406.1, p < 0.001) and interaction (F (1,16) = 4.920, p = .041) accounted for the increase of exercised rats' (EX- and EX+) physical performance. The Tukey test evidenced a significant increase in EX- and EX+ compared with C- and C+ respectively (*Figure 18c*).

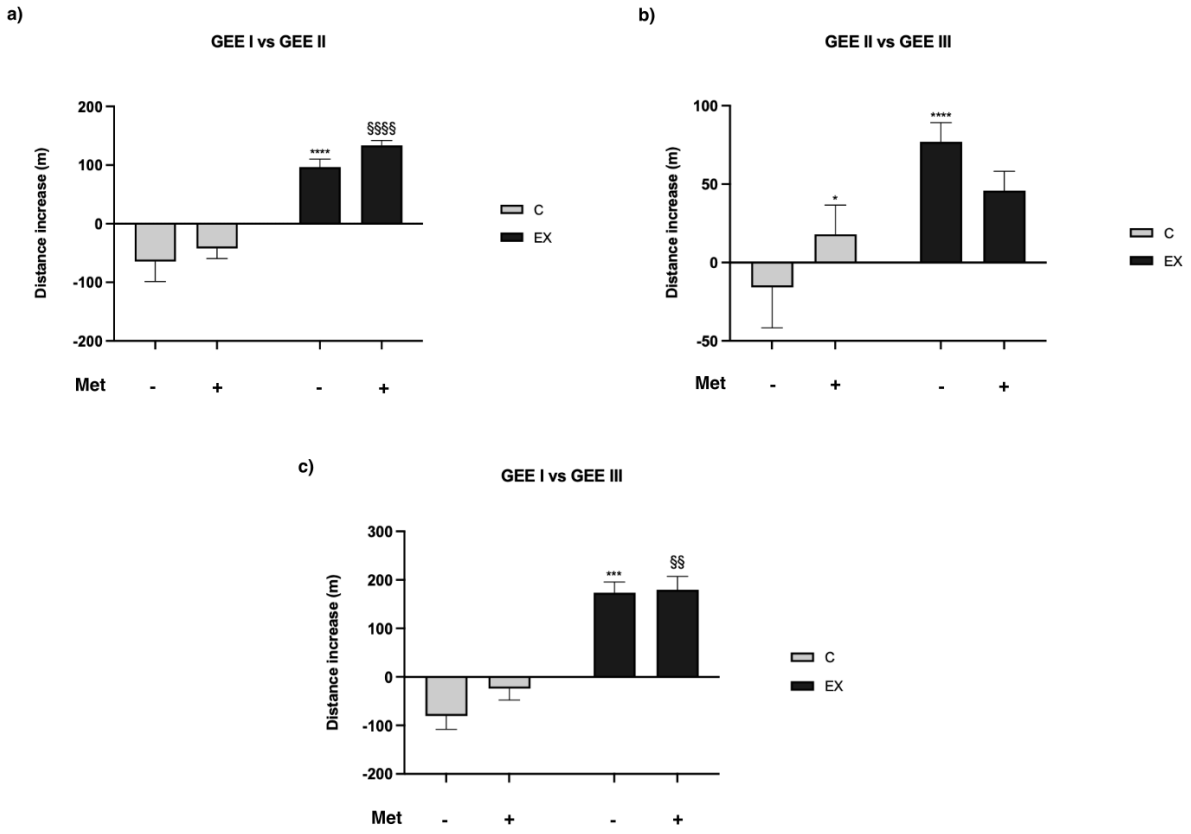

Figure 18. Comparison of the three GEE tests: evaluation of rats' physical performance. Met administration, training, and interaction influence rats' physical performance. Average increase in the distance covered by each group at every subsequent GEE was used to evaluate the performance, through the comparison between GEE I and GEE II (a), GEE II and GEE III (b), GEE I and GEE III (c). Statistical analysis was performed using two-way ANOVA followed by Tukey test. * ($p<0.05$), *** ($p<0.001$), **** ($p<0.0001$) for differences *versus* C-; §§ ($p<0.01$), §§§§ ($p<0.0001$) for differences *versus* C+.

We next performed a t-test within the control and the exercised groups, to evaluate the action of Met treatment on physical performance. Despite the control groups did not have a great physical performance, t-test reported a "late-positive effect" of Met administration in the comparison between the GEE II and GEE III ($p = .045$) and between the GEE I and GEE III ($p = .0084$) (*Figure 19b and 19c*).

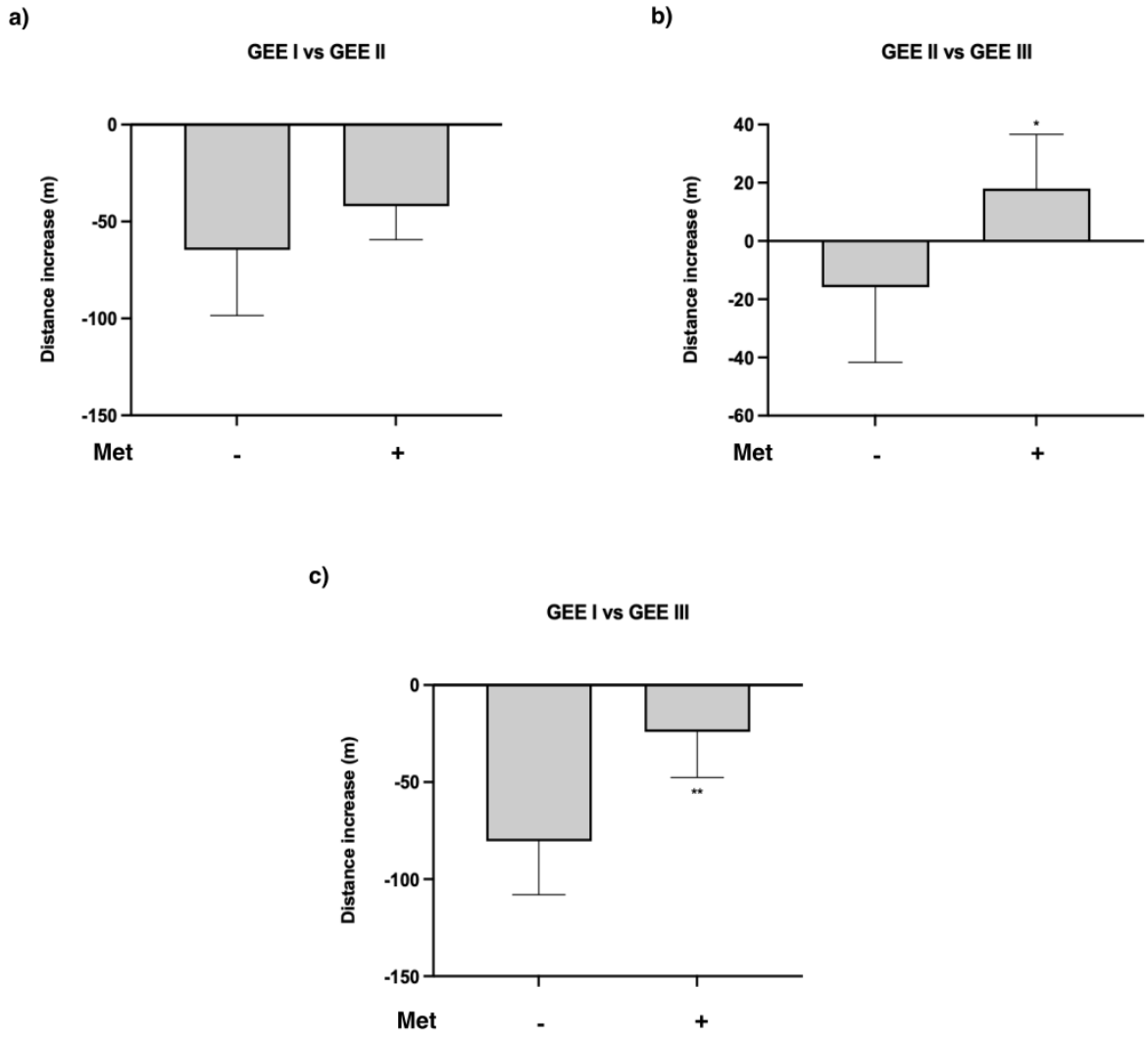

Figure 19. Comparison of the three GEE tests within the control groups (C- and C+). Met treatment increase C+ rats' physical performance. T-test was performed to evaluate statistical differences between GEE I and GEE II (a), GEE II and GEE III (b) and GEE I and GEE III (c). * ($p<0.05$), ** ($p<0.01$) for differences *versus* C-.

As regards the exercised groups, t-test reported an "early-positive effect" of Met treatment, evident in the comparison between the first and the second GEE ($p = .047$; *Figure 20a*). This effect was no more visible in the comparison between the second and the third GEE, as the EX- increase in the distance covered was higher than the EX+ ($p = .004$; *Figure 20b*). The t-test on GEE I *versus* GEE III reported no differences, as the same distance was covered at the end of the three GEEs (*Figure 20c*).

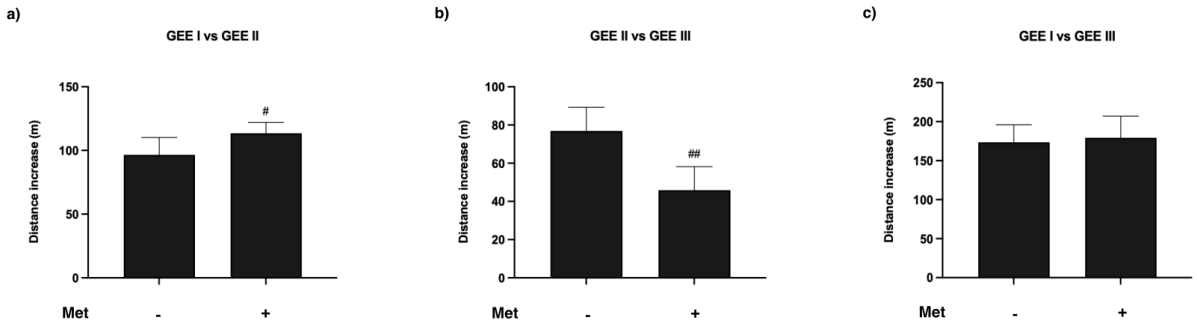

Figure 20. Comparison of the three GEE tests within the exercised groups (EX- and EX+). Met administration exerts an "early-positive effect" on EX+ rats' physical performance. T-test was performed to evaluate statistical differences between GEE I and GEE II (a), GEE II and GEE III (b), GEE I and GEE III (c). # ($p<0.05$), ## ($p<0.01$) for differences *versus* EX-.

4.1.3. Blood parameters

In *Table 4* are reported the results obtained from the blood analysis.

	C-	C+	EX-	EX+
ALT (U/L)	53,8 ± 9,88	48 ± 7,07	38,6 ± 12,36	31 ± 4,74
AST (U/L)	323,6 ± 75,49	249,8 ± 29,91	350 ± 89,20	263,8 ± 50,95
Total cholesterol (mg/dl)	54,4 ± 8,79	61,8 ± 7,40	56 ± 5,24	58,6 ± 6,80
Creatinine (mg/dl)	0,456 ± 0,02	0,450 ± 0,03	0,486 ± 0,06	0,464 ± 0,07
PCR (mg/dl)	0,01 ± 0	0,01 ± 0	0,01 ± 0	0,01 ± 0
Glucose (mg/dl)	259 ± 54,11	267 ± 47,44	308,4 ± 59,50	297,4 ± 37,27
Triglycerides (mg/dl)	125,8 ± 25,62	101,4 ± 39,21	122,2 ± 51,09	87,4 ± 34,90
HDL (mg/dl)	24 ± 2,74	28 ± 2,45	25,2 ± 0,84	25,2 ± 2,86
Urea (mg/dl)	48,6 ± 3,13	47,8 ± 5,85	45,8 ± 5,93	50,4 ± 5,59
CK-MB (U/L)	1794 ± 260,35	1670 ± 250,20	1606 ± 403,34	1208 ± 174,99
LDH (U/L)	2454,2 ± 410,96	2174,2 ± 185,66	2436,2 ± 681,21	1789,4 ± 236,22

Table 4. Blood parameters analysis

T-test performed to investigate possible differences between SED and C due to the last GEE test, indicated only a significant increase of ALT levels in C- with respect to SED (t (6) = 2.81, p = .031) (*Figure 21a*).

Two-way ANOVA performed to evidence statistical differences among controls and exercised rats, showed that training decreased ALT levels (F (1,14) = 14.10, p = .0021).

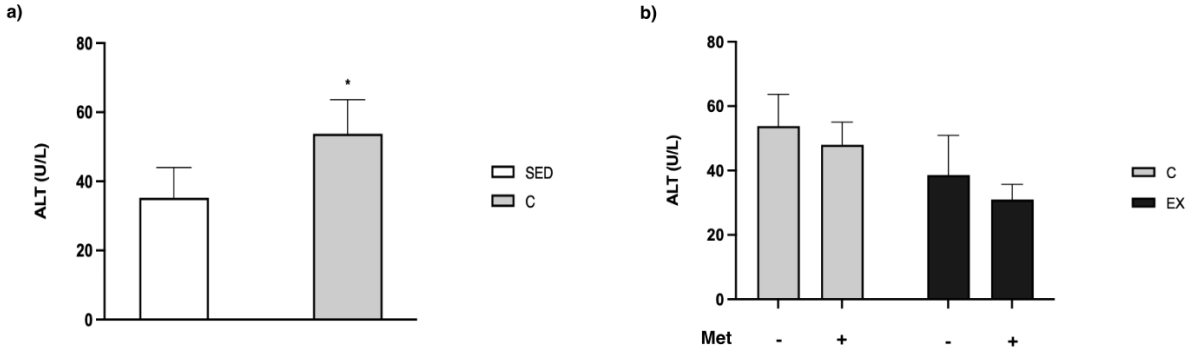

Figure 21. Blood ALT evaluation. (a) T-test was performed to evaluate possible differences between SED and C-. * ($p<0.05$) for differences *versus* SED. (b) Two-way ANOVA followed by Tukey test was performed among C-, C+, EX- and EX+: training F (1,14) = 14.10, p = .0021. No differences emerged from the Tukey post hoc test.

As regards aspartate transferase (AST), the results obtained showed that Met treatment reduced its levels (two-way ANOVA: drug administration F (1,16) = 7.46, p = .015) (*Figure 22*).

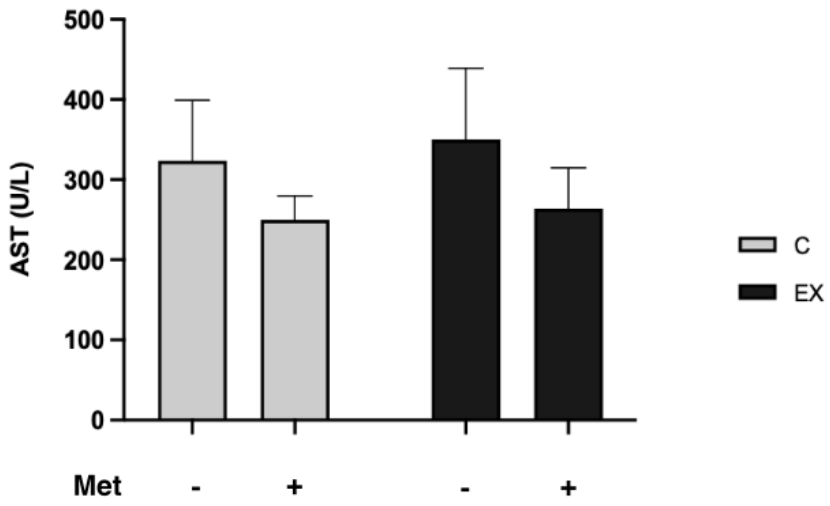

Figure 22. Blood AST evaluation. Two-way ANOVA followed by Tukey test was performed among C-, C+, EX- and EX+: drug administration F (1,16) = 7.46, p = .015. No differences emerged from the Tukey post hoc test.

Met treatment also led to variations in lactate dehydrogenase (LDH) levels, as evidenced by two-way ANOVA (F (1,16) = 5.94, p = .027) (*Figure 23*).

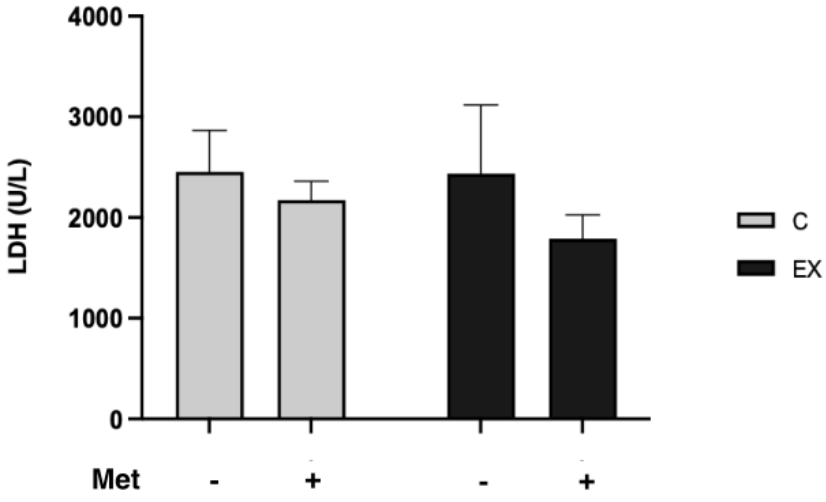

Figure 23. Blood LDH evaluation. Two-way ANOVA followed by Tukey test was performed among C-, C+, EX- and EX+: drug administration F (1,16) = 5.94, p = .027. No differences emerged from the Tukey post hoc test.

Creatine phosphokinase – MB (CK-MB) was modified by training (two-way ANOVA: F (1,16) = 6.53, p = .021) (*Figure 24*).

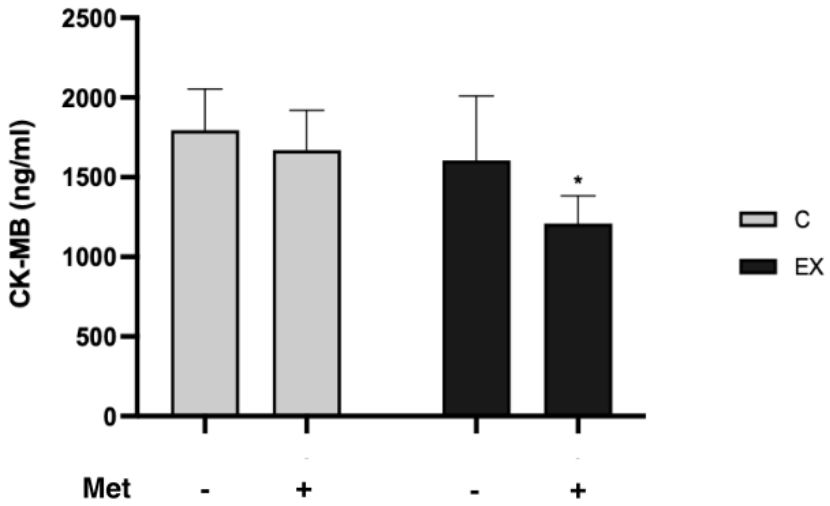

Figure 24. Blood CK-MB evaluation. Two-way ANOVA followed by Tukey test was performed among C-, C+, EX- and EX+: training F (1,16) = 6.53, p = .021. No differences emerged from the Tukey post hoc test.

As regards multiple comparisons among groups for blood parameters, the lack of significant differences is probably due to the scarce numerousness of the samples and the high SD of the values.

4.1.4. Myokines in serum and in total muscle lysate

A panel of 12 myokines was evaluated in samples of serum and total muscle lysate. As regards the myokines in serum, statistical differences emerged in irisin, fibroblast growth factor 21 (FGF21), osteocrin and secreted protein acidic and rich in cysteine (SPARC).

Two-way ANOVA reported that drug administration accounted for the increase in irisin (F (1,16) = 4.50, p = .050) and FGF21 (F (1,16) = 20.21, p = .0004). Nevertheless, Tukey's post-hoc test evidenced a meaningful difference only in FGF21 levels in C+ vs C- and in EX+ vs EX- (*Figures 25 and 26*).

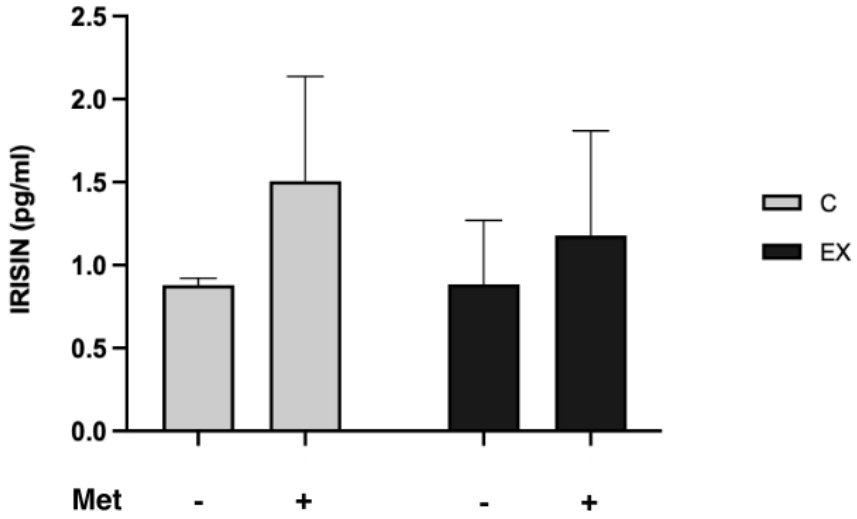

Figure 25. Evaluation of myokines in serum: irisin. Two-way ANOVA followed by Tukey test was performed among C-, C+, EX- and EX+: drug administration F (1,16) = 4.50, p = .050. No differences emerged from the Tukey post hoc test.

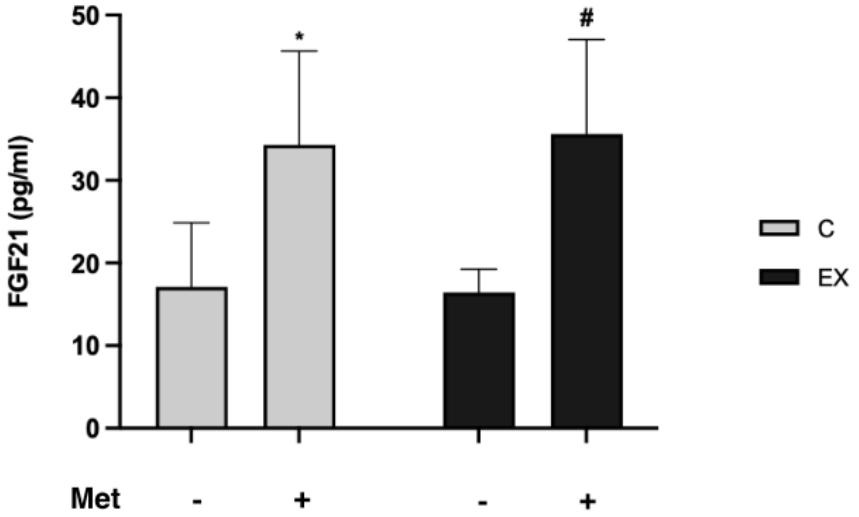

Figure 26. Evaluation of myokines in serum: FGF-21. Statistical analysis was performed using two-way ANOVA followed by Tukey test. * ($p<0.05$) for differences *versus* C-; # ($p<0.05$) for differences *versus* EX-.

Osteocrin serum levels were modulated by drug administration (F (1,16) = 7.796, p = .013), training (F (1,16) = 8.792, p = .009), and interaction (F (1,16) = 11.31, p = .004), as reported by the two-way ANOVA. Tukey's post-hoc test evidenced significant lower levels in C+ and EX- compared with C- (*Figure 27*).

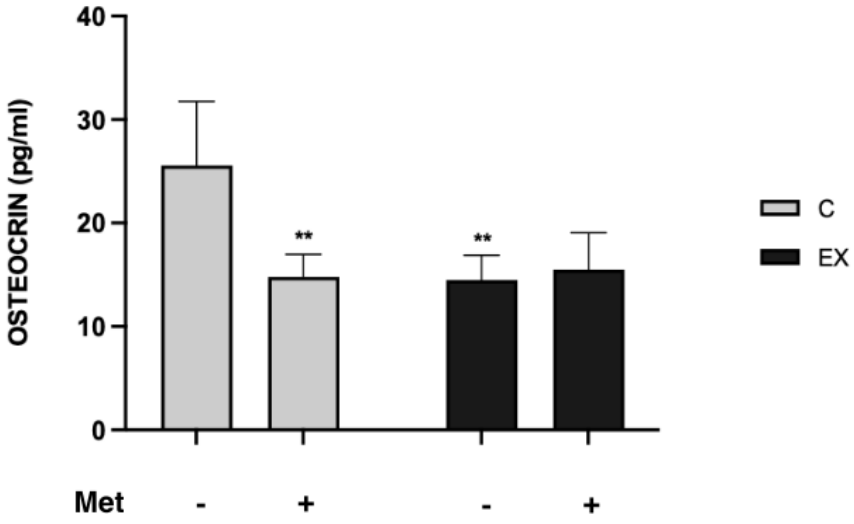

Figure 27. Evaluation of myokines in serum: osteocrin. Statistical analysis was performed using two-way ANOVA followed by Tukey test. ** ($p<0.01$) for differences *versus* C-.

As regards SPARC data, the two-way ANOVA pointed out that drug administration (F (1,16) = 7.072, p = .017) led to a serum increase of this myokine (*Figure 28*).

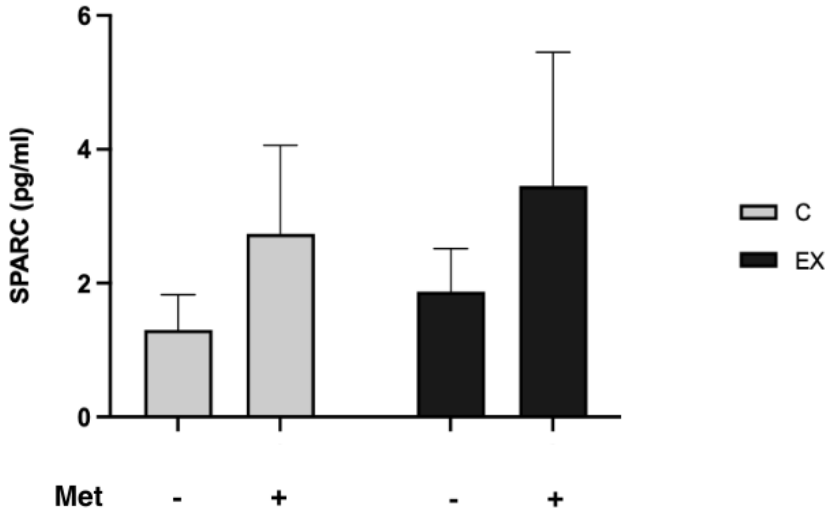

Figure 28. Evaluation of myokines in serum: SPARC. Two-way ANOVA followed by Tukey test was performed among C-, C+, EX- and EX+: drug administration F (1,16) = 7.072, p = .017. No differences emerged from the Tukey post hoc test.

The same analysis was conducted in total muscle lysate samples, but statistical differences emerged only in fractalkine. Two-way ANOVA reported that drug administration (F (1,16) = 68.66, $p < 0.0001$) and training (F (1,16) = 9.907, p = .004) accounted for the decrease of this protein in muscle tissue. Tukey post-hoc test evidenced significant differences in both C+ and EX- *versus* C-, and in EX+ *versus* EX- (*Figure 29*).

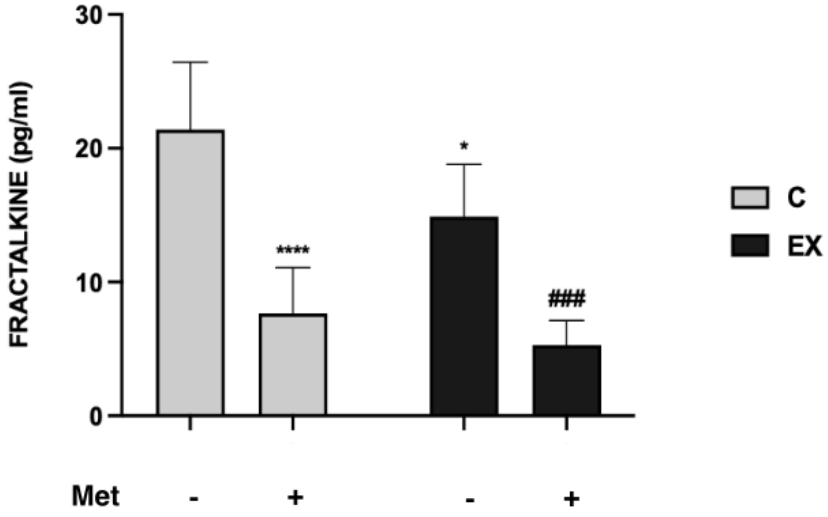

Figure 29. Evaluation of myokines in muscle: fractalkine. Statistical analysis was performed using two-way ANOVA followed by Tukey test. * ($p<0.05$), **** ($p<0.0001$) for differences *versus* C-; ### ($p<0.001$) for differences *versus* EX-.

As for blood parameters, also for some of the analysed myokines, the lack of significant differences among groups (Tukey test) could be due to the scarce numerousness of the samples and the high SD of the values.

4.1.5. Western Blot analysis on total muscle lysate

With the WB technique, we analysed the expression of some muscle proteins involved in signalling pathways that can be modulated by physical exercise or Met treatment.

We evaluated the expression of myosin heavy chain (MYH1/2), a muscle structural protein, as well as the levels of the main MRFs. We then analysed AMPK and some factors involved directly and indirectly in its pathway such as ACCß, PGC-1α, GSK3ß, AKT and mTOR.

Muscle mitochondrial fraction was also analysed, in particular the expression levels of PGC-1α and Cytochrome C (Cyt C).

MYH1/2 levels were higher in C+ and EX- respect to C-, and in EX+ compared with EX-. Two-way ANOVA showed that drug administration (F (1,20) = 585.2, $p < 0.0001$), training (F (1,20) = 43.53, $p < 0.0001$) and interaction (F (1,20) = 23.90, $p < 0.0001$) intervene in modulating MYH1/2 expression (*Figure 30*).

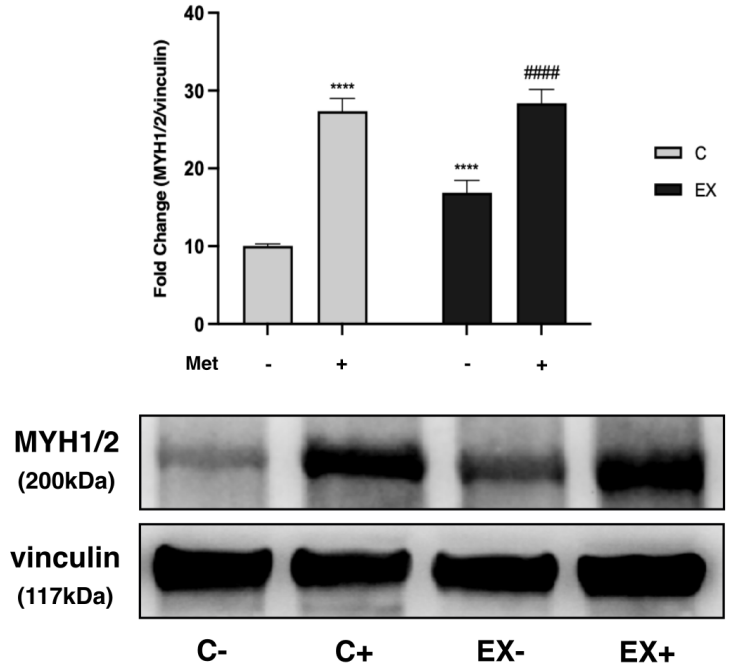

Figure 30. Western Blot analysis on MYH1/2 expression in total muscle lysate. Representative images of WB for MYH1/2 in total muscle lysates. Histograms represent band density expressed as fold change compared with C-. Vinculin was used as loading control. Data are representative of four independent WB. Statistical analysis was performed using two-way ANOVA followed by Tukey test. **** ($p<0.0001$) for differences *versus* C-; #### ($p<0.0001$) for differences *versus* EX-.

As regards the MRFs, t-test performed to compare SED and C- showed an increase in C- for all the myogenic factors analysed (t (10) = from 7.7 to 13.7, $p < 0.0001$).

Myf5 expression increased in C+ and decreased in EX- respect to C-. Myf5 levels were higher in EX+ than in C+ and EX-. Two-way ANOVA evidenced that drug administration (F (1,20) = 673.6, $p < 0.0001$) and interaction (F (1,20) = 35.77, $p < 0.0001$) were involved in Myf5 modulation (*Figure 31*).

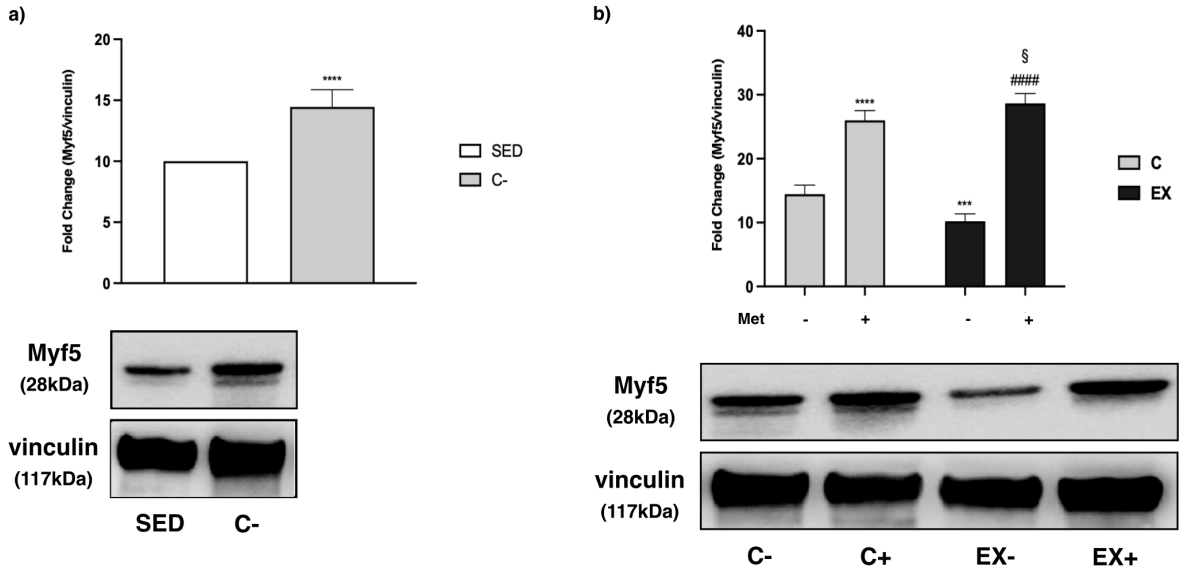

Figure 31. Western Blot analysis on Myf5 expression in total muscle lysate. Representative images of WB for Myf5 in total muscle lysates. Vinculin was used as loading control. Data are representative of four independent WB. (a) Histograms represent band density expressed as fold change compared with SED. Statistical analysis was performed using the t-test. **** ($p<0.0001$) *versus* SED. (b) Histograms represent band density expressed as fold change compared with C-. Statistical analysis was performed using two-way ANOVA followed by Tukey test. **** ($p<0.0001$) for differences *versus* C-; #### ($p<0.0001$) for differences *versus* EX-.

For what concerns MyoD levels, the only difference emerged from the multiple comparisons concerns the higher expression in EX- with respect to C-. Two-way ANOVA reported that training (F (1,20) = 17.36, p = .0005) and interaction (F (1,20) = 9.104, p = .0068) alter MyoD levels in total muscle lysate (*Figure 32*).

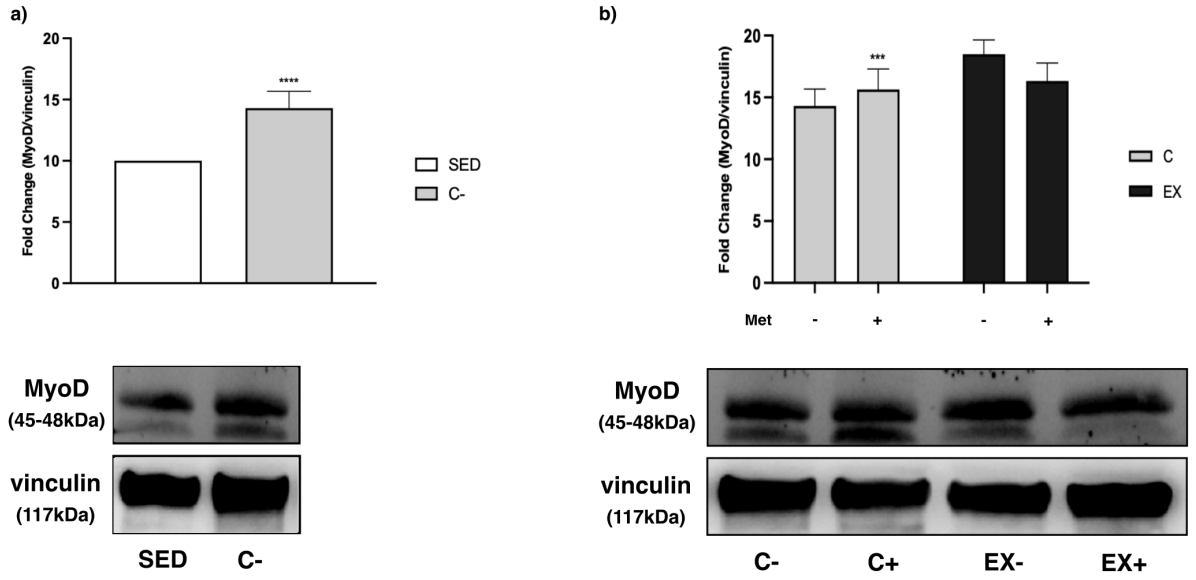

Figure 32. Western Blot analysis on MyoD expression in total muscle lysate. Representative images of WB for MyoD in total muscle lysates. Vinculin was used as loading control. Data are representative of four independent WB. (a) Histograms represent band density expressed as fold change compared with SED. Statistical analysis was performed using the t-test. **** ($p<0.0001$) *versus* SED. (b) Histograms represent band density expressed as fold change compared with C-. Statistical analysis was performed using two-way ANOVA followed by Tukey test. *** ($p<0.001$) for differences *versus* C-.

PAX7 decreased in the trained groups, in particular its levels were lower in EX- and EX+ compared with C- and C+ respectively. Moreover, C+ resulted significantly increased with respect to C-. Two-way ANOVA reported that drug administration (F (1,20) = 11.72, p = .0027), training (F (1,20) = 108.2, $p < 0.0001$) and interaction (F (1,20) = 6.902, $p < 0.0001$) modulate PAX7 expression (*Figure 33*).

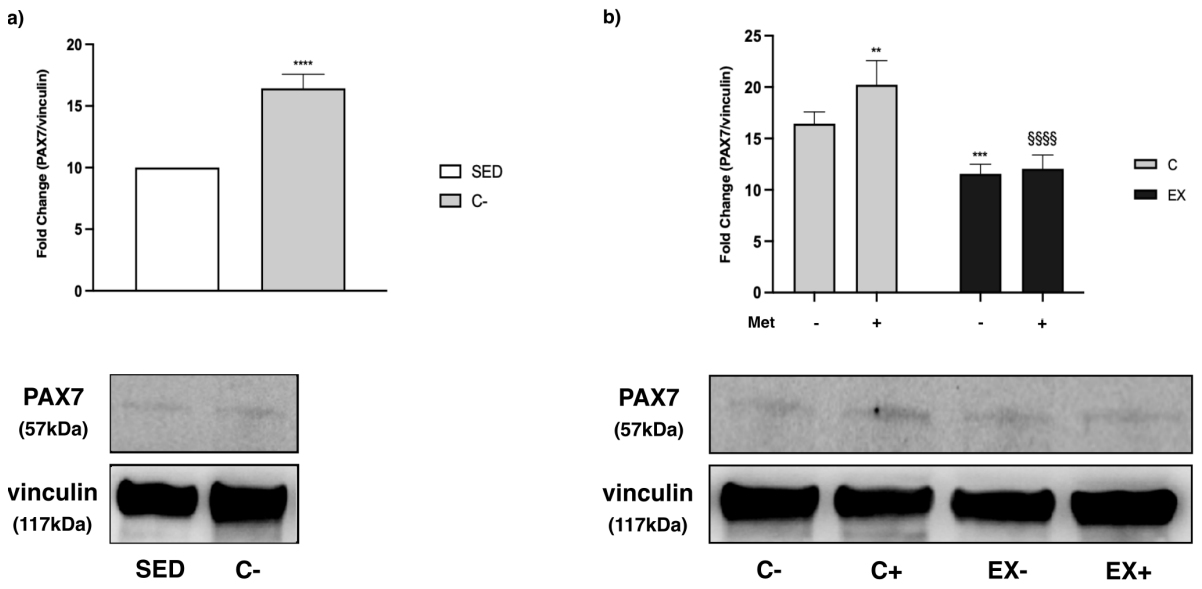

Figure 33. Western Blot analysis on PAX7 expression in total muscle lysate. Representative images of WB for PAX7 in total muscle lysates. Vinculin was used as loading control. Data are representative of four independent WB. (a) Histograms represent band density expressed as fold change compared with SED. Statistical analysis was performed using the t-test. **** ($p<0.0001$) *versus* SED. (b) Histograms represent band density expressed as fold change compared with C-. Statistical analysis was performed using two-way ANOVA followed by Tukey test. ** ($p<0.01$), *** ($p<0.001$) for differences *versus* C-; §§§§ ($p<0.0001$) for differences *versus* C+.

As regards AMPK activation, expressed as p-AMPK/AMPK *ratio*, t-test between SED and C- reported an increase in AMPK phosphorylation levels in C- (t (10) = 13.50, $p<0.0001$) (*Figure 34a*).

Two-way ANOVA analysis evidenced an involvement of drug administration (F (1,20) = 562.7, $p < 0.0001$), training (F (1,20) = 31.03, $p < 0.0001$) and interaction (F (1,20) = 8.991, p = .0071) in altering AMPK activation levels. Multiple comparisons reported a significant increase in p-AMPK/AMPK *ratio* in C+ *versus* C-, and in EX+ *versus* EX-. Moreover, AMPK activation in EX+ was meaningfully lower than that observed in C+ (*Figure 34b*).

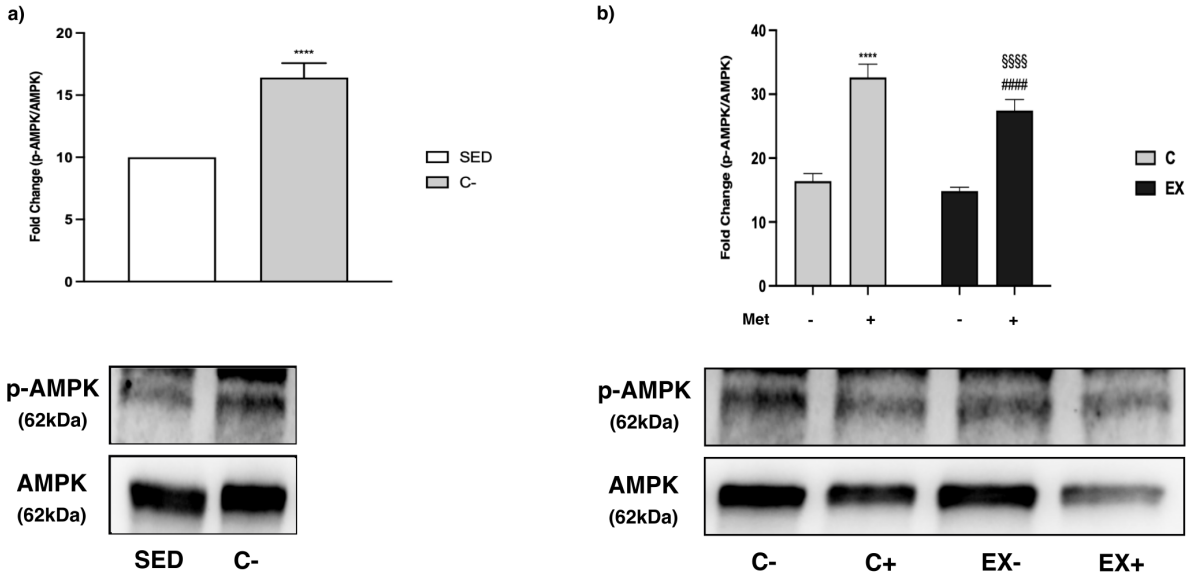

Figure 34. Western Blot analysis on AMPK activation level in total muscle lysate. Representative images of WB for p-AMPK/AMPK *ratio* in total muscle lysates. Phosphorylation level is presented as the *ratio* between phosphorylated and total protein. Data are representative of four independent WB. (a) Histograms represent band density expressed as fold change compared with SED. Statistical analysis was performed using the t-test. **** ($p<0.0001$) *versus* SED. (b) Histograms represent band density expressed as fold change compared with C-. Statistical analysis was performed using two-way ANOVA followed by Tukey test. **** ($p<0.0001$) for differences *versus* C-; §§§§ ($p<0.0001$) for differences *versus* C+; #### ($p<0.0001$) for differences *versus* EX-.

We next analysed some factors involved in the AMPK pathway, of which ACCß, that when phosphorylated is inactivated. Drug administration (F (1,20) = 155.1, $p < 0.0001$), training (F (1,20) = 260.1, $p < 0.0001$) and interaction (F (1,20) = 88.95, $p < 0.0001$) intervene in modulating ACCß phosphorylation, as evidenced by two-way ANOVA. In particular, p-ACC/ACCß *ratio* increased in trained rats, both in EX- and in EX+, compared with the respective control groups (C- and C+). Furthermore, the increase observed in EX+ was significantly higher than EX- (*Figure 35*).

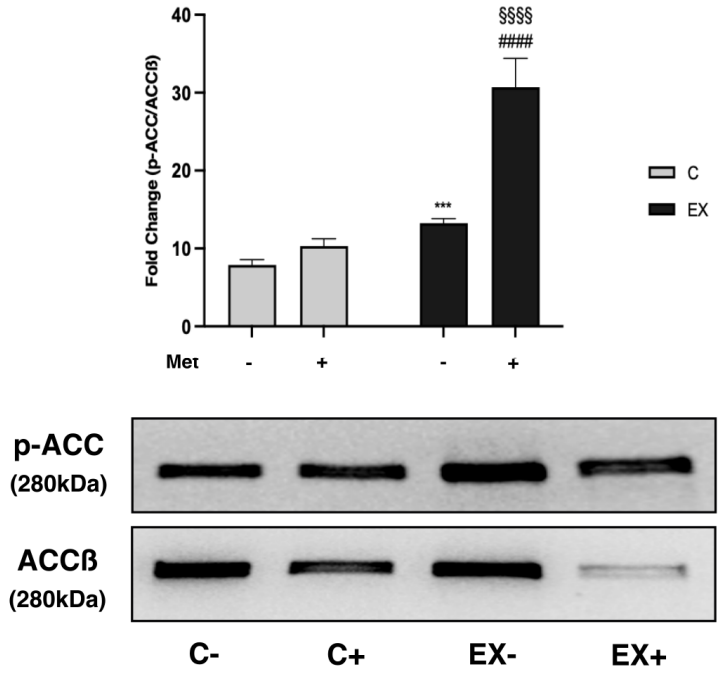

Figure 35. Western Blot analysis on ACCß phosphorylation in total muscle lysate. Representative images of WB for p-ACC/ACCß *ratio* in total muscle lysates. Histograms represent band density expressed as fold change compared with C-. Phosphorylation level is presented as the *ratio* between phosphorylated and total protein. Data are representative of four independent WB. Statistical analysis was performed using two-way ANOVA followed by Tukey test. *** ($p<0.001$) for differences *versus* C-; §§§§ ($p<0.0001$) for differences *versus* C+; #### ($p<0.0001$) for differences *versus* EX-.

Another AMPK downstream factor is PGC-1α. Two-way ANOVA reported that drug administration (F (1,20) = 103.0, $p < 0.0001$), training (F (1,20) = 196.2, $p < 0.0001$) and interaction (F (1,20) = 9.240, $p = .0065$) altered PGC-1α expression. Multiple comparisons evidenced that PGC-1α levels were lower in C+ than C-, increased in trained groups even though with a less augmentation in EX+ (*Figure 36*).

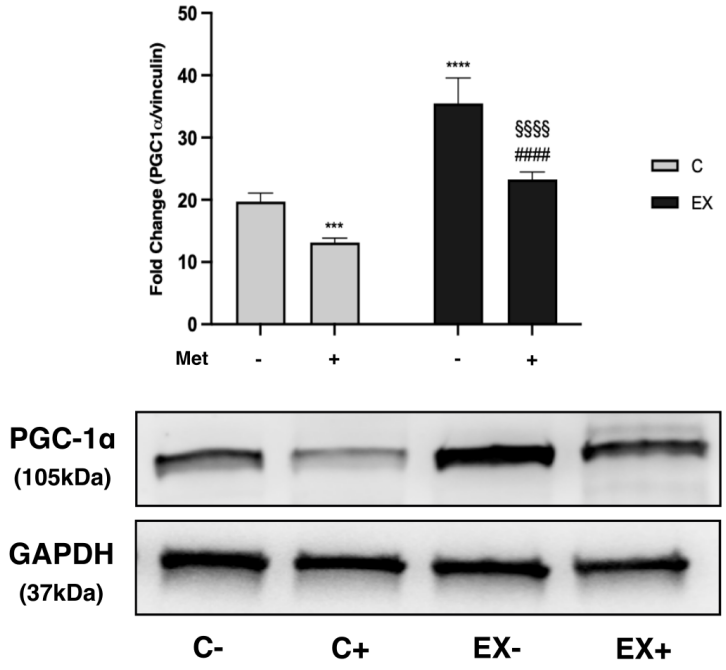

Figure 36. Western Blot analysis on PGC-1α expression in total muscle lysate. Representative images of WB for PGC-1α in total muscle lysates. Histograms represent band density expressed as fold change compared with C-. GAPDH was used as loading control. Data are representative of four independent WB. Statistical analysis was performed using two-way ANOVA followed by Tukey test. *** ($p<0.001$), **** ($p<0.0001$) for differences *versus* C-; §§§§ ($p<0.0001$) for differences *versus* C+; #### ($p<0.0001$) for differences *versus* EX-.

For what concerns PGC-1α expression in the mitochondrial fraction, it increased in C+ and further in EX- with respect to C- although it reached the higher expression level in EX+ group. Two-way ANOVA reported that drug administration (F (1,20) = 68.47, $p < 0.0001$), training (F (1,20) = 179.3, $p < 0.0001$) and interaction (F (1,20) = 7.334, p = .0135) modified mitochondrial PGC-1α expression (*Figure 37a*).

To confirm these results, we evaluated the expression of Cyt C - a protein induced by PGC-1α - and we obtained the same trend as for PGC-1α (*Figure 37b*).

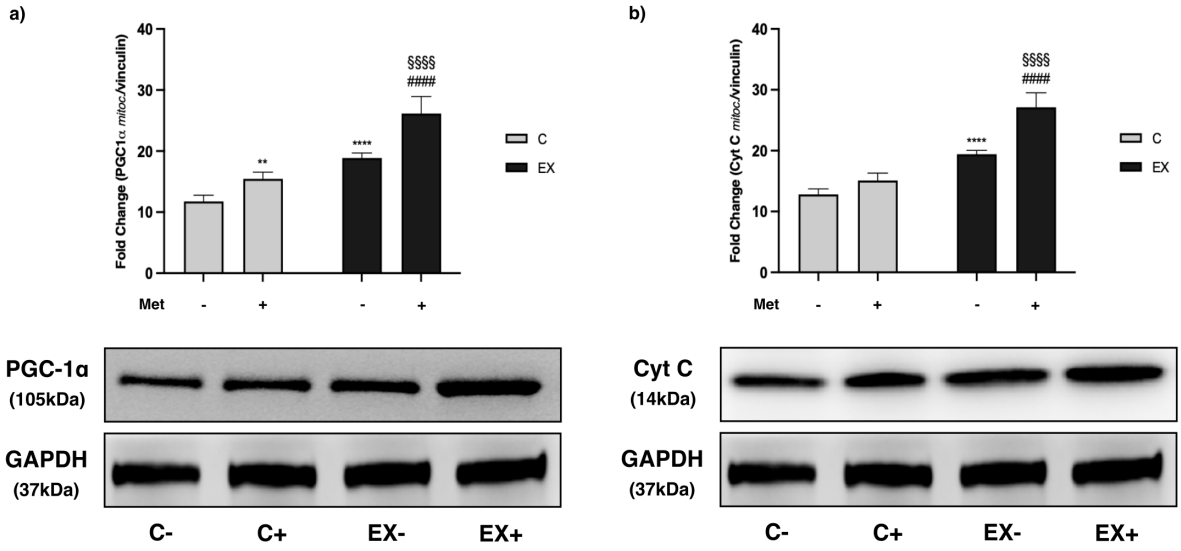

Figure 37. Western Blot analysis on PGC-1α and Cyt C expression in total muscle lysate. Representative images of WB for PGC-1α (a) and Cyt C (b) in the muscle mitochondrial fraction. Histograms represent band density expressed as fold change compared with C-. GAPDH was used as loading control. Data are representative of four independent WB. Statistical analysis was performed using two-way ANOVA followed by Tukey test. ** ($p<0.01$), **** ($p<0.0001$) for differences *versus* C-; §§§§ ($p<0.0001$) for differences *versus* C+; #### ($p<0.0001$) for differences *versus* EX-.

GSK3ß is a kinase whose phosphorylation means inactivation [45]. p-GSK3ß/GSK3ß *ratio* was higher in C+ and EX- *versus* C-, and in EX+ with respect to both EX- and C+. Two-way ANOVA evidenced that drug administration (F (1,20) = 141.4, $p < 0.0001$), training (F (1,20) = 137.3, $p < 0.0001$) and interaction F (1,20) = 38.31, $p < 0.0001$) modulate GSK3ß phosphorylation (*Figure 38*).

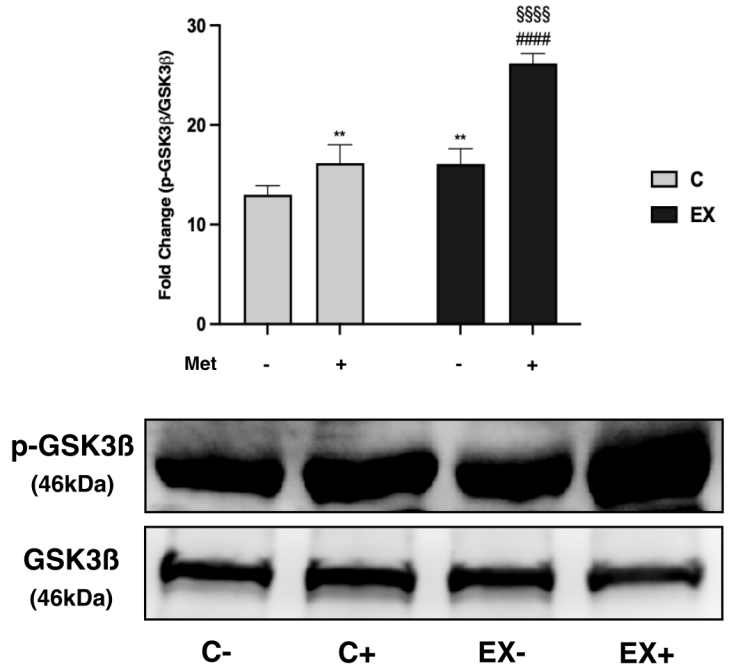

Figure 38. Western Blot analysis on GSK3ß phosphorylation in total muscle lysate. Representative images of WB for p-GSK3ß/GSK3ß *ratio* in total muscle lysates. Histograms represent band density expressed as fold change compared with C-. Phosphorylation level is presented as the *ratio* between phosphorylated and total protein. Data are representative of four independent WB. Statistical analysis was performed using two-way ANOVA followed by Tukey test. ** ($p<0.01$) for differences *versus* C-; §§§§ ($p<0.0001$) for differences *versus* C+; #### ($p<0.0001$) for differences *versus* EX-.

AKT activity could be influenced by insulin and plays a role in muscle protein synthesis regulation [46]. Two-way ANOVA reported an involvement of drug administration (F (1,20) = 398.4, $p < 0.0001$), training (F (1,20) = 85.16, $p < 0.0001$) and interaction (F (1,20) = 418.8, $p < 0.0001$) in modulating AKT phosphorylation. From the multiple comparisons we noticed an increase in EX+ p- AKT levels compared to EX- and C+ (*Figure 39*).

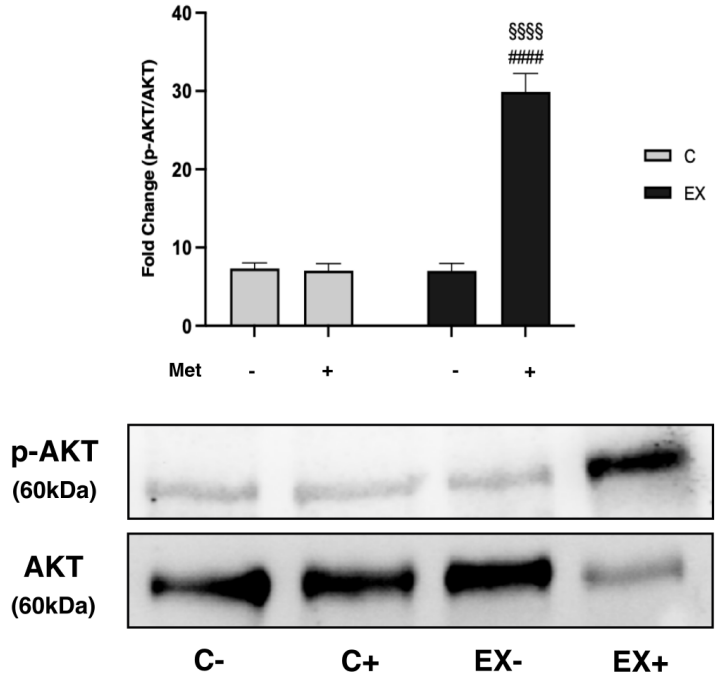

Figure 39. Western Blot analysis on AKT phosphorylation in total muscle lysate. Representative images of WB for p-AKT/AKT *ratio* in total muscle lysates. Histograms represent band density expressed as fold change compared with C-. Phosphorylation level is presented as the *ratio* between phosphorylated and total protein. Data are representative of four independent WB. Statistical analysis was performed using two-way ANOVA followed by Tukey test. §§§§ ($p<0.0001$) for differences *versus* C+; #### ($p<0.0001$) for differences *versus* EX-.

mTOR is a protein that can be modulated directly and indirectly both by AMPK and by AKT[47]. Statistical analysis indicated that drug administration (F (1,20) = 179.1, $p < 0.0001$) and training (F (1,20) = 246.3, $p < 0.0001$) increased mTOR phosphorylation. From the multiple comparisons emerged that EX- and C+ had a higher phosphorylation of mTOR than C-. Moreover, there was a significant increase of p-mTOR/mTOR ratio in EX+ compared with EX- and C+ (*Figure 40a*). Representative images of p-p70S6K and p70S6K are shown in *Figure 40b*, even though no statistical analysis was performed on this kinase as the levels of total protein were too low to be quantified.

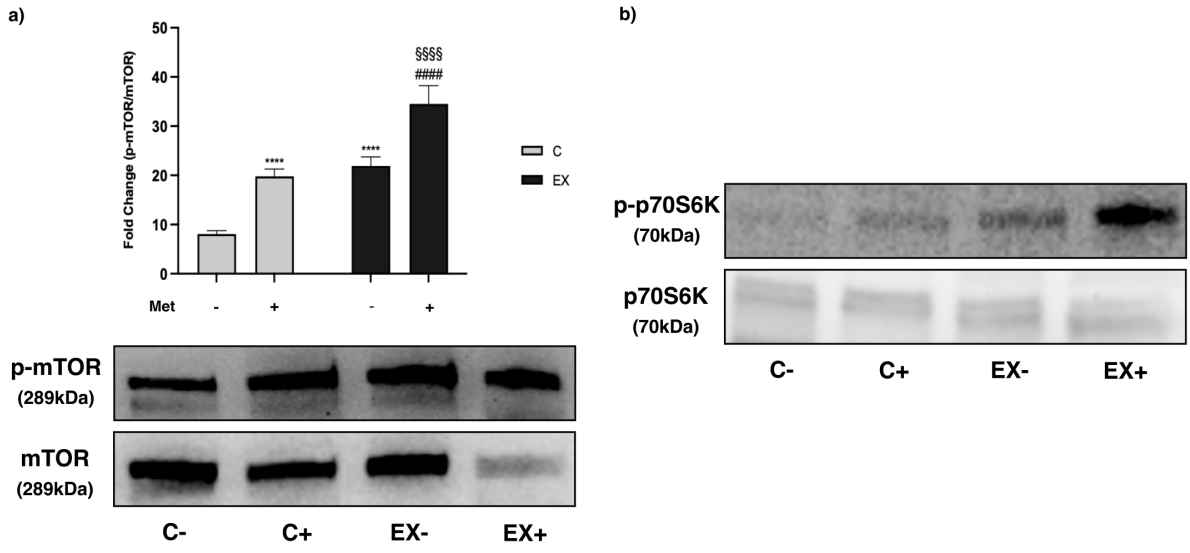

Figure 40. Western Blot analysis on mTOR and p70S6K phosphorylation in total muscle lysate. Representative images of WB for (a) p-mTOR/mTOR *ratio* and (b) p-p70S6K and p70S6K in total muscle lysates. (a) Histograms represent band density expressed as fold change compared with C-. Phosphorylation level is presented as the *ratio* between phosphorylated and total protein. Data are representative of four independent WB. Statistical analysis was performed using two-way ANOVA followed by Tukey test. **** ($p<0.0001$) for differences *versus* C-; §§§§ ($p<0.0001$) for differences *versus* C+; #### ($p<0.0001$) for differences *versus* EX-.

4.2. *In vitro* study

4.2.1. Effects of Met on proliferating C2C12

We examined the proliferation of C2C12 cells cultured in GM supplemented with different concentrations of Met (250µM, 1mM and 10mM) for 24h, 48h and 72h. Met had an antiproliferative effect on C2C12 myoblasts. In cells exposed to 10mM Met we observed a statistically significant reduction in proliferation compared with control at all times tested. 250µM Met decreased cell proliferation only after 72h treatment, while 1mM Met reduced cell growth already starting from 48h (*Figure 41*).

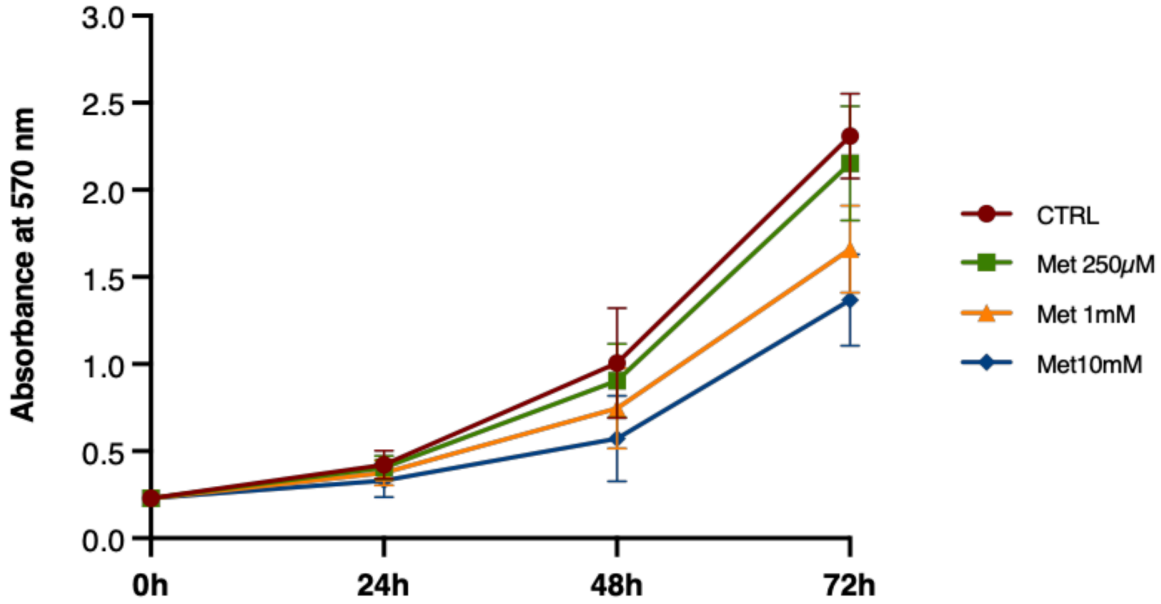

Figure 41. Evaluation of C2C12 proliferation at different time points and with different Met concentrations. Proliferating cells were treated with 250μM, 1mM and 10mM Met for 24h, 48h and 72h. Statistical analysis was performed using two-way ANOVA followed by Bonferroni's multiple comparison test. Statistically significant differences between CTRL and Met-treated cells: 24h Met10mM vs CTRL ($p<0.001$); 48h Met1mM and Met10mM vs CTRL ($p<0.0001$); 72h Met250μM vs CTRL ($p<0.05$), Met1mM and Met10mM vs CTRL ($p<0.0001$).

In C2C12 exposed to the same experimental conditions, we evaluated by Western Blot (WB) analysis the effects of Met treatment on AMPK activity. A meaningful increase was found after the exposure to 1mM and 10mM Met at every time point compared with control cells (CTRL) (*Figure 42*).

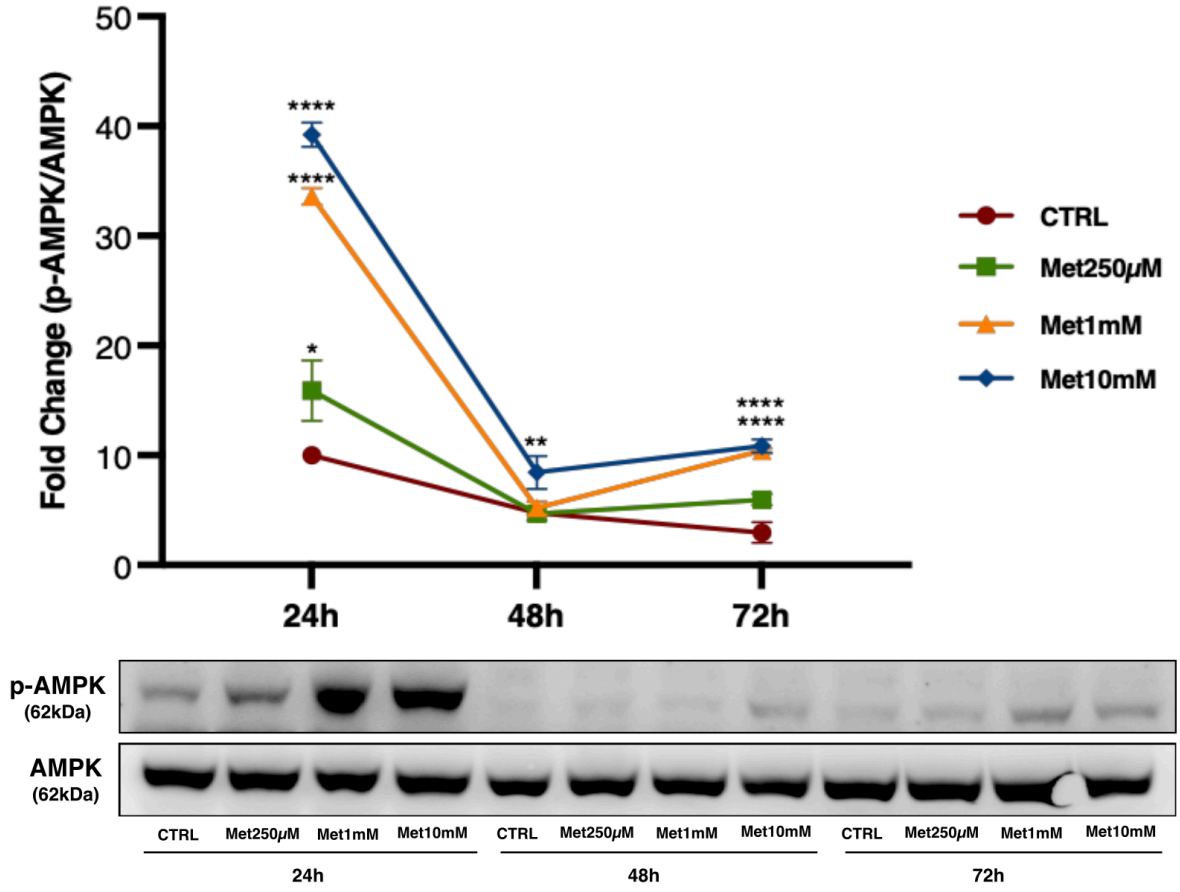

Figure 42. Western Blot analysis on AMPK activation in total cell lysate. Representative image of WB for AMPK and p-AMPK in total cell lysate from C2C12 treated with 250µM, 1mM and 10mM Met for 24h, 48h and 72h. The graph represents band density expressed as a fold change of p-AMPK/AMPK *ratio* compared with CTRL from four independent experiments. * ($p<0.05$), ** ($p<0.01$), **** ($p<0.0001$) for differences *versus* CTRL using two-way ANOVA followed by Bonferroni's multiple comparison test.

Cell cycle arrest, cytotoxicity and apoptosis induction are the major causes of cell proliferative inhibition. To understand the mechanism by which metformin inhibited proliferation of C2C12 cells, we tested whether metformin induced cytotoxicity or apoptosis. Cell viability was monitored by the TB exclusion test (*Figure 43a*) and LDH release (*Figure 43b*). TB and

LDH assays did not show statistical differences as regard the number of dead cells and cytotoxicity at any Met concentration and time point, compared with CTRL.

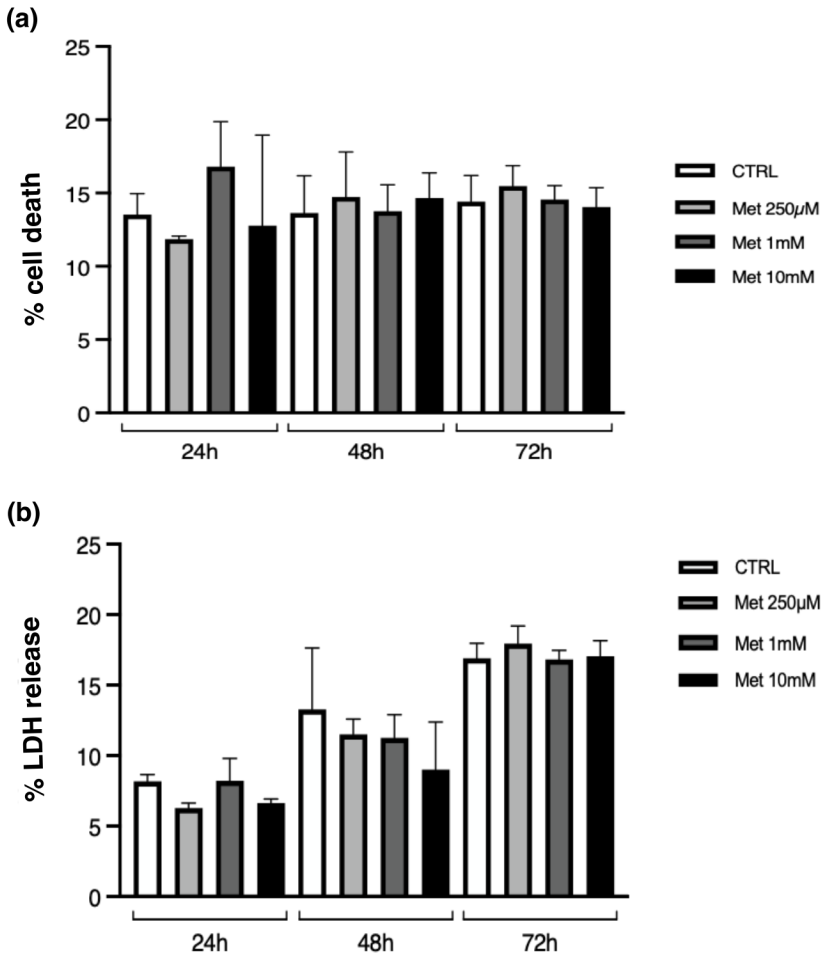

Figure 43. TB exclusion test and LDH release assessment on C2C12 cells. TB exclusion test (a) and LDH release assessment (b) were performed. Statistical analysis of the differences between control and treated cells was conducted for each time point using one-way ANOVA. No differences were observed ($p>0.05$).

To elucidate whether metformin induced apoptosis WB analysis was performed to evaluate the expression of caspase 3, which plays an important role in programmed cell death. The caspase-3 expression in C2C12 cells did not vary neither in control nor in treated cells at any Met concentration and time point (data not shown).

At last, to establish whether Met influenced cell cycle progression, we determined the distribution of Met-treated C2C12 cells in the different phases of the cell cycle using flow cytometry at 24h (*Figure 44a*), 48h (*Figure 44b*) and 72h (*Figure 44c*).

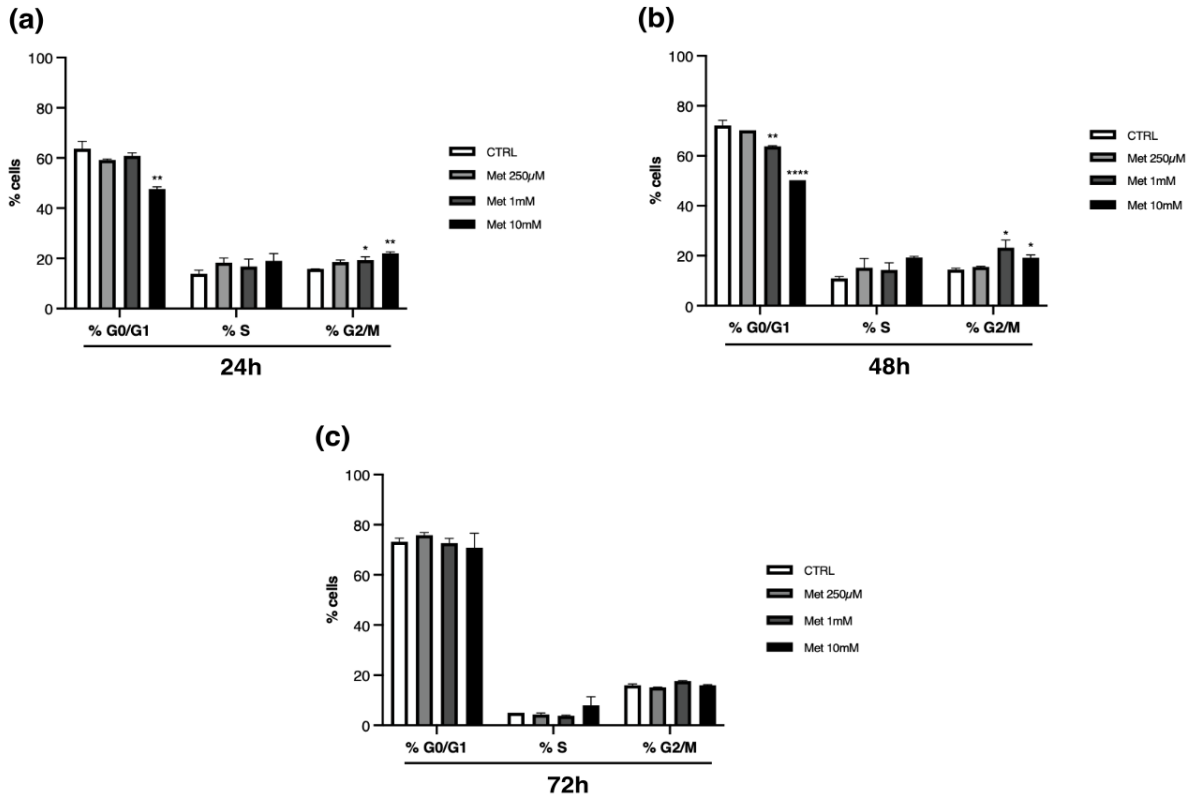

Figure 44. FACS analysis on C2C12 cell cycle progression. Histograms represent flow cytometry analysis of the three different phases of the cell cycle. Cell percentage was reduced in G0/G1 phase and increased in G2/M. Statistical differences are evident at 24h (a), even more at 48h (b), and disappear at 72h (c). Statistical analysis of the differences between control and treated cells was performed for each time point and phase using one-way ANOVA followed by Bonferroni's multiple comparison test. * ($p<0.05$), ** ($p<0.01$), **** ($p<0.0001$) for differences *versus* CTRL.

The fraction of cells in G0/G1 decreased after the exposure to 10mM Met for 24h, and even more after 48h. At this time point also 1mM Met determined a significant reduction in G0/G1 cells compared with control. No differences existed in the percentage of cells in S phase. As regards cells in G2/M phase, a significant increase was found in cells treated with 1mM and

10mM Met for 24h and 48h compared with control. All the previously observed differences were undetectable at 72h.

4.2.2. Effects of Met on myoblast differentiation

We next asked whether Met could affect myogenic differentiation process. Proliferating myoblasts were induced to differentiate by incubation in DM for a maximum of 96h and exposed to 10mM Met, added fresh to the medium every 24h.

We analysed the expression of MYH1/2, PAX7, MyoD, Myf5 and p21.

MYH1/2 expression was statistically significant in CTRL only at 96 hours, while in the Met 10mM cells it was never expressed (*Figure 45a*).

The expression of PAX7 decreased both in CTRL and in Met10mM over time. The levels of PAX7 in treated cells were lower than the control already starting from 24h but decreased in a more attenuated manner compared with CTRL cells (*Figure 45b*).

Myf5 levels were lower in Met10mM cells compared with CTRL, with a significant difference at 24h. In control and treated cells, we observed an opposite trend of expression at 72h and 96h, with an increase in Met10mM and a decrease in CTRL (*Figure 45c*).

MyoD was meaningfully less expressed in Met10mM than in CTRL cells at 24h and 48h. While MyoD levels significantly decreased in CTRL over time, in Met10mM cells MyoD expression remained rather stable but significantly higher than control at 72h and 96h (*Figure 45d*).

p21 expression was always significantly lower in Met10mM compared with the CTRL cells, except for the 24h time point. In cells treated with Met, p21 meaningfully decreased over time (*Figure 45e*).

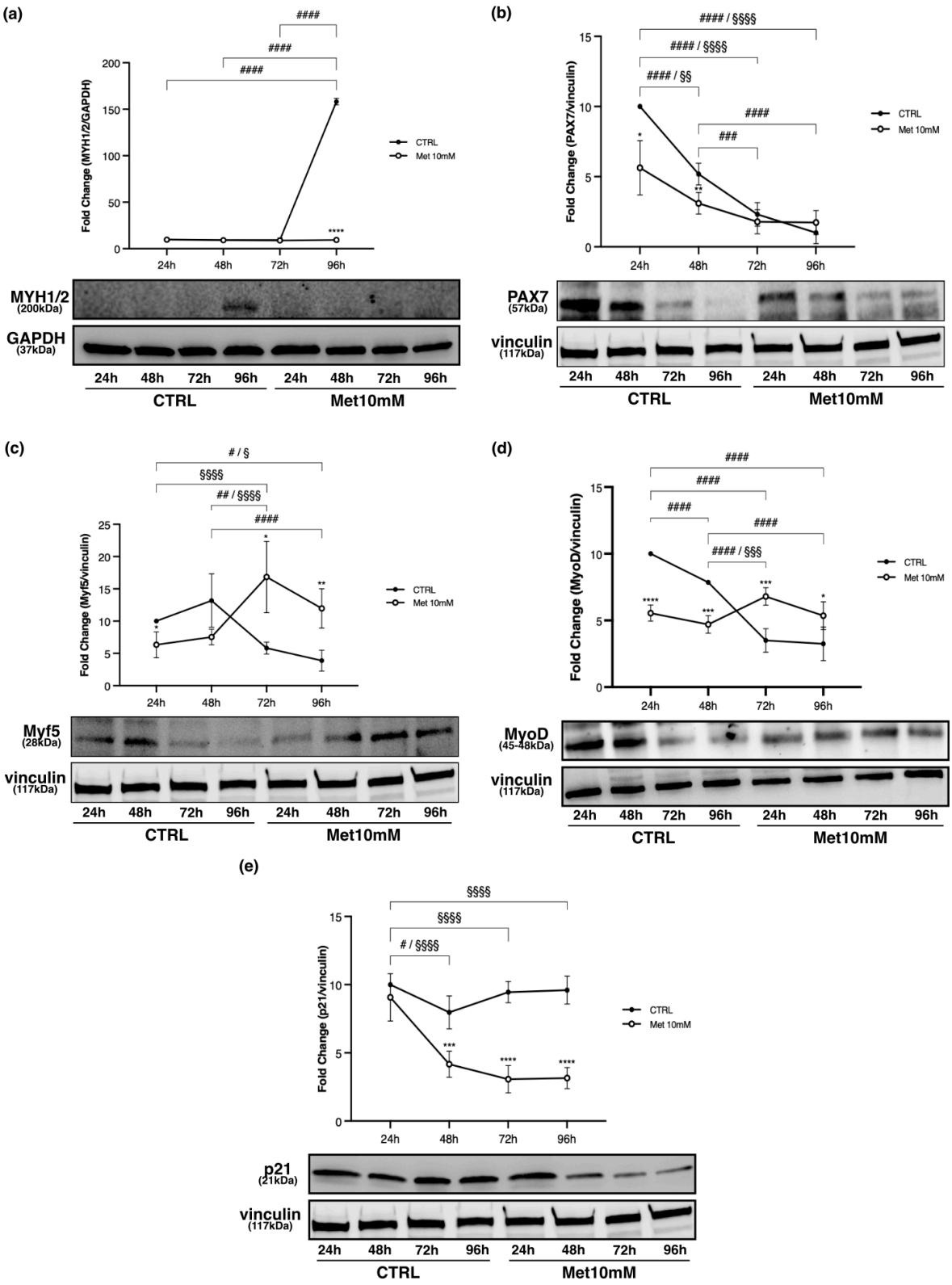

Figure 45. Western Blot analysis on differentiating C2C12. Proliferating C2C12 cells were shifted in DM and treated with 10mM Met for 24h, 48h, 72h and 96h. Representative images of WB for MYH1/2 (a), PAX7 (b), Myf5 (c), MyoD (d) and p21 (e) in total cell lysates. The graphs represent band density expressed as fold change

compared with CTRL. GAPDH and vinculin were used as loading control. Data are representative of four independent experiments. Statistical analysis was performed using two-way ANOVA followed by Bonferroni's multiple comparison test. * ($p<0.05$), ** ($p<0.01$), *** ($p<0.001$), **** ($p<0.0001$) for differences between CTRL and Met; # ($p<0.05$), ## ($p<0.01$), ### ($p<0.001$), #### ($p<0.0001$) for differences within CTRL; § ($p<0.05$), §§ ($p<0.01$), §§§ ($p<0.001$), §§§§ ($p<0.0001$) for differences within Met.

We also evaluated the activation of AMPK (p-AMPK/AMPK *ratio*) and the expression of factors involved in its pathway.

AMPK activation level was always significantly higher in Met10mM cells with respect to CTRL at every time point, with a tendency to decrease both in control and in Met-treated cells over time (*Figure 46a*).

As regards the expression PGC-1α, no differences were evident between CTRL and Met10mM cells at 24h. Subsequently, PGC-1α significantly increased over time both in treated and in untreated cells, even though the increase was always lower in CTRL than Met cells. While the increase was maximal at 72h in CTRL, PGC-1α kept on rising also after 72h in Met10mM (*Figure 46b*).

Met induced a significant increase of acetyl-CoA carboxylase ß (ACCß) phosphorylation compared with control at each time point. Moreover, there was a significant reduction of the phosphorylation of this enzyme both in CTRL and in Met 10mM cells over time (*Figure 46c*).

In CTRL cells phosphorylation of GSK3ß significantly increased at 48h, it was reduced at 72h, and it plunged at 96h. In treated cells GSK3ß was not phosphorylated at any time (*Figure 46d*).

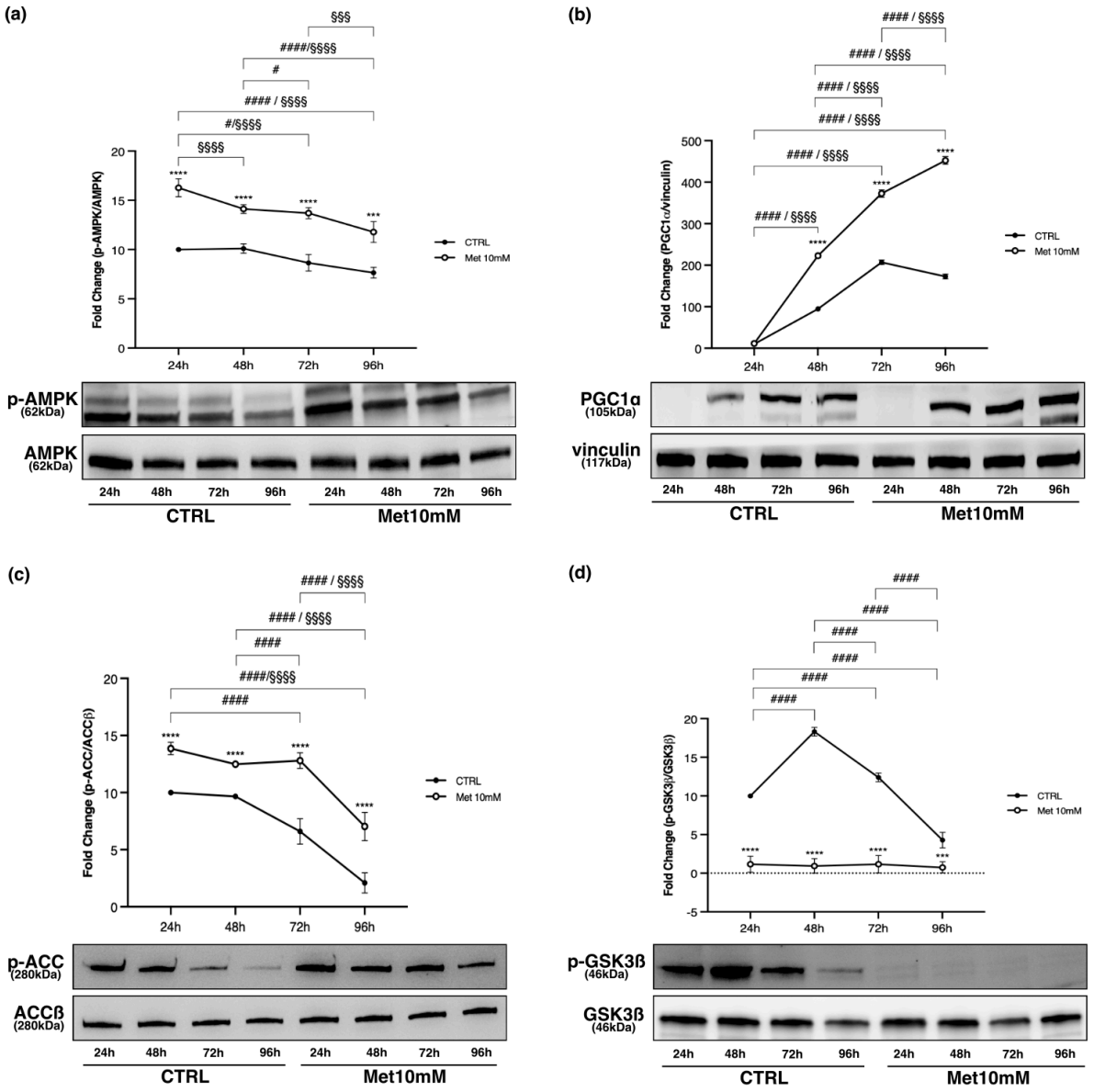

Figure 46. Western Blot analysis on differentiating C2C12: AMPK pathway. Met maintains GSK3ß in its activated status. Proliferating C2C12 cells were shifted in DM and treated with 10mM Met for 24h, 48h, 72h and 96h. Representative images of WB for p-AMPK and AMPK (a), PGC-1α (b), p-ACC and ACCß (c), p-GSK3ß and GSK3ß (d) in total cell lysates. The graphs represent band density expressed as fold change compared with CTRL. Phosphorylation level is presented as the *ratio* between phosphorylated and total protein; PGC-1α was normalized to vinculin. Data are representative of four independent experiments. Statistical analysis was performed using two-way ANOVA followed by Bonferroni's multiple comparison test. *** ($p<0.001$), **** ($p<0.0001$) for differences between CTRL and Met; # ($p<0.05$), #### ($p<0.0001$) for differences within CTRL; §§§ ($p<0.001$), §§§§ ($p<0.0001$) for differences within Met.

4.2.3. Concentration-dependent effects of Met on myotubes

The levels of MYH1/2, Myf5, MyoD, p21, p-AMPK/AMPK *ratio*, PGC-1α, p-ACC/ACCß *ratio* and p-GSK3ß/GSK3ß *ratio* were evaluated in myotubes exposed to the same concentrations used in proliferating C2C12 (250μM, 1mM and 10mM Met).

The expression of MYH1/2 significantly decreased at all Met concentrations compared with CTRL. A significant reduction was also observed in Met1mM and Met10mM cells with respect to Met250μM (*Figure 47a*).

Expression levels of the myogenic factors Myf5 and MyoD were significantly higher in the cells treated with 10mM Met, compared with CTRL and cells exposed to the other two drug concentrations (*Figures 47b and 47c*).

Met treatment reduced the levels of p21 compared with control in a concentration-dependent manner (*Figure 47d*).

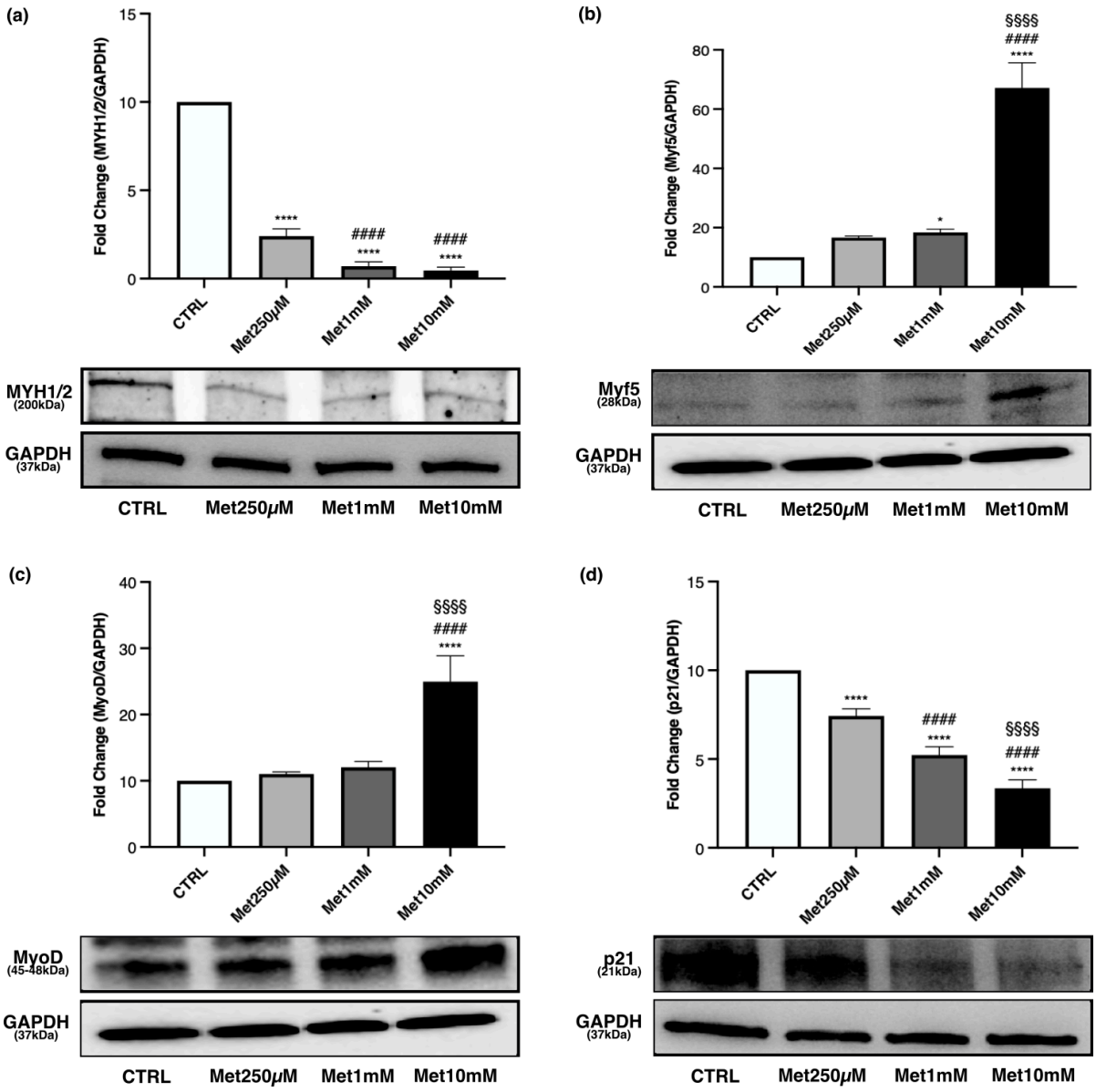

Figure 47. Western Blot analysis on myotubes treated with Met. Differentiated C2C12 were incubated in DM + Met at three different concentrations (250µM, 1mM, 10mM) for 24h. Representative images of WB for MYH1/2 (a), Myf5 (b), MyoD (c) and p21 (d) in total cell lysates. Histograms represent band density expressed as fold change compared with CTRL. GAPDH was used as loading control. Data are representative of four independent experiments. Statistical analysis was performed using one-way ANOVA followed by Bonferroni's multiple comparison test. * ($p<0.05$), **** ($p<0.0001$) for differences *versus* CTRL; #### ($p<0.0001$) for differences *versus* Met250µM; §§§§ ($p<0.0001$) for differences *versus* Met1mM.

1mM and 10mM Met treatment increased the phosphorylation level of AMPK compared with control and 250µM Met, even though the greatest effect on the activation of AMPK was observed after exposure to 10mM Met (*Figure 48a*).

The treatment with 10mM Met led to an increased expression of PGC-1α, which was statistically significant compared with CTRL, Met250µM and Met1mM cells (*Figure 48b*).

p-ACC/ACCß *ratio* increased in myotubes exposed to the two highest drug concentrations, with the maximal effect observed at 10mM Met (*Figure 48c*).

A statistically significant reduction was observed in the phosphorylation levels of GSK3ß after treatment with 1mM and 10mM Met compared with control and 250µM Met. A noteworthy decrease in p-GSK3ß/GSK3ß *ratio* was noticed in Met10mM cells (*Figure 48d*).

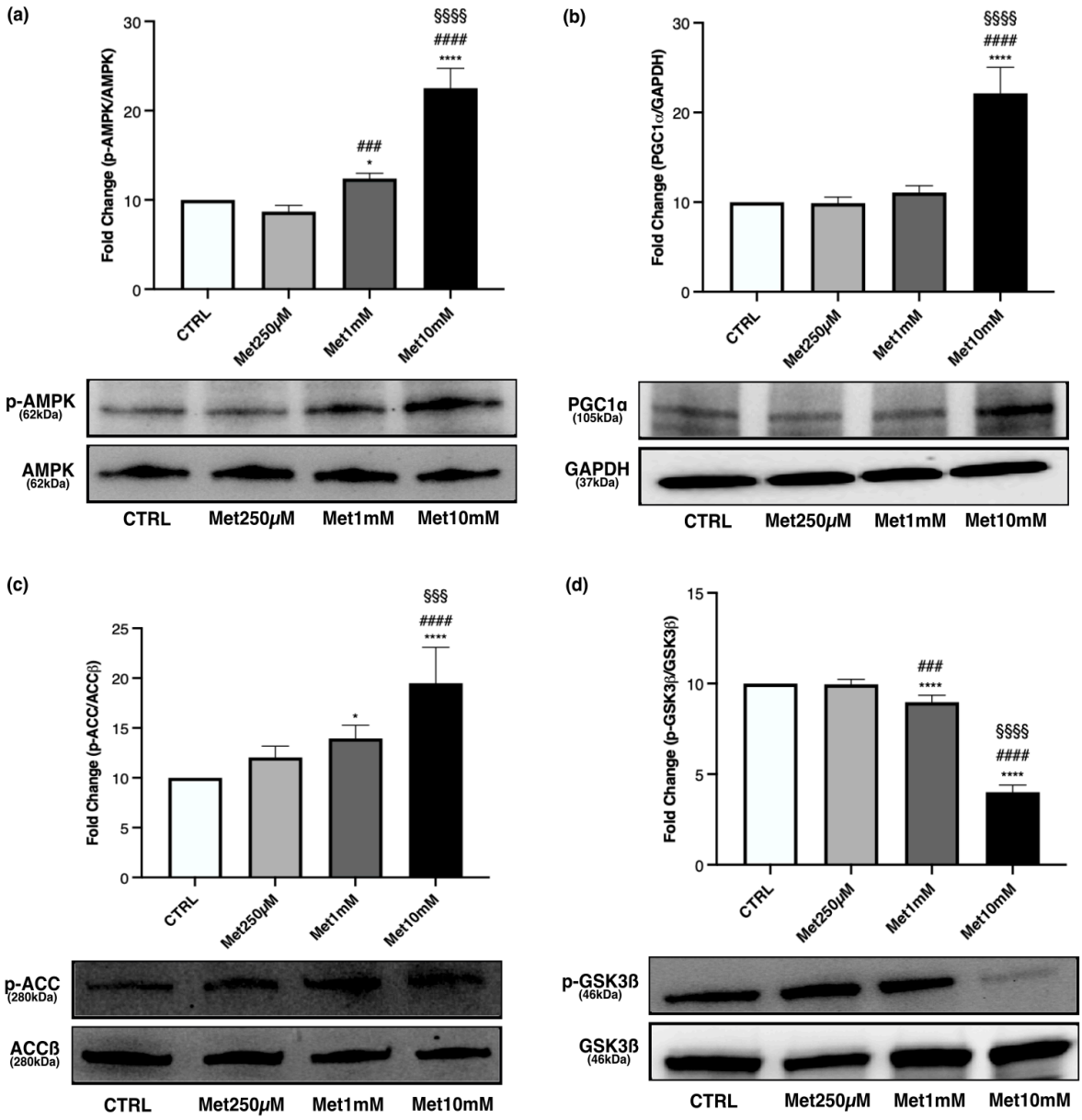

Figure 48. Western Blot analysis on myotubes treated with Met: AMPK pathway. High Met concentrations activate AMPK, increase PGC-1α expression and ACCß phosphorylation. p-GSK3ß/GSK3ß *ratio* decreases especially with 10mM Met. Differentiated C2C12 were incubated in DM + Met at three different concentrations (250μM, 1mM, 10mM) for 24h. Representative images of WB for p-AMPK and AMPK (a), PGC-1α (b), p-ACC and ACCß (c), p-GSK3ß and GSK3ß (d) in total cell lysates. Histograms represent band density expressed as fold change compared with CTRL. Phosphorylation level is presented as the *ratio* between phosphorylated and total protein; PGC-1α was normalized to GAPDH. Data are representative of four independent experiments.

Statistical analysis was performed using one-way ANOVA followed by Bonferroni's multiple comparison test. * ($p<0.05$), **** ($p<0.0001$) for differences *versus* CTRL; ### ($p<0.001$), #### ($p<0.0001$) for differences *versus* Met250μM; §§§ ($p<0.001$), §§§§ ($p<0.0001$) for differences *versus* Met1mM.

It has been reported that 400μM and 500μM Met may promote myogenic differentiation and myotube formation, whereas higher doses (1mM and 10mM) inhibit the differentiation process [48]. To verify if the effect of Met on myogenic differentiation might be related to the drug dose, we examined the same panel of factors in myotubes exposed to concentrations of Met included in the range 250μM-1mM (250μM, 400μM, 600μM, 800μM, 1mM).

Met induced a statistically significant reduction of MYH1/2 expression already starting from 400μM, with a more evident decrease at 800μM and 1mM (*Figure 49a*).

Compared with CTRL, the expression of the myogenic factor Myf5 significantly decreased after 400μM Met treatment and increased when myotubes were exposed to higher concentrations, especially to 800μM (*Figure 49b*). Furthermore, p21 levels showed a significant reduction in treated cells with a concentration-dependent trend (*Figure 49c*).

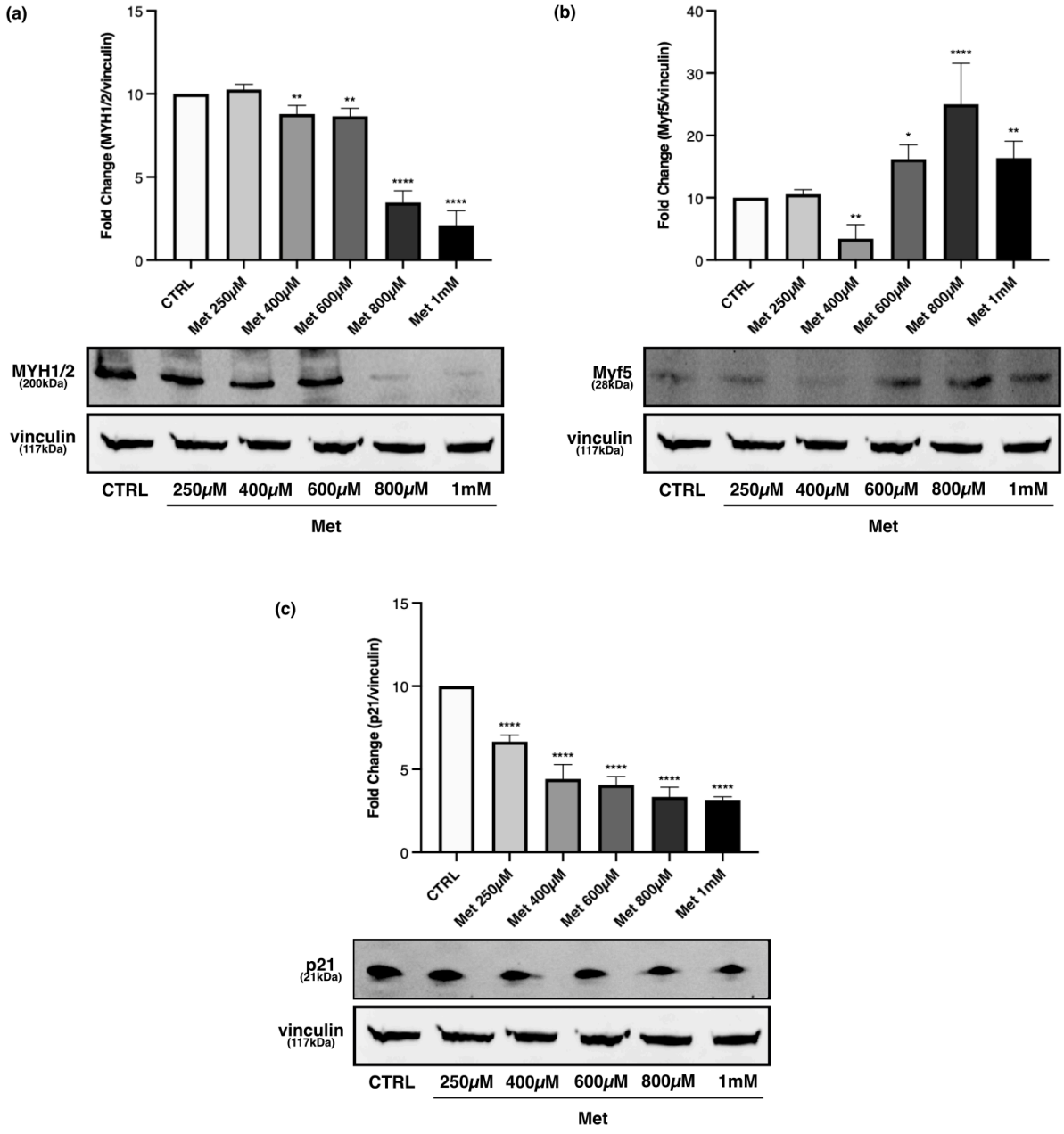

Figure 49. Western Blot analysis on myotubes treated with different Met concentrations. Differentiated C2C12 were incubated in DM + Met at the following concentrations: 250μM, 400μM, 600μM, 800μM, 1mM, for 24h. Representative images of WB in total cell lysate are shown. (a) Met reduces MYH1/2 protein expression starting from 400μM, with a more evident decrease at 800μM and 1mM. (b) The expression levels of Myf5 decreases after 400μM Met treatment and increases at higher concentrations especially at 800μM. (c) Met reduces p21 levels in a concentration-dependent manner. Histograms represent band density expressed as fold change compared with CTRL. Vinculin was used as loading control. Data are representative of four independent

experiments. Statistical analysis was performed using one-way ANOVA followed by Bonferroni's multiple comparison test. * ($p<0.05$), ** ($p<0.01$), **** ($p<0.0001$) for differences *versus* CTRL.

Met activated AMPK starting from 400µM, and the p-AMPK/AMPK *ratio* progressively raised as the drug concentration increased (*Figure 50a*).

As regards PGC-1α, Met treatment did not modify its expression, except for 1mM Met that induced a weak but statistically significant increase compared with CTRL (*Figure 50b*).

Met treatment led to a significant decrease of GSK3ß phosphorylation starting from the 400µM concentration compared with control (*Figure 50c*).

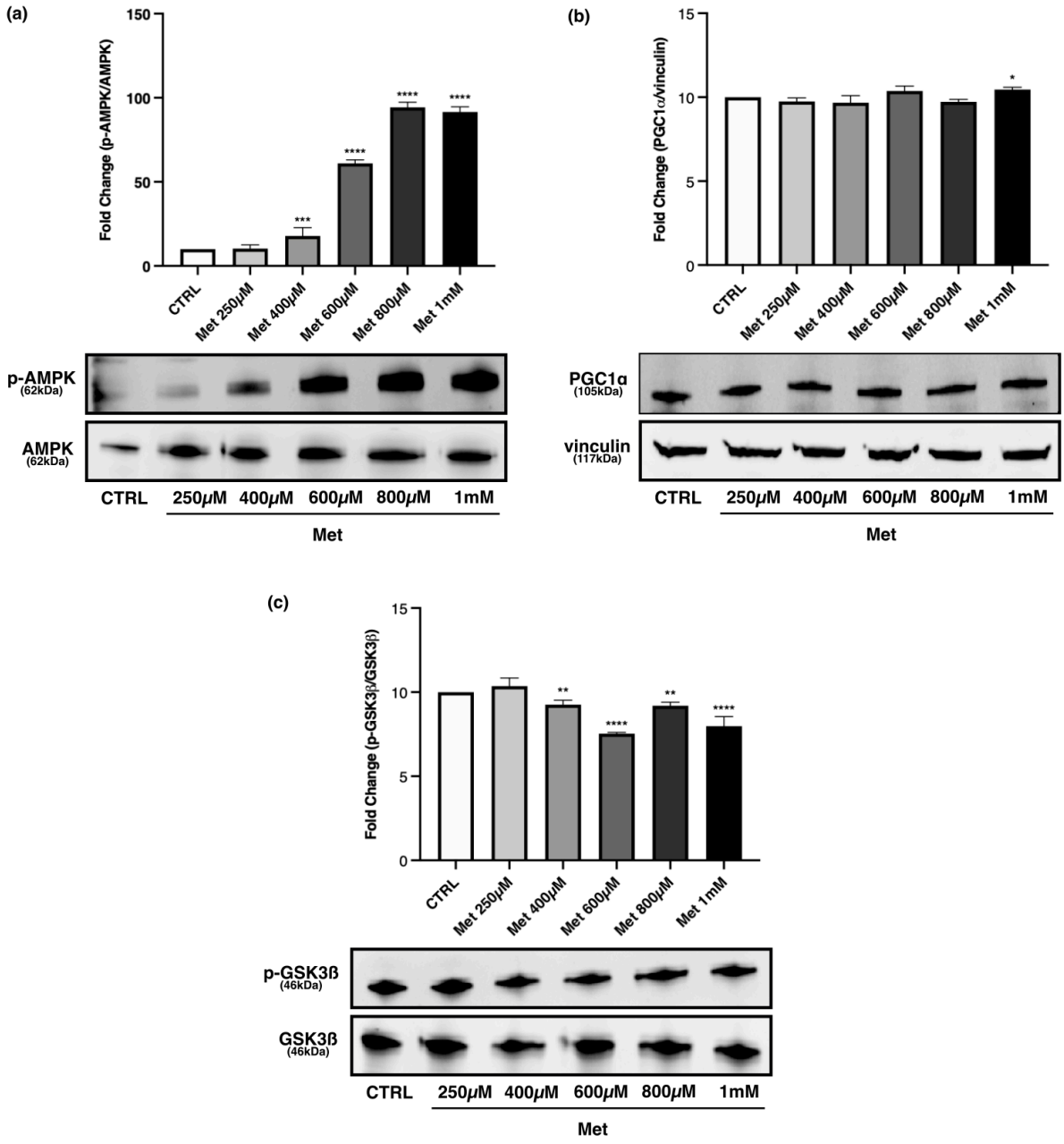

Figure 50. Western Blot analysis on myotubes treated with different Met concentrations: AMPK pathway. Differentiated C2C12 were incubated in DM + Met at the following concentrations: 250µM, 400µM, 600µM, 800µM, 1mM, for 24h. Representative images of WB in total cell lysate are shown. (a) Met activates AMPK starting from 400µM and the p-AMPK/AMPK ratio progressively raises until 800µM and remains stable at the concentration of 1mM. (b) Met induces a weak but statistically significant increase of PGC-1α expression only at 1mM. (c) Phosphorylation status of GSK3ß decreases starting from the exposure to 400µM Met. Histograms represent band density expressed as fold change compared with CTRL. Phosphorylation level is presented as the *ratio* between phosphorylated and total protein; PGC-1α was normalized to vinculin. Data are representative of

four independent experiments. Statistical analysis was performed using one-way ANOVA followed by Bonferroni's multiple comparison test. * ($p<0.05$), ** ($p<0.01$), *** ($p<0.001$), **** ($p<0.0001$) for differences *versus* CTRL.

4.2.4. Time-dependent effects of Met on myotubes

We evaluated on myotubes the time-dependent effects of 10mM Met on the proteins previously analysed.

Met induced a statistically significant decrease of MYH1/2 levels in a time-dependent manner compared with control (*Figure 51a*).

Myf5 expression statistically increased in Met10mM cells at every time point with respect to control, with a maximal effect at 48h (*Figure 51b*).

p21 levels in treated cells was lower than control at 24h, and it was further reduced after 48h (*Figure 51c*).

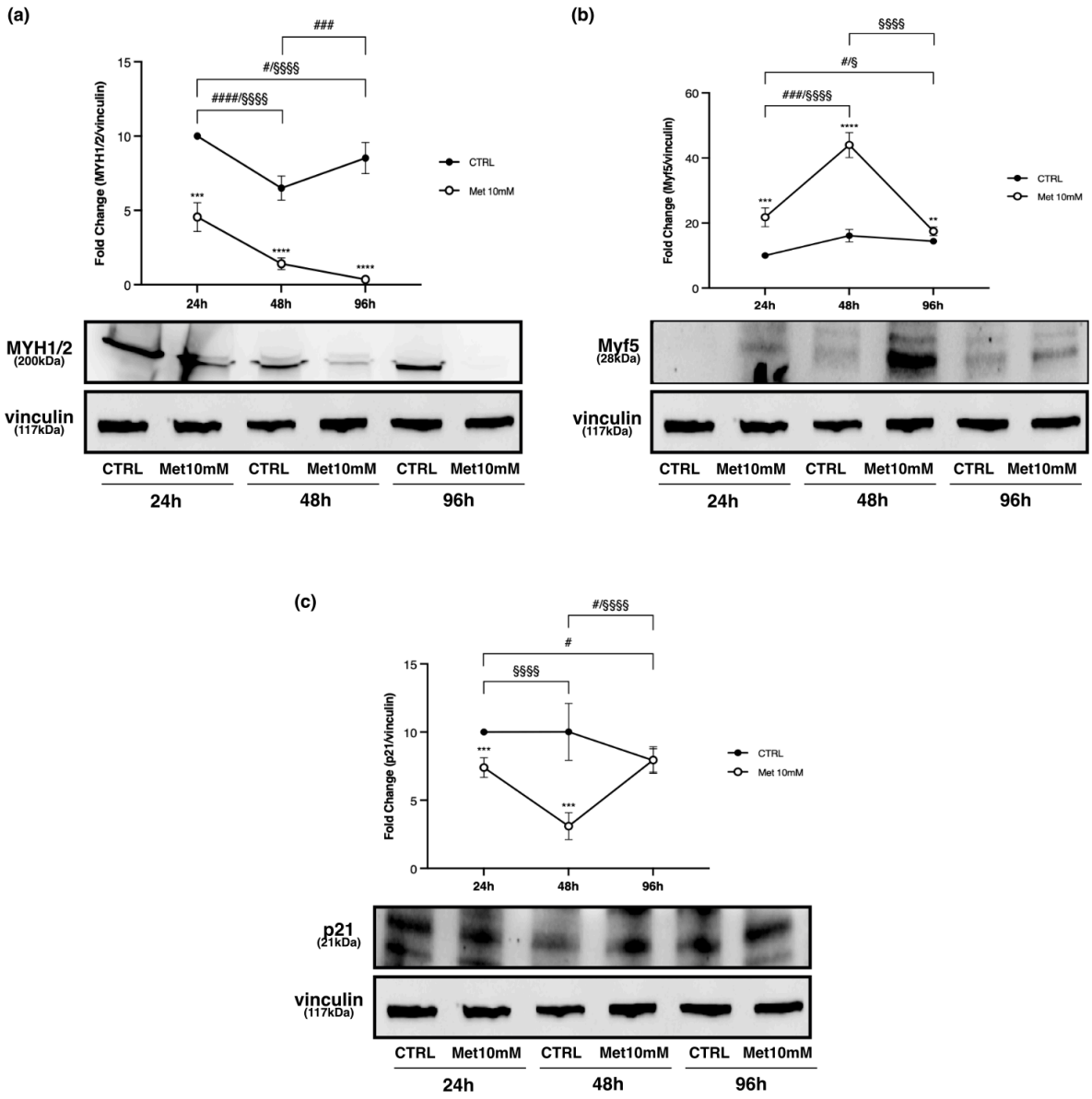

Figure 51. Western Blot analysis on myotubes treated with Met for 24h, 48h, and 96h. Differentiated C2C12 were incubated in DM + 10mM Met for 24h, 48h and 96h. Representative images of WB in total cell lysate are shown. (a) Met reduces MYH1/2 expression in a time-dependent manner. (b) Met increases Myf5 expression with the maximal effect at 48h. (c) Met reduces p21 levels in a time-dependent manner with the maximal effect at 48h. The graphs represent band density expressed as fold change compared with CTRL. Vinculin was used as loading control. Data are representative of four independent experiments. Statistical analysis was performed using two-way ANOVA followed by Bonferroni's multiple comparison test. ** ($p<0.01$), *** ($p<0.001$), **** ($p<0.0001$) for differences between CTRL and Met; # ($p<0.05$), ### ($p<0.001$), #### ($p<0.0001$) for differences within CTRL; § ($p<0.05$), §§§§ ($p<0.0001$) for differences within Met.

p-AMPK/AMPK *ratio* was always higher in treated myotubes compared with control at every time point, with a maximal activation at 48h (*Figure 52a*).

PGC-1α expression significantly increased only at 24h in Met10mM cells compared with CTRL. No statistical differences were observed between treated and untreated cells at 48h and 96h (*Figure 52b*).

The p-GSK3ß/GSK3ß *ratio* increased in a time-dependent manner both in control and in treated cells, but the phosphorylation levels in Met10mM cells were always lower than those in CTRL with a statistically significant difference at 24h and 48h (*Figure 52c*).

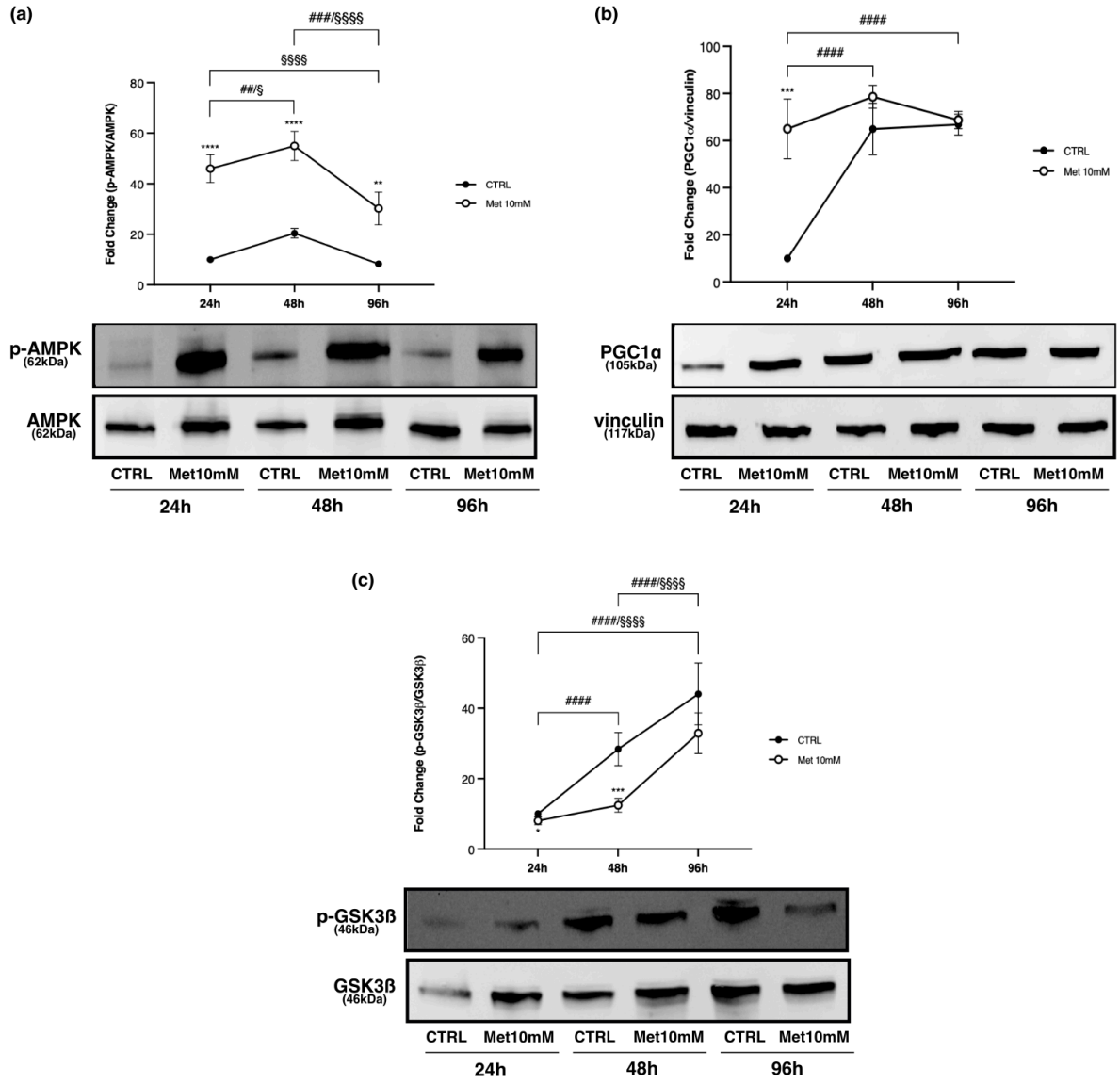

Figure 52. Western Blot analysis on myotubes treated with Met for 24h, 48h, and 96h: AMPK pathway. Differentiated C2C12 were incubated in DM + 10mM Met for 24h, 48h and 96h. Representative images of WB in total cell lysate are shown. (a) Met increases p-AMPK/AMPK *ratio* compared with CTRL. (b) Met increases PGC-1α expression only at 24h. (c) p-GSK3ß/GSK3ß *ratio* increases in a time-dependent manner both in CTRL and in Met cells; GSK3ß phosphorylation was significantly lower in treated cells compared to CTRL at 24h and 48h. The graphs represent band density expressed as fold change compared with CTRL. Phosphorylation level is presented as the *ratio* between phosphorylated and total protein; PGC-1α was normalized to vinculin. Data are representative of four independent experiments. Statistical analysis was performed using two-way ANOVA followed by Bonferroni's multiple comparison test. * ($p<0.05$), ** ($p<0.01$), *** ($p<0.001$), **** ($p<0.0001$) for

differences between CTRL and Met; #### ($p<0.0001$) for differences within CTRL; § ($p<0.05$), §§§§ ($p<0.0001$) for differences within Met.

4.2.5. Cotreatment "Met-Compound C": effects on myotubes

Compound C (CC) co-administered with 10mM Met dampened the effects of the drug on the parameters analysed.

Figure 53a shows that the CC attenuated the reduction in MYH1/2 expression induced by 10mM Met. Similarly, CC counteracted the effect of Met on Myf5 expression (*Figure 53b*). As regards p21 levels, cotreatment "Met-CC" not only counteracted the reduction induced by Met but led to a significant increase of the protein compared with control (*Figure 53c*). Furthermore, CC inhibited the upregulation of PGC-1α induced by Met (*Figure 53d*).

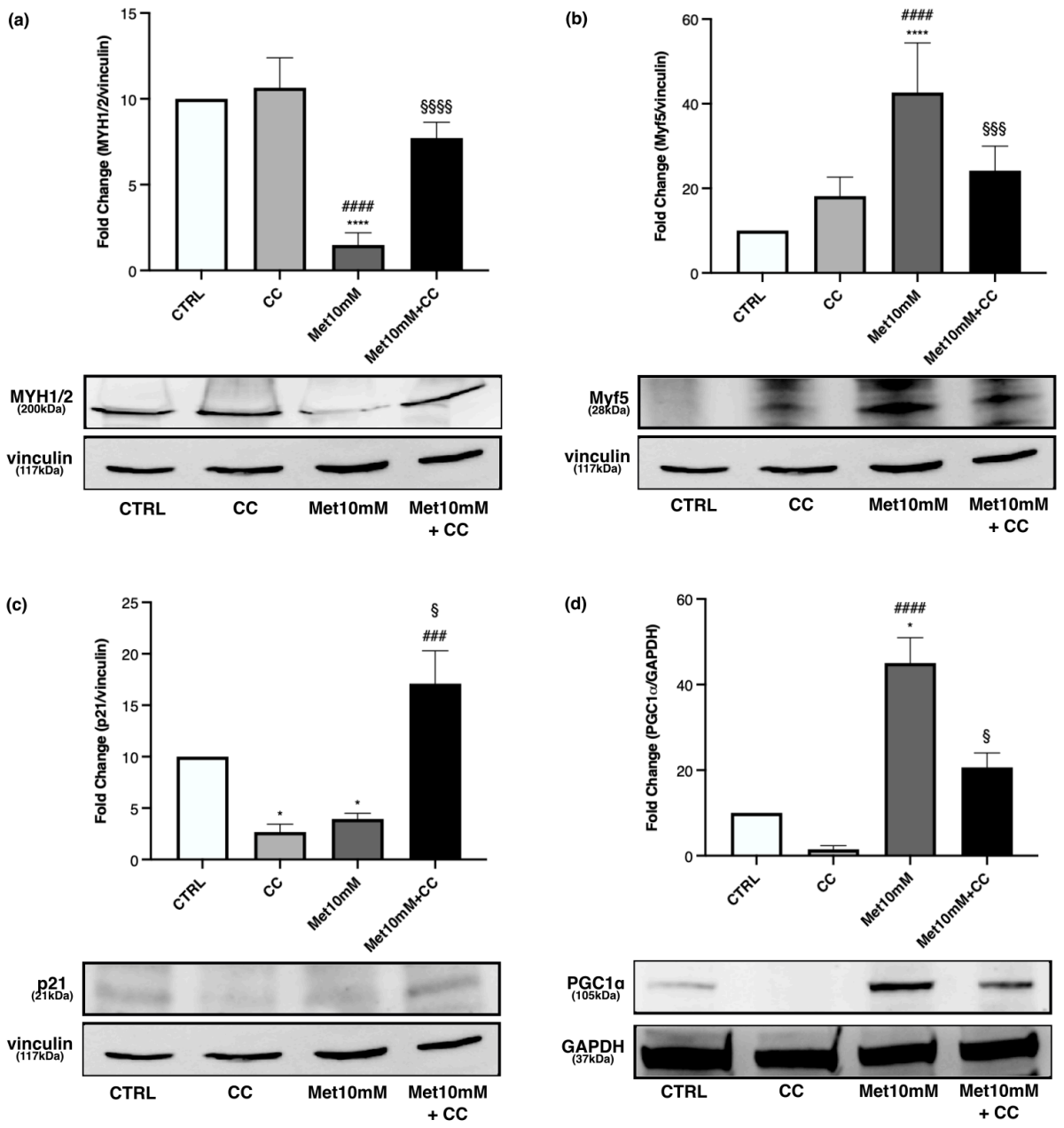

Figure 53. Western Blot analysis on myotubes treated with Met and/or CC. Myotubes were exposed to 10mM Met alone or combined with 10μM CC for 24h. Representative images of WB in total cell lysate are shown: MYH1/2 (a), Myf5 (b), p21(c), PGC-1α (d). Histograms represent band density expressed as fold change compared with CTRL. Vinculin and GAPDH were used as loading control. Data are representative of four independent experiments. Statistical analysis was performed using one-way ANOVA followed by Bonferroni's multiple comparison test. * ($p<0.05$), **** ($p<0.0001$) for differences *versus* CTRL, ### ($p<0.001$), #### ($p<0.0001$) for differences *versus* CC, § ($p<0.05$), §§§ ($p<0.001$), §§§§ ($p<0.0001$) for differences *versus* Met10mM.

4.2.6. Cotreatment “Met-lithium chloride”: effects on myotubes

Lithium chloride **(**LiCl) itself increased MYH1/2 levels in myotubes. The cotreatment “Met-LiCl” did not modify the effect of Met on MYH1/2 expression (*Figure 54a*).

Met action on Myf5 and p21 was not affected by the addition of LiCl in the culture medium (*Figures 54b and 54c*).

A significant increase in PGC-1α was induced by LiCl alone, while the cotreatment “Met-LiCl” did not alter the effects of Met (*Figure 54d*).

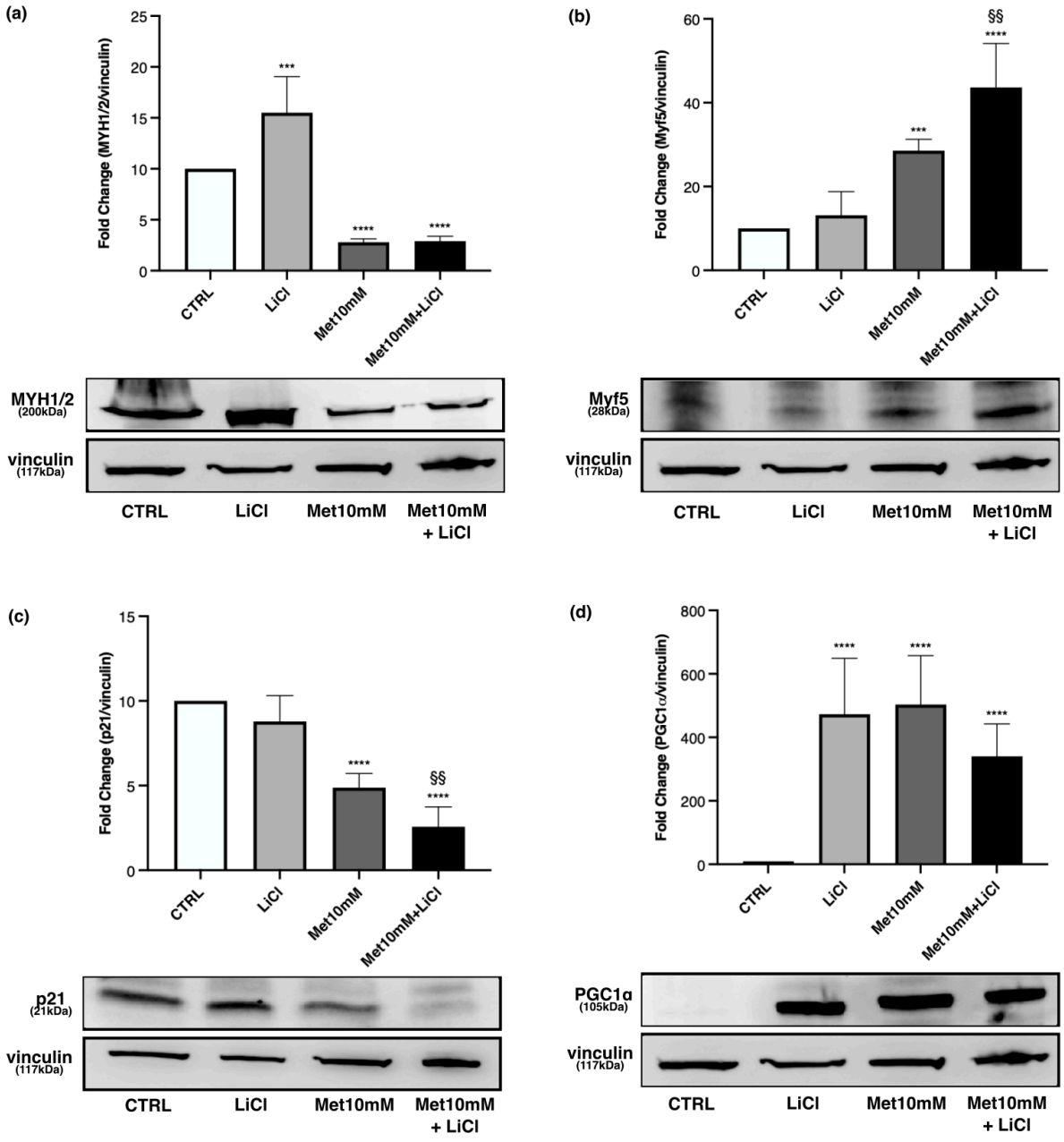

Figure 54. Western Blot analysis on myotubes treated with Met and/or LiCl. Myotubes were exposed to 10mM Met alone or combined with 10mM LiCl for 24h. Representative images of WB in total cell lysate are shown: MYH1/2 (a), Myf5 (b), p21(c), PGC-1α (d). Histograms represent band density expressed as fold change compared with CTRL. Vinculin was used as loading control. Data are representative of four independent experiments. Statistical analysis was performed using one-way ANOVA followed by Bonferroni's multiple comparison test. *** ($p<0.001$), **** ($p<0.0001$) for differences *versus* CTRL, §§ ($p<0.01$) for differences *versus* Met10mM.

5. DISCUSSION

5.1. *In vivo* study

Met is a biguanide oral antidiabetic drug that is traditionally used for the management of type 2 diabetes. Its therapeutic effects are based on a combination of improvement of peripheral uptake and utilisation of glucose, a decrease in the hepatic glucose output, a decreased rate of intestinal absorption of carbohydrates, and an enhancement in insulin sensitivity without causing side effects related to hypoglycemia [49]. Therefore, this drug can be used by healthy athletes to enhance their physical performance during a competition, taking advantage of insulin anabolic properties without falling into hypoglycemic risk related to insulin assumption. Moreover, differently from insulin, Met is not inserted in the WADA list of prohibited substances, so the healthy athlete who assumes it may not result positive to the doping test.

In the first part of the study, we aimed to investigate the effects of Met on physical performance *in vivo* on a healthy murine model to clarify if this drug could be considered a doping substance.

The first parameters we evaluated were food consumption and body weight increase, as previous studies reported that Met administration could have anorexic properties, and physical exercise can reduce food consumption and body weight as well. From our results we noticed no differences among groups as regards both the evaluated parameters.

Therefore, we decided to investigate the possible changes in muscle weight due to Met treatment and/or physical exercise by evaluating the muscle weight/body weight *ratio*. We observed that Met administration increased muscle weight, both alone and combined with training, suggesting a contribution of this antidiabetic drug in muscle anabolism improvement by impacting on insulin sensitivity [7].

To evaluate how training and Met administration affected rat physical performance we submitted animals to the GEE test at the beginning of the experimental period , at the middle and at the end. From the comparisons between GEE I – GEE II, GEE II – GEE III and GEE I – GEE III emerged that physical training led to a better rats' performance, in terms of covered distance, with respect to the untrained ones (C- and C+). From a deepened analysis of the results within the EX groups, we noticed that rats in EX+ group reached the better performance in the first four weeks of the experimental period, whereas the rats in EX- reached their better performance in the later four weeks. Surprisingly, we did not notice a further increase in EX+ when we compared the first GEE with the last GEE. As aforementioned, we also investigated the potential differences within the control groups, and we noticed a "less-decreased" performance of C+ rats in the second part of the experimental period. The same Met effect on C+ performance emerged also in the comparison between GEE I and GEE III. Taken together, these results suggest that Met treatment exerts a higher effect on physical performance when associated with training, even though its effects consist only in speeding up the positive effects of exercise on the performance without ameliorating it.

Rats blood was collected immediately after their sacrifice, thereafter blood analysis was performed.

Significant differences emerged in ALT, AST, LDH and CK-MB.

ALT is an enzyme that belongs to the transferases family and is responsible for the transport of amino groups produced by skeletal muscle after protein catabolism. ALT blood levels increase after tissue damage, such as muscle damage associated with an acute exercise [50].

AST is an enzyme present in the liver as well as in other tissues such as muscles, and it catalyses a reaction of transamination. Just like ALT, also AST levels increase after acute exercise, and it is likely due to its release from muscle cells [51,52].

LDH is an oxidoreductase that intervenes during the glycolysis in case of oxygen deficiency, with a subsequent NADH accumulation. Therefore, LDH oxidises NADH into NAD^+ using pyruvate as an oxidising molecule, later reduced into lactic acid with a high concentration in muscles. Circulating LDH levels increase during tissue damage and even more in case of tissue necrosis. For this reason, LDH is considered a marker of muscle stress [53].

CK is an enzyme expressed in tissues that need high amounts of adenosine triphosphate (ATP) such as skeletal muscle, brain, and heart, but also in smaller amounts in other visceral tissues. In these tissues, the kinase is responsible for the reversible conversion of creatine, and using ATP forms phosphocreatine (PCr) and adenosine diphosphate (ADP) [51]. CK is a dimeric molecule made up of two subunits (M and B), that can be combined to form: CK-MM, CK-BB, CK-MB. This latter form is highly expressed in myocardium, therefore is a marker of myocardial injury, but also in skeletal muscle (5 to 7%). Some evidence reported peak values of CK-MB in endurance athletes [51,54].

In our study, we noticed an increase in ALT levels in C- compared with SED, and this augment could probably result from muscle damage that occurred during the last GEE performed 48h before the sacrifice of rats. Moreover, the increase in ALT levels was also evident in C+, whereas in EX- and significantly in EX+ this blood parameter was low. This result suggests that training, and even more when it is associated with Met administration, could protect skeletal muscle against damages that can occur after a bout of endurance exercise.

Similar results were obtained as regards AST and LDH. In both cases Met administration decreased the levels of the two parameters, suggesting a potential role of this antidiabetic drug in protecting muscle from damage due to the last GEE. We found statistical differences also in CK-MB. The levels of this kinase decreased after exercise training, but the greater decrease was observed after Met treatment combined with training, suggesting – again – that Met associated with physical training prevented tissue damage caused by endurance exercise.

Skeletal muscle is actively involved in the synthesis and secretion of some proteins named myokines. In particular, muscle contraction during physical activity has an important role in activating the release of myokines, which can exert autocrine, paracrine and/or endocrine effects to regulate skeletal muscle growth [55–57]. Therefore, muscle contractile activity is an important regulator of the expression and secretion of myokines. In our study we analysed the levels of myokines in serum and skeletal muscle, with the aim to point out potential differences among groups related to physical training, Met administration and Met-training combination. After Met treatment, we observed an increase in FGF21, irisin, osteocrin and SPARC in serum, and a decrease in fractalkine in muscle.

FGF21 is an endocrine hormone, produced in various peripheral tissues, including skeletal muscle. Several studies suggest that FGF21 could be an excellent molecule to treat type 2 diabetes and could also be involved in the mechanism of metabolic enhancement, proper of some antidiabetic drugs. It has been demonstrated that Met increases FGF21 expression in mouse liver, therefore augmenting its secretion and serum levels through a mechanism of complex I inhibition, dependent on activating transcription factor 4 (ATF4) [58,59]. From our results emerged that drug administration increased serum FGF21 levels, independently from physical training. Moreover, FGF21 levels did not increase in EX- rats, suggesting that training does not influence the circulating levels of this myokine. As regards FGF21 levels in skeletal muscle, its values were under-determinable, confirming that this myokine does not accumulate in the tissue where it is produced as it is rapidly secreted. In addition, the results obtained on FGF21 support the inducing effect of Met on the myokine (as recently reported in literature) and demonstrate the efficacy of the drug administration modality adopted in our experimental protocol.

Irisin is a polypeptide hormone released into the blood after physical exercise. The increase in its circulating levels occurs from a stimulation of PPAR-γ and PGC-1α production, which

resulted in irisin increase as a product of its precursor fibronectin type III domain-containing protein 5 (FNDC5). Irisin influences glucose metabolism in skeletal muscle and also acts as a mediator of physical exercise effects on adipose tissue metabolism, by converting white adipose tissue (WAT) into brown adipose tissue (BAT). Moreover, irisin decreases body weight and insulin resistance as well. Plasma irisin levels increase both after endurance and resistance exercise, with a higher secretion after aerobic exercise [49,57]. From our analysis, statistical differences regarding irisin levels only emerged in serum samples, and we noticed that drug administration meaningfully increased irisin serum levels. It has been demonstrated that Met increases intramuscular irisin precursor (FNDC5) mRNA/protein expression and blood irisin levels in mice [49]. Since irisin levels are reported to increase also after physical exercise but our data did not highlight any differences between EX- and C-, we can hypothesise that the intensity of the training protocol used in our study was not enough to gain this effect. These results confirm the inducing role of Met on this myokine and, once again, demonstrate the effectiveness of the drug administration protocol.

Osteocrin is a peptide primarily expressed in skeletal muscle, and it has been demonstrated that it augments in type 2 diabetic mice. Indeed, blood and muscle levels of osteocrin are associated with fasting blood glucose levels and insulin resistance index in type 2 diabetes [60]. We were not able to understand which mechanism led to the result obtained in our study as regards osteocrin levels in serum samples. We can hypothesise that Met administration and physical training may support insulin activity also in health conditions. If so, osteocrin levels could be lower in rats submitted to Met treatment and/or training.

SPARC is a multifunctional myokine expressed in satellite cells and muscle fibres that may promote myoblast differentiation. Moreover, it can be released into the bloodstream by skeletal muscle after aerobic exercise and its expression can increase when AMPK is activated [61,62]. Our results show that Met administration increased SPARC serum levels, with a slight

increase also after physical training. This may confirm a role of Met in activating AMPK, resulting in SPARC expression, and its involvement in cell differentiation.

In muscle samples, the only myokine that showed significant differences among groups was fractalkine. This myokine is a chemokine produced by muscle cells and it can be both soluble and membrane anchored. It is mainly involved in muscle regeneration, with a direct effect on myogenic cells. Moreover, fractalkine levels increase in skeletal muscle after resistance exercise [63–65]. The results obtained highlight a role of Met in regulating this myokine expression in skeletal muscle. Indeed, we observed a reduction of fractalkine levels in rats treated with Met. We can suppose that fractalkine decrease observed after Met treatment could be a consequence of a protective effect of the drug from the muscle damages induced by exercise. In absence of damages the regenerative process does not need to be turned on.

Further investigations were performed on skeletal muscle samples, with the aim to investigate the possible differences in the expression levels of some proteins involved in energy production, that can be modified after physical exercise and/or after Met administration.

AMPK is an energy-sensing kinase expressed in human cells, regulated by cellular energy deficit, and activated by a phosphorylation on the threonine in response to various cellular stresses. When AMP/ATP and ADP/ATP ratios increase in the cell, there is an augmentation in AMPK activation related to a diminished energy availability. High intensity and short duration exercise leads to an increased AMPK activation, whereas a less intensity exercise not always leads to variation in AMPK activation [66,67]. It is known that AMPK plays a role in recovering the energetic homeostasis by turning on pathways that produce ATP, such as fatty acid oxidation by inhibiting ACCß through its phosphorylation, and mitochondrial biogenesis by means of PGC-1α levels increase in mitochondria. From the obtained results emerged that AMPK is highly activated after Met treatment but also after GEE test, both in trained and untrained conditions.

Once activated AMPK phosphorylates and inhibits ACCß, the muscular isoform of ACC, leading to a decrease of malonil-CoA and a subsequent increase of fatty acid oxidation [68]. We observed that training and even more its combination with Met treatment inhibited ACCß by increasing its phosphorylation levels. As aforementioned, AMPK can also increase the expression of another downstream factor: PGC-1α. It has been reported that in muscle submitted to physical exercise PGC-1α, once activated, translocates from the nucleus to the mitochondrial subsarcolemma, where it is involved in mitochondrial biogenesis [69]. According to this, our analysis reported an increase of PGC-1α in the mitochondrial fraction, supported by a similar trend of Cyt C, one of its downstream factors. Taken together, these results suggest that Met could have a role in restoring the energetic homeostasis via the AMPK pathway.

AKT is a kinase defined as the most important signal transducer of insulin, indeed its activation increases when stimulated by the hormone. AKT inhibits hepatic gluconeogenesis and enhances both glycogen synthesis and glycolysis [46]. All these effects are also associated with Met antidiabetic action. Our results showed a significant increase of p-AKT/AKT *ratio* only in EX+ but we hypothesise that AKT phosphorylation could be brought to light for a short period of time after its activation, therefore not so easy to notice in an *in vivo* model. Nevertheless, we observed an increase in p-GSK3ß/GSK3ß *ratio* after treatment and exercise that can be attributed to AKT activation, as GSK3ß is phosphorylated by this kinase.

GSK3ß is a constitutively active kinase that exerts multiple actions on different pathways [70]. One of its main functions is to inhibit the glycogen synthase (GS), leading to a decreased synthesis of glycogen. Insulin counteracts the GSK3ß effect on GS through AKT activation, that in turn inhibits GSK3ß by phosphorylating it on Ser9. It has been reported that physical training also increases the phosphorylation of GSK3ß [71]. Taken together, our results suggest that the combination Met treatment-exercise can enhance the single effects of drug administration and training on GSK3ß.

mTOR activity can be influenced both by AMPK and AKT pathways, although with different outcomes [47]. Indeed, AMPK inhibits mTOR whereas AKT determines its activation. Once activated, mTOR phosphorylates p70S6K, resulting in an increased protein synthesis. From our *in vivo* results emerged that both AMPK and AKT signalling pathways are activated by Met treatment. Nevertheless, we suppose that the AKT signalling on mTOR prevails on that of AMPK, as our data showed a weak but still evident increase in p70S6K phosphorylation.

In our study we evaluated the activation level of mTOR by considering its phosphorylation on Ser2448, which promotes mTOR activity according to literature [72].

Recently it has been reported that the phosphorylation on Ser2448 leads to inactivation of mTOR as part of an inhibitory feedback mechanism induced by the activated form of p70S6K, that switches off mTOR signal[7,73] .

Therefore, we can suppose that our result on mTOR signal reflects the action of two processes that regulate its activation in an opposite way.

The activation of protein synthesis in our treated muscles is supported by the increased levels of MYH1/2, a muscle structural protein. Indeed, our analysis reported a marked increase in MYH1/2 expression after Met administration, training and when they are combined. Nevertheless, we observed that the main effect on myosin heavy chain increase is due to Met administration rather than the eight weeks training.

We also investigate the variations related to the main MRFs such as PAX7, MyoD and Myf5. The results obtained on MRFs suggested that physical training, Met administration, and also an exercise carried on until exhaustion - as GEE test was - influence the expression pattern of the considered myogenic factors. The levels of MRFs vary according to the activation state of the SCs and the different phases of the cell cycle in which they are. On the basis of our results, we can hypothesise that training, Met administration and GEE influence SCs' status but we cannot define the exact entity of their action.

Despite these potentially favourable effects of Met on the contractile proteins and on the muscle energetic metabolism, why did we not see an enhancement in EX+ rats' physical performance? To find out an answer to this question, we decided to deepen the effects of Met on skeletal muscle by using C2C12 cells, an *in vitro* model that allowed us to study the outcomes of the drug treatment on proliferating and differentiating myoblast and on myotubes.

5.2. *In vitro* study

The aim of the *in vitro* study was to investigate the effects of Met on myoblast proliferation and differentiation and to understand the role of AMPK in the mechanism of action of the drug.

We observed that Met inhibited C2C12 proliferation in a concentration- and time-dependent manner without increasing cell mortality or inducing cytotoxicity and apoptosis, according to other authors [74]. In addition, AMPK activation was detected in proliferating cells after treatment with Met. Specifically, the increase in AMPK phosphorylation was more evident in cells treated with 1mM and 10mM Met after 24h and much less, but still detectable, after 48h and 72h. The time lag observed between the increase in AMPK phosphorylation (maximal at 24h) and the inhibition of cell proliferation (maximal at 72h) suggests that Met antiproliferative effect is not a direct consequence of the AMPK activation, but some other cellular events are probably interposed between the two phenomena.

The analysis of the cell cycle showed that after treatment with 1mM and 10mM Met the percentage of myoblasts in G0/G1 phase was lower, while that of cells in G2/M was higher compared with control. These differences were evident after 24h of treatment, even more at 48h, and disappeared after 72h. We suppose that the loss of differences among control and treated cells after 72h was most likely due to the achievement of confluence in CTRL in the time span between 48h and 72h.

Thus, our work highlights that Met-treated myoblasts decrease their proliferation rate and reside in the G2/M phase of cell cycle rather than control. These effects are associated with an increase in AMPK activation in the cells.

Williamson *et al.* [75] observed that AICAR treatment of myoblast cultures, besides increasing AMPK phosphorylation, altered cell cycle transition with a cell arrest in G1. Taken together, Williamson's and our findings suggest that the AMPK system plays a role in the regulation of

cell proliferation, and we can speculate that the kinase is involved in Met effects on myoblast growth and cell cycle progression.

However, AICAR-induced AMPK activation altered cell cycle transition by inducing cell stop in G0/G1 phase, while in our study Met causes a significant increase in the percentage of cells in G2/M. Our findings agree with those obtained by Pavlidou *et al.* [74] who observed a delay in cell transition through the G2/M phase after Met treatment.

In the present study, Met inhibited C2C12 myoblast differentiation as demonstrated by the lack of expression of MYH1/2, a marker of completed differentiation, in treated cells in comparison with controls in myoblasts induced to differentiate.

Moreover, a different expression pattern of the main MRFs was also evident in myoblasts induced to differentiate in presence of Met. We observed a progressive decrease of MyoD and Myf5 expression levels in differentiating CTRL. Conversely, an increase in MyoD expression and even more in Myf5 was evident in Met-treated cells over time, even though their levels were lower than controls at 24h and 48h.

It has been reported that when proliferating myoblasts are induced to differentiate by serum deprivation in the medium, a significant proportion of cells escapes from terminal differentiation. Kitzmann *et al*. [76] showed that MyoD and Myf5 expression patterns became mutually exclusive when C2C12 cells were induced to differentiate, with Myf5 staining present in cells which fail to differentiate. To further analyse the regulation of MyoD and Myf5 expression, authors synchronised proliferating myoblasts. Analysis of MyoD and Myf5 expression during cell cycle progression revealed that MyoD was absent in G0, peaked in mid-G1, fell to its minimum level at G1/S and made up from S to M. In contrast, Myf-5 protein was high in G0, decreased during G1 and reappeared at the end of G1 to remain stable until mitosis [76].

We can speculate that myoblasts induced to differentiate in presence of 10mM Met do not undergo a permanent exit from the cell cycle, but their cycle progression is arrested in G2/M phase. Indeed, these cells show high expression of both MyoD and Myf5 as reported by Kitzmann *et al.* [76] for cells from S to M phase.

The analysis of PAX7 expression profile over time in control and treated cells seems to support an alteration of the differentiation process by Met. Indeed, since PAX7 is downregulated during myogenic differentiation [77] and we observed that PAX7 downregulation was delayed by Met treatment, we may speculate that the drug could affect the differentiation process in C2C12 cells.

We then analysed the expression of p21, an inhibitor of the cell cycle. The increase in p21 level is crucial for the irreversible exit from the cell cycle and the end of the differentiation process. In differentiating cells treated with Met we observed that p21 protein expression decreased over time compared with control. p21 binds to and inhibits the activity of cyclin-CDK2, -CDK1, and -CDK4/6 complexes, and thus acts as a regulator of cell cycle progression from G1 to S phase. Moreover, in a landmark study, Spencer and co-workers [78] identified a quiescence decision point temporally located in late G2/M phase requiring high levels of p21. Cells with low p21 levels failed to enter G0 arrest.

Therefore, myoblasts treated with Met and induced to differentiate were detained in G2 probably because p21 levels were not enough to commit them to enter G0 arrest.

As already observed in proliferating myoblasts, also in differentiating cells, Met treatment induced a remarkable rise of AMPK phosphorylation.

Our results are consistent with the findings of Williamson *et al.* [75] showing that AICAR-treated myoblasts undergoing differentiation had a reduced myotube formation and myosin accumulation together with a reduced p21 expression.

Thus, we can suppose that Met affects myoblasts differentiation through an AMPK-dependent mechanism.

In addition, we observed that Met induced an increase in PGC-1α expression and phosphorylation of ACCß in differentiating myoblasts. ACCß is a downstream target enzyme of AMPK, and its phosphorylation promotes the oxidative metabolism in skeletal muscle. A link between PGC-1α and AMPK is widely reported, indeed PGC-1α has been described as a mediator of some transcriptional outputs triggered by metabolic sensors like AMPK [79].

Williamson *et al.* [75] demonstrated that the activation of AMPK by AICAR in proliferating and differentiating myoblasts or in myotubes reduced p21 protein expression through a PGC-1α-dependent mechanism. Based on our data, we cannot support a direct involvement of PGC-1α in Met effects on myoblasts, however PGC-1α levels rise in differentiating cells treated with Met much more than in CTRL in the same experimental conditions.

A noteworthy result shown in the present research concerns the activation state of GSK3ß in differentiating cells. Indeed, this kinase resulted non-phosphorylated, therefore fully active in cells treated with Met at every time point, whereas its phosphorylation state was already well evident in CTRL at 24h and further increased at 48h. An important negative regulatory role for GSK3ß in myogenesis has been revealed by van der Velden and co-workers [80] who demonstrated that the promyogenic effects of Insulin-like Growth Factor-1 (IGF-1) require GSK3ß inactivation. Therefore, these data rule out the possibility that also GSK3ß could be involved in Met effects on myoblasts differentiation.

In the present study we aimed to evaluate the effects of Met also in myotube cultures. Primarily, we tested Met at the concentrations used in cell proliferation (250µM, 1mM and 10mM), then we focused on a panel of Met concentrations included in the range 250µM-1mM. Indeed, it has been reported that Met may affect myogenic differentiation with a dual action depending on the concentration employed [48]. Altogether, the effects caused by Met in

myotubes were comparable to those induced in myoblasts. Some of them were already evident at low concentrations of Met and showed an approximative concentration-dependent trend, such as phosphorylated AMPK increase and p21 and MYH1/2 decrease. As regards GSK3ß, its phosphorylation decreased starting from 400μM Met with little ups and downs until 1mM and plunged with 10mM Met treatment. The increase in PGC-1α expression was only evident at the highest drug concentration.

Interestingly, as regards Myf5, we observed a significant reduction of its levels after 400μM Met treatment, whereas its expression increased when myotubes were exposed to higher concentrations. It is to note that Met induced AMPK activation in these cells starting from 400μM. Therefore, if we assume that the effects of Met on myotubes are mediated by an AMPK-dependent mechanism, we can speculate that 400μM Met is not enough to create cellular conditions needed to carry out the effects of drug on myotubes.

In addition, we showed that generally the effects of Met on myotubes reach their maximum level after 48h of treatment and tend to decrease over time, except for the PGC-1α increase. Indeed, PGC-1α expression raised in myotubes treated with Met after exposure to the highest concentration only at 24h, with no statistical difference *versus* CTRL at 48h and 96h. Therefore, Met effect on PGC-1α expression in myotubes seems to be transient and to require high concentrations of the drug. The lack of statistically significant difference between control and treated cells both at 48h and 96h is due to an increased PGC-1α expression also in CTRL at 48h, probably correlated with the increment of AMPK phosphorylation observed in these cells at the same time point.

As we underlined above, when proliferating or differentiating myoblasts or myotubes were treated with Met, a significant increase of AMPK activation was evident. In each of these cell types, Met-induced activation of AMPK was accompanied by a series of other cellular events

that have already been partially demonstrated in the same cell types after AMPK activation by AICAR treatment [75].

Based on these analogies, we hypothesised that Met effects in skeletal muscle cells are mediated by AMPK. Moreover, our findings showed that GSK3ß could also be involved in Met inhibition of myoblast differentiation.

Therefore, to test the contribution of AMPK or GSK3ß to the effects of Met on myotubes we evaluated how Met affected Myf5, p21, PGC-1α and MYH1/2 expression in myotubes when a specific inhibitor of AMPK or GSK3ß was added in culture. In this work we studied the effects of Met on myoblasts proliferation and differentiation and determined the role of AMPK in the mechanism of action of the drug. We observed that AMPK inhibition by CC attenuated the effects of Met on the expression of all the analysed proteins, supporting the hypothesis that Met impairs skeletal muscle differentiation through an AMPK-dependent mechanism. As regards GSK3ß, to investigate whether its inhibition could attenuate Met effects on myotubes, we employed a pharmacological inhibition with LiCl [81]. The addition of LiCl in the culture medium of treated myotubes did not counteract the action of Met on p21 and Myf5 expression. As regards MYH1/2, LiCl did not change the effects of Met, nevertheless LiCl alone increased MYH1/2 expression. Inhibition of GSK3ß by LiCl caused an augment of PGC-1α comparable to that induced by Met. This result is consistent with reports that connect knock-down of GSK3ß, as well as its pharmacological inhibition, to increased PGC-1α transcript and protein abundance during myogenic differentiation and in fully differentiated myotubes [82,83]. As Met and LiCl increased PGC-1α expression themselves compared with control, but their association did not lead to an additional increase in PGC-1α, we may speculate that a common mechanism is involved in their final effect on PGC-1α expression, even though this hypothesis needs to be further investigated.

6. CONCLUSIONS

The results obtained *in vitro* highlight that Met inhibits myoblasts differentiation by arresting cells in G2/M phase. We can suppose that a similar effect may be induced in skeletal muscle SCs, affecting - at least temporarily - the renewing process. Therefore, we can speculate that Met speeds up the positive effects of training on physical performance by increasing the contractile ability of muscle through a higher expression of MYH1/2 and by restoring the energetic homeostasis via the activation of AMPK. Nevertheless, if Met affects the regenerative potential of muscle SCs as previously hypothesised, the prolonged and continuous exposure to Met may hamper the repair of skeletal muscle after training-induced damage. In this *scenario*, the reduced levels of fractalkine observed in muscle of Met-treated rats could be evaluated as an additional negative effect of Met on skeletal muscle, responsible for a lower regenerative potential of the muscle cells instead of a less need to regenerate them. Similarly, the increase in Myf5 levels observed both *in vivo* and *in vitro* after Met treatment may be due to a lower SCs inclination to differentiate, according to what we noticed *in vitro*. Further experiments are needed to support this hypothesis.

Publication

Maniscalco E, Abbadessa G, Giordano M, Gasso L, Borrione P, Racca S. “Metformin regulates myoblast differentiation through an AMPK-dependent mechanism.” submitted to PLOS ONE (we are going to provide the requested revisions).

7. REFERENCES

1 Shen L, Meng X, Zhang Z, Wang T. Physical exercise for muscle atrophy. In: *Advances in Experimental Medicine and Biology*. Springer New York LLC, 2018, pp 529–545.

2 Frontera WR, Ochala J. Skeletal Muscle: A Brief Review of Structure and Function. Behav Genet. 2015;45(2):183–195.

3 Plaza-Diaz J, Izquierdo D, Torres-Martos Á, Baig AT, Aguilera CM, Ruiz-Ojeda FJ. Impact of Physical Activity and Exercise on the Epigenome in Skeletal Muscle and Effects on Systemic Metabolism. *Biomedicines*. 2022;10(1). doi:10.3390/biomedicines10010126.

4 Calcagno G. Modificazioni metaboliche indotte dall'esercizio fisico. .

5 Dumont NA, Bentzinger CF, Sincennes MC, Rudnicki MA. Satellite cells and skeletal muscle regeneration. *Compr Physiol*. 2015;5(3):1027–1059.

6 Hawke TJ, Garry DJ. invited review Myogenic satellite cells: physiology to molecular biology. 2001http://www.jap.org.

7 Thomson D. The Role of AMPK in the Regulation of Skeletal Muscle Size, Hypertrophy, and Regeneration. *Int J Mol Sci*. 2018;19(10):3125.

8 Hoffman NJ, Parker BL, Chaudhuri R et al. Global Phosphoproteomic Analysis of Human Skeletal Muscle Reveals a Network of Exercise-Regulated Kinases and AMPK Substrates. *Cell Metab*. 2015;22(5):922–935.

9 Aragón-Vela J, Solis-Urra P, Ruiz-Ojeda FJ, Álvarez-Mercado AI, Olivares-Arancibia J, Plaza-Diaz J. Impact of exercise on gut microbiota in obesity. Nutrients. 2021;13(11). doi:10.3390/nu13113999.

10 Rivera-Brown AM, Frontera WR. Principles of exercise physiology: Responses to acute exercise and long-term adaptations to training. *PM and R*. 2012;4(11):797–804.

11 Savikj M, Zierath JR. Train like an athlete: applying exercise interventions to manage type 2 diabetes. Diabetologia. 2020;63(8):1491–1499.

12 Trevor AJ, Katzung BG, Masters SB. Ormoni pancreatici, farmaci antidiabetici e glucagone. In: *Katzung & Trevor's Farmacologia - quesiti a scelta multipla e compendio della materia*. PICCIN, pp 429–438.

13 PDB-101. https://pdb101.rcsb.org.

14 Beale EG. Insulin Signaling And Insulin Resistance. 2013 doi:10.231/JIM.0b013e3182746f95.

15 Rang HP, Dale MM, Ritter JM, Flower RJ. Pancreas endocrino e controllo del glucosio ematico. In: *Farmacologia*. ELSEVIER MASSON, pp 400–412.

16 Kalra S, Arora S, Kapoor N. Classification of Non-Insulin Glucose Lowering Drugs. *J Pak Med Assoc*. 2022;72(1):181–182.

17 Bailey CJ. Metformin: historical overview. *Diabetologia*. 2017;60(9):1566–1576.

18 Lamoia TE, Shulman GI. Cellular and Molecular Mechanisms of Metformin Action. Endocr Rev. 2021;42(1):77–96.

19 Magdalena Markowicz-Piasecka, Kristiina M. Huttunen, Łukasz Mateusiak, Elżbieta Mikiciuk-Olasik, Joanna Sikora. Is Metformin a Perfect Drug? Updates in Pharmacokinetics and Pharmacodynamics. *Curr Pharm Des*. 2017;23:1–19.

20 Galuska D, Nolte LA, Zierath JR, Wallberg-Henriksson H. Effect of metformin on insulin-stimulated glucose transport in isolated skeletal muscle obtained from patients with NIDDM. *Diabetologia*. 1994;37(8):826–832.

21 Cusi K, Consoli A, DeFronzo RA. Metabolic effects of metformin on glucose and lactate metabolism in noninsulin-dependent diabetes mellitus. *J Clin Endocrinol Metab*. 1996;81(11):4059–4067.

22 Hundal RS, Krssak M, Dufour S et al. Mechanism by which metformin reduces glucose production in type 2 diabetes. *Diabetes*. 2000;49(12):2063–2069.

23 Foretz M, Hébrard S, Leclerc J et al. Metformin inhibits hepatic gluconeogenesis in mice independently of the LKB1/AMPK pathway via a decrease in hepatic energy state. *Journal of Clinical Investigation*. 2010;120(7):2355–2369.

24 Barbieri R. Metformin for the treatment of polycystic ovary syndrome. *Obstetrics & Gynecology*. 2003;101(4):785–793.

25 Cabreiro F, Au C, Leung K-Y et al. Metformin Retards Aging in C. elegans by Altering Microbial Folate and Methionine Metabolism. *Cell*. 2013;153(1):228–239.

26 Hong J, Zhang Y, Lai S et al. Effects of Metformin Versus Glipizide on Cardiovascular Outcomes in Patients With Type 2 Diabetes and Coronary Artery Disease. *Diabetes Care*. 2013;36(5):1304–1311.

27 Zemdegs J, Martin H, Pintana H et al. Metformin Promotes Anxiolytic and Antidepressant-Like Responses in Insulin-Resistant Mice by Decreasing Circulating Branched-Chain Amino Acids. *The Journal of Neuroscience*. 2019;39(30):5935–5948.

28 Langone F, Cannata S, Fuoco C et al. Metformin Protects Skeletal Muscle from Cardiotoxin Induced Degeneration. *PLoS One*. 2014;9(12):e114018.

29 Dong X, Hui T, Chen J et al. Metformin Increases Sarcolemma Integrity and Ameliorates Neuromuscular Deficits in a Murine Model of Duchenne Muscular Dystrophy. *Front Physiol*. 2021;12. doi:10.3389/fphys.2021.642908.

30 Pavlidou T, Marinkovic M, Rosina M et al. Metformin Delays Satellite Cell Activation and Maintains Quiescence. *Stem Cells Int*. 2019;2019:1–19.

31 Kang MJ, Moon JW, Lee JO et al. Metformin induces muscle atrophy by transcriptional regulation of myostatin via HDAC6 and FoxO3a. *J Cachexia Sarcopenia Muscle*. 2022;13(1):605–620.

32 International Olympic Committee. https://www.olympic.org/the-ioc.

33 WADA. https://www.wada-ama.org.

34 Thevis M, Geyer H, Schänzer W. Identification of oral antidiabetics and their metabolites in human urine by liquid chromatography/tandem mass spectrometry-a matter for doping control analysis. *Rapid Communications in Mass Spectrometry*. 2005;19(7):928–936.

35 Falcieri E, Burattini S, Ferri ° P et al. C2C12 murine myoblasts as a model of skeletal muscle development: morpho-functional characterization. 2004.

36 Senesi P, Montesano A, Luzi L, Codella R, Benedini S, Terruzzi I. Metformin Treatment Prevents Sedentariness Related Damages in Mice. *J Diabetes Res*. 2016;2016:1–11.

37 Soya H, Nakamura T, Deocaris CC et al. BDNF induction with mild exercise in the rat hippocampus. *Biochem Biophys Res Commun*. 2007;358(4):961–7.

38 Inoue K, Okamoto M, Shibato J et al. Long-Term Mild, rather than Intense, Exercise Enhances Adult Hippocampal Neurogenesis and Greatly Changes the Transcriptomic Profile of the Hippocampus. *PLoS One*. 2015;10(6):e0128720.

39 Shima T, Matsui T, Jesmin S et al. Moderate exercise ameliorates dysregulated hippocampal glycometabolism and memory function in a rat model of type 2 diabetes. *Diabetologia*. 2017;60(3):597–606.

40 Matsui T, Liu Y-F, Soya M, Shima T, Soya H. Tyrosine as a Mechanistic-Based Biomarker for Brain Glycogen Decrease and Supercompensation With Endurance Exercise in Rats: A Metabolomics Study of Plasma. *Front Neurosci*. 2019;13:200.

41 Zheng J, Liu W, Zhu X et al. Pterostilbene Enhances Endurance Capacity via Promoting Skeletal Muscle Adaptations to Exercise Training in Rats. *Molecules*. 2020;25(1). doi:10.3390/molecules25010186.

42 Penna C, Perrelli MG, Raimondo S et al. Postconditioning induces an anti-apoptotic effect and preserves mitochondrial integrity in isolated rat hearts. *Biochim Biophys Acta Bioenerg*. 2009;1787(7):794–801.

43 Bradford MM. A rapid and sensitive method for the quantitation of microgram quantities of protein utilizing the principle of protein-dye binding. *Anal Biochem*. 1976;72(1–2):248–254.

44 Mosmann T. Rapid colorimetric assay for cellular growth and survival: Application to proliferation and cytotoxicity assays. *J Immunol Methods*. 1983;65(1–2):55–63.

45 Fang X, Yu SX, Lu Y, Bast RC, Woodgett JR, Mills GB. Phosphorylation and inactivation of glycogen synthase kinase 3 by protein kinase A. *Proc Natl Acad Sci U S A*. 2000;97(22):11960–5.

46 Sakai G, Inoue I, Suzuki T et al. Effects of the Activation of Three Major Hepatic Akt Substrates on Glucose Metabolism in Male Mice. *Endocrinology*. 2017;158(8):2659–2671.

47 Shackelford DB, Shaw RJ. The LKB1-AMPK pathway: metabolism and growth control in tumour suppression. *Nat Rev Cancer*. 2009;9(8):563–75.

48 Jiang L-L, Liu L. Effect of metformin on stem cells: Molecular mechanism and clinical prospect. *World J Stem Cells*. 2020;12(12):1455–1473.

49 Yano N, Zhao YT, Zhao TC. The Physiological Role of Irisin in the Regulation of Muscle Glucose Homeostasis. *Endocrines*. 2021;2(3):266–283.

50 Nathwani RA, Pais S, Reynolds TB, Kaplowitz N. Serum alanine aminotransferase in skeletal muscle diseases. *Hepatology*. 2005;41(2):380–382.

51 Cialoni D, Brizzolari A, Sponsiello N et al. Serum Cardiac and Skeletal Muscle Marker Changes in Repetitive Breath-hold Diving. *Sports Med Open*. 2021;7(1). doi:10.1186/s40798-021-00349-z.

52 Otto-Ślusarczyk D, Graboń W, Mielczarek-Puta M. Aspartate aminotransferase - key enzyme in the human systemic metabolism. *Postepy Hig Med Dosw*. 2016;70:219–230.

53 Elustondo PA, White AE, Hughes ME, Brebner K, Pavlov E, Kane DA. Physical and Functional Association of Lactate Dehydrogenase (LDH) with Skeletal Muscle Mitochondria. *Journal of Biological Chemistry*. 2013;288(35):25309–25317.

54 Cabaniss C. Daniel. Creatine Kinase. .

55 So B, Kim H-J, Kim J, Song W. Exercise-induced myokines in health and metabolic diseases. *Integr Med Res*. 2014;3(4):172–179.

56 Huh JY. The role of exercise-induced myokines in regulating metabolism. *Arch Pharm Res*. 2018;41(1):14–29.

57 Zumárraga Franco Javier, Argüelles Castilla Sandro, Ayala Gómez Antonio, Cano Rodríguez Mercedes. Physical exercise and myokines. *Approaches to Aging Control*. 2019;23.

58 Kim KH, Jeong YT, Kim SH et al. Metformin-induced inhibition of the mitochondrial respiratory chain increases FGF21 expression via ATF4 activation. *Biochem Biophys Res Commun*. 2013;440(1):76–81.

59 Wang Y, Dang N, Sun P, Xia J, Zhang C, Pang S. The effects of metformin on fibroblast growth factor 19, 21 and fibroblast growth factor receptor 1 in high-fat diet and streptozotocin induced diabetic rats. *Endocr J*. 2017;64(5):543–552.

60 Shimomura M, Horii N, Fujie S et al. Decreased muscle-derived musclin by chronic resistance exercise is associated with improved insulin resistance in rats with type 2 diabetes. *Physiol Rep*. 2021;9(9):e14823.

61 Petersson SJ, Jørgensen LH, Andersen DC, Nørgaard RC, Jensen CH, Schrøder HD. SPARC is up-regulated during skeletal muscle regeneration and inhibits myoblast differentiation. *Histol Histopathol*. 2013;28(11):1451–60.

62 Songsorn P, Ruffino J, Vollaard NBJ. No effect of acute and chronic supramaximal exercise on circulating levels of the myokine SPARC. *Eur J Sport Sci*. 2017;17(4):447–452.

63 Szukiewicz D, Szewczyk G, Pyzlak M et al. Anti-inflammatory Action of Metformin with Respect to CX3CL1/CX3CR1 Signaling in Human Placental Circulation in Normal-Glucose Versus High-Glucose Environments. *Inflammation*. 2018;41(6):2246–2264.

64 Rutti S, Arous C, Schvartz D et al. Fractalkine (CX3CL1), a new factor protecting β-cells against TNFα. *Mol Metab*. 2014;3(7):731–41.

65 Strömberg A, Olsson K, Dijksterhuis JP, Rullman E, Schulte G, Gustafsson T. CXCL1-a macrophage chemoattractant induced by a single bout of exercise in human skeletal muscle. *American Journal of Physiology-Regulatory, Integrative and Comparative Physiology*. 2016;310(3):R297–R304.

66 Jessen N, Sundelin EIO, Møller AB. AMP kinase in exercise adaptation of skeletal muscle. *Drug Discov Today*. 2014;19(7):999–1002.

67 Zhou G, Myers R, Li Y et al. Role of AMP-activated protein kinase in mechanism of metformin action. *Journal of Clinical Investigation*. 2001;108(8):1167–1174.

68 Dean D, Daugaard JR, Young ME et al. Exercise diminishes the activity of acetyl-CoA carboxylase in human muscle. *Diabetes*. 2000;49(8):1295–300.

69 O'Neill HM, Lally JS, Galic S et al. Skeletal muscle ACC2 S212 phosphorylation is not required for the control of fatty acid oxidation during exercise. *Physiol Rep*. 2015;3(7):e12444.

70 Beurel E, Grieco SF, Jope RS. Glycogen synthase kinase-3 (GSK3): Regulation, actions, and diseases. Pharmacol Ther. 2015;148:114–131.

71 Markuns JF, Wojtaszewski JF, Goodyear LJ. Insulin and exercise decrease glycogen synthase kinase-3 activity by different mechanisms in rat skeletal muscle. *J Biol Chem*. 1999;274(35):24896–900.

72 Reynolds TH, Bodine SC, Lawrence JC. Control of Ser2448 phosphorylation in the mammalian target of rapamycin by insulin and skeletal muscle load. *J Biol Chem*. 2002;277(20):17657–62.

73 Figueiredo VC, Markworth JF, Cameron-Smith D. Considerations on mTOR regulation at serine 2448: implications for muscle metabolism studies. Cellular and Molecular Life Sciences. 2017;74(14):2537–2545.

74 Pavlidou T, Rosina M, Fuoco C et al. Regulation of myoblast differentiation by metabolic perturbations induced by metformin. *PLoS One*. 2017;12(8):e0182475.

75 Williamson DL, Butler DC, Alway SE. AMPK inhibits myoblast differentiation through a PGC-1α-dependent mechanism. *American Journal of Physiology-Endocrinology and Metabolism*. 2009;297(2):E304–E314.

76 Kitzmann M, Carnac G, Vandromme M, Primig M, Lamb NJC, Fernandez A. The Muscle Regulatory Factors MyoD and Myf-5 Undergo Distinct Cell Cycle–specific Expression in Muscle Cells. *Journal of Cell Biology*. 1998;142(6):1447–1459.

77 Olguin HC, Olwin BB. Pax-7 up-regulation inhibits myogenesis and cell cycle progression in satellite cells: a potential mechanism for self-renewal. *Dev Biol*. 2004;275(2):375–388.

78 Spencer SL, Cappell SD, Tsai F-C, Overton KW, Wang CL, Meyer T. The Proliferation-Quiescence Decision Is Controlled by a Bifurcation in CDK2 Activity at Mitotic Exit. *Cell*. 2013;155(2):369–383.

79 Cantó C, Auwerx J. PGC-1α, SIRT1 and AMPK, an energy sensing network that controls energy expenditure. *Curr Opin Lipidol*. 2009;20(2):98–105.

80 van der Velden JLJ, Langen RCJ, Kelders MCJM, Wouters EFM, Janssen-Heininger YMW, Schols AMWJ. Inhibition of glycogen synthase kinase-3β activity is sufficient to stimulate myogenic differentiation. *American Journal of Physiology-Cell Physiology*. 2006;290(2):C453–C462.

81 Ma Z, Zhong Z, Zheng Z, Shi X-M, Zhang W. Inhibition of Glycogen Synthase Kinase-3β Attenuates Glucocorticoid-Induced Suppression of Myogenic Differentiation In Vitro. *PLoS One*. 2014;9(8):e105528.

82 Theeuwes WF, Gosker HR, Langen RCJ et al. Inactivation of glycogen synthase kinase-3β (GSK-3β) enhances skeletal muscle oxidative metabolism. *Biochimica et Biophysica Acta (BBA) - Molecular Basis of Disease*. 2017;1863(12):3075–3086.

83 Theeuwes WF, Gosker HR, Langen RCJ, Pansters NAM, Schols AMWJ, Remels AHV. Inactivation of glycogen synthase kinase 3β (GSK-3β) enhances mitochondrial biogenesis during myogenesis. *Biochimica et Biophysica Acta (BBA) - Molecular Basis of Disease*. 2018;1864(9):2913–2926.